DOCTORAL THESIS

UNIVERSITAT POLITÈCNICA DE CATALUNYA BARCELONATECH

Novel lubrication system to improve the excessive wear in wind turbine yaw and pitch gears

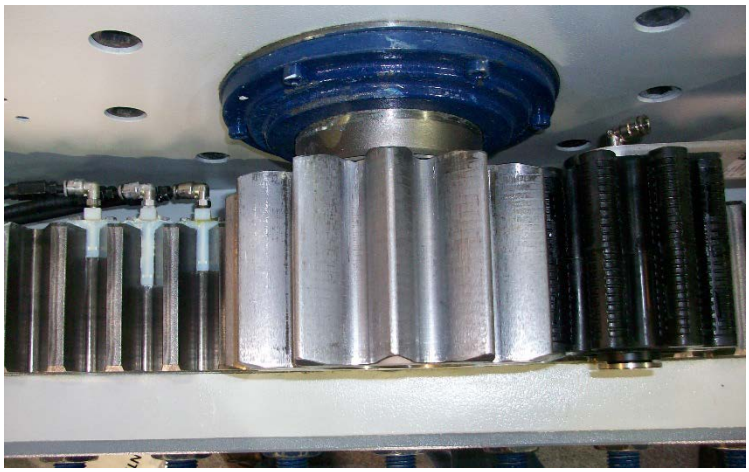

Josep Farré Lladós

Novel lubrication system to improve the excessive wear in wind turbine yaw and pitch gears

Josep Farré Lladós

Mechanical Engineering Department

Technical University of Catalonia

SUPERVISORS:

Jasmina Casals Terré[1] and Lars-Göran Westerberg[2]

[1]UPC - Technical University of Catalonia Department of Mechanical Engineering
[2]Luleå University of Technology Division of Fluid and Experimental Mechanics

Printed by the Technical University of Catalonia, Barcelona 2015

www.upc.edu

This project/research has been supported by KIC InnoEnergy. KIC InnoEnergy is a company supported by the European Institute of Innovation and Technology (EIT), and has the mission of delivering commercial products and services, new businesses, innovators and entrepreneurs in the field of sustainable energy through the integration of higher education, research, entrepreneurs and business companies.

To all my family, especially Laia, Montse and my parents Josep Mª and Montse.

ABSTRACT

Manufacturers of wind turbines have observed a new phenomenon that appears in high power wind turbines: excessive wear in the teeth located at 0º in the pitch bearing.

In order to design more efficient wind turbines, manufacturers are increasing the rotor diameter to capture more kinetic energy from the wind to generate more energy, therefore the stress in the joints/unions is increased, which leads to the elastic deformation of the system. These stresses and deformations increase in all parts of the wind turbine, the foundations and the tower, yaw, nacelle, drive train and blade unions. All these cases are mainly static unions, except the drive train that transmits torque, the yaw system that turns the nacelle and the pitch system that turns each blade around its axis.

The weight of the blades under movement, always working in the most efficient position, causes micro-movements allowed by the elastic deformations and the backlash of the gear transmission that induce an excessive wear at the zero degree position. The same phenomenon is observed in the yaw system, though to a lesser extent. Despite the manufacturer's efforts, a solution that could be implemented in the near future or easily retrofitted in the wind turbines does not yet exist.

The aim of this PhD project is to improve the lubrication of the pitch and yaw gear systems of wind turbines through the use of a novel lubrication system based on an array of micro-fabricated channels fitted at the gears' root (dedendum). A micro-nozzle to continuously inject fresh grease in between the teeth in contact has been designed, manufactured and installed in a test bench of a 2 MW wind turbine pitch system. The test bench has been used to characterize the fatigue behavior of the gear surface using conventional wind turbine greases under real cyclic loads, showing a delay of $2x10^4$ cycles in the appearance of wear.

The proposed micro-nozzle is expected to be compatible with and easily implemented into both newly designed and in-market models. This novel lubrication system will inject fresh lubricant to the gear contact area even when the wind turbine is generating electricity.

CONTENTS

ACKNOWLEDGMENTS

I would like to thank everyone who has contributed to this PhD project, and in particular:

My supervisor, Jasmina Casals Terré, for supporting and guiding my work, and profiling and sparking my creativity to improve my own ideas.

My co-supervisor, Lars-Göran Westerberg, for supporting and guiding my work and receiving me warmly at the LTU University.

Our project partners Klüber Lubrication, Laualgun Bearings, Grupo Técnico Rivi and KIC InnoEnergy for supporting my work; especially Albert Pros Castellà, Haritz Maiz, Jorge Damián, Eduardo Vicente, Mikel Lasa and Antoni Martinez for their thoughtful advice and the ideas contributed.

My UPC colleagues Mercedes Jimenez, Eulalia Griful, Miguel Mudarra, Pep Simó, Roberto Castilla, José Marin, Esteve Codina for their advice during the project.

The members of the LTU mechanical elements department and fluid dynamics department, especially Jinxia Li, Henrik Lycksam, Torbjörn Green for their enthusiastic reception and for teaching me the µPIV technology.

The institution ETSEIAT and the staff of the UPC, LTU, Oficina de Patents i Llicències UPC, FundacióCIM BarcelonaTech, Klüber Lubrication GmbH Ibérica S. en C., Klüber Lubrication Munchen SE & Co. KG., Laualgun Bearings, S.A., Grupo Técnico Rivi S.L., KIC InnoEnergy S.E., ACC1Ó Generalitat de Catalunya, EADA Business school, Arco, Arquitectura de Comunicació S.A. including Xavier Tamarit, Ari-Pekka Holm, Victor Camargos, Sergio Benjumea, Rafael Marin, Montse Gelonch, Anna Monistrol, Ed Weenk, Libe Iruretagoiena, Jana Kim Koehler, Michele Maniglia, Alejandra Molina, Melisenda Murphy Solari, Nuria Marin.

My colleagues for interesting discussions, project feedback, and food for thought.

And last, but not least, all my family.

PART I: Summary

1. Introduction

Renewable energies and more specifically wind power generation have, in recent years, been a sector that has grown in market share with significant energy generation. In the wind sector, this growth has led to the design and implementation of machines with greater power generation capacities.

In order to design more efficient wind turbines, manufacturers are increasing the rotor diameter to capture more kinetic energy from the wind and **increase energy generation**; therefore the stresses and deformations are increasing in all parts of the wind turbine, such as the foundations, yaw, nacelle, tower and drive train unions. Most of these unions are static, except for: the drive train that transmits torque, the yaw system that turns the nacelle and the pitch system that turns the blade around its axis. During dynamic operation of the wind turbine, the yaw and pitch bearings suffer from sequential traction – compression stresses that cause millions of micro-movements per cycle between the gear teeth. Therefore the thickness of the lubricant between the teeth is reduced and direct contact between metal surfaces occurs. The wind turbine manufacturers observed a new phenomenon that appears in high power wind turbines: **excessive wear in the tooth located at 0º** in the pitch bearing as shown in Figure 2.9.

Currently, to slow this phenomenon the pitch gear lubrication at the zero degree position is carried out during unwind periods or programmed stops. These programmed stops cause **important losses in electricity generation** [1]. Moreover, the low efficiency of the current lubrication systems generates the need for a preventive maintenance plan to avoid the abrasive particles accelerating premature failure due to wear. For instance, in a 6 MW wind turbine, the preventive maintenance costs for the pitch and yaw gear per year can be estimated at around 5500 €/year and energy production loses in 3200 €/year as Casals-Terré [2] reports.

Reducing preventive maintenance and eliminating the corrective maintenance due to wear in the pitch and yaw gears is a **challenge** on which the wind turbine industry is currently focused to **maximize the reliability of offshore turbines**.

The forecast in the wind market states that high rotor dimensions in wind turbines will be in demand together with an increase in the expected life cycle of these machines. Gamesa [3] for example offers 30 years of operation. All these situations will worsen the wear in the gear teeth at the zero degree position.

The aim of this PhD thesis is to **reduce the wear** through a **novel lubrication system** based on an array of micro-fabricated channels fitted at the gears' root called **MiCRoLuBGeaR,** which improve the lubrication of the pitch and yaw gear systems of wind turbines. The solution

is expected to be compatible with and easily implemented into both newly designed and in-market models.

In chapter 2, a representative number of patented solutions will be reported and comparatively discussed. In chapter 3 the micro-manufacturing method to avoid the novel lubrication device is introduced and in chapter 4 the use of micro-channels in the lubrication field is introduced. Chapter 5 validates the proof of concept of the device and model and integrates the system in a real gear. Furthermore, the system is validated using FEM simulations and in a test bench under real loads.

2. Excessive wear in yaw and pitch gears

A wind turbine is an electric generator that obtains the power from the wind. There are two types of wind turbines depending on the position of its axis: vertical and horizontal. The following diagram shows the different parts of a horizontal-axis wind turbine:

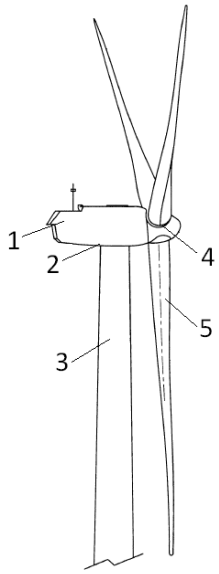

Figure 2.1: Wind turbine general view. 1- Nacelle, 2- Yaw system, 3- Tower, 4- Pitch system, 5- Blade

1. – Nacelle: part located at the top at the wind turbine that contains all generating components such as the generator, the gearbox, the drive train, the brake assembly.

2. – Yaw: the system that rotates the nacelle to position the blades in the optimal direction for the wind.

3. – Tower: part that provides the required elevation to the blades to perform in laminar wind flow.

4. – Pitch: the system that rotates the blades around their vertical axis to change their aerodynamic characteristics.

5. – Blade: the part of the wind turbine that transforms the kinetic energy of the wind into torque at the drive train.

The wind turbine blades (#5 in Figure 2.1) transform the kinetic energy of the wind into torque at the drive train. To regulate the changes in wind speed over time, the pitch system (#4 in Figure 2.1) moves each blade around its vertical axis, changing its aerodynamic

characteristics. The *blade leading edge* is the frontal part of the blade that first makes contact with the air-flow. The *blade trailing edge* as shown in Figure 2.2 is the rear part of the blade, where the air-flow finishes its contact with the blade. When the air-flow passes along a specific airfoil it causes a pressure difference at the blade, which is transmitted as torque to the drive train of the wind turbine.

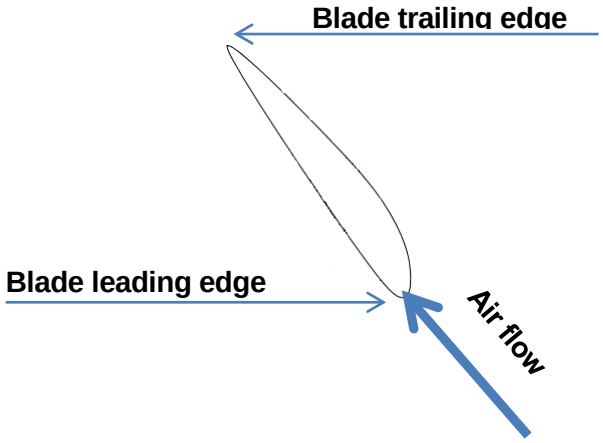

Figure 2.2: Airfoil

Gamesa Innovation [4] described the different pitch system types currently installed in wind turbines: pinion-crown, hydraulic and cogged belt systems. Manufacturers like General Electric [5] and Alstom [6] use the electric pitch system while Gamesa [3] and Acciona [7] install the hydraulic system. The pros and cons of each system were summarized by MOOG [8], manufacturer of pitch systems, and presented in Table 2.1.

Figure 2.3 shows the most important parts of the electric pitch with the pinion-crown system. They are the:

- Drive Motor: transforms the electric power into angular mechanical power.
- Gearbox: decreases the motor revolutions per minute to move the blade more slowly. The pinion gear performs the power transmission from the gearbox to the bearing.
- Blade bearing: allows the blade to rotate along its axis to change its aerodynamics.
- Blade: transforms the kinetic energy of the wind into mechanical angular power.
- Pitch control: controls the position of the blade.

When the pitch control receives the signal to actuate from the turbine control system as Figure 2.3 represents, it connects the drive motor, which through the gearbox, transmits an angular velocity to the blade bearing. Thus, the blades are rotated around their vertical axis, changing

their aerodynamic characteristics as shown in Figure 2.2. The pitch system actuates in each of the blades in the same way, as shown in Figure 2.4.

	Hydraulic	Electric
Design/composition	Consists of a hydraulic Power Unit (HPU) in the nacelle and three actuators with control valves and accumulators in the hub.	Includes three sets of motors/gears, drives, controllers, and energy storage units. Consists of from 3 to 8 switchgear cabinets depending on the functions assembled in each cabinet.
Strengths	High forces, no need for gears. No backlash. Fail-safe, powered by accumulator.	Low energy consumption. Quiet operation (no pump).
Weaknesses	Management of hydraulic fluid, possible oil leakage. High energy consumption as pump runs continuously. Repetitive maintenance including filtration and oil replacement. Fluid rotary union required. Accumulator pressure loss.	Maintenance of batteries. Backlash. Increased probability of failure due to higher number of components (energy storage unit, motor/gear, controller).
Cost	Initial cost lower: running cost higher due to higher maintenance cost.	Initial cost higher: running cost lower due to lower maintenance cost.
Maintenance	Cylinder seals need to be replaced every 7 to 10 years.	Largely maintenance free except battery change.
Working Environment	Noisy due to pump. Risk of oil leakage.	Little room for movement in hub.
Image	Highly reliable due to proven fail-safe functionality.	Environmentally friendly system.

Table 2.1: Comparison between hydraulic and electric pitch from MOOG [8]

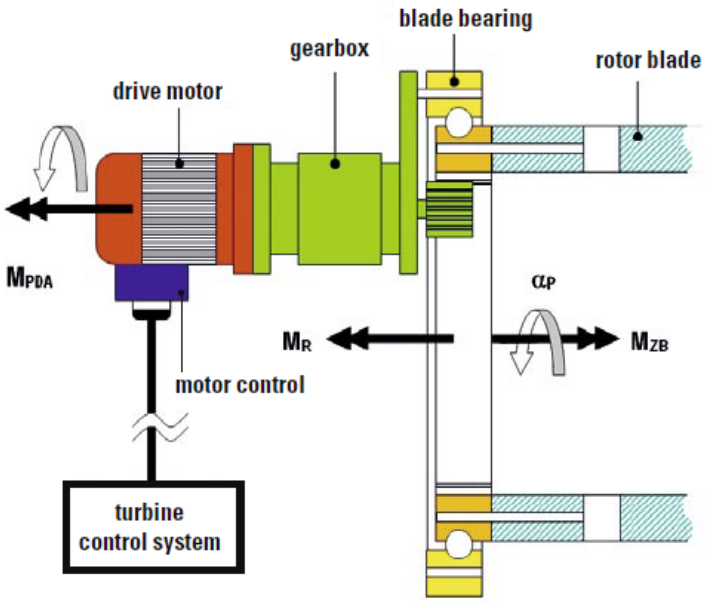

Figure 2.3: Generic gear pitch system and its main components by Manjock [9]

In case of electrical power supply failure; a system to move the wind turbine to a secure position is needed, with the blades in the idling position. For this purpose some pitch system designers, like MOOG [8], integrate an energy storage system to supply electricity to the pitch actuators in case of failure as shown in Figure 2.4.

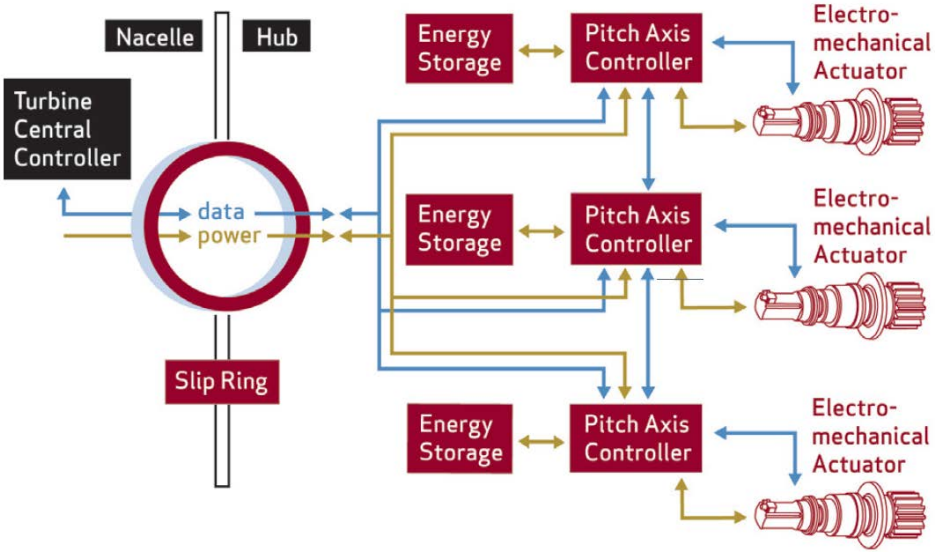

Figure 2.4: Pitch system schema by MOOG [8]

In wind turbines, the blade leading edge as shown in Figure 2.2 needs to be kept in the correct direction with respect to the wind in order to capture the maximum kinetic energy, according

to Wobben [10]. The yaw system (Figure 2.5), rotates the whole nacelle along its vertical axis according to the wind direction (#2 in Figure 2.1).

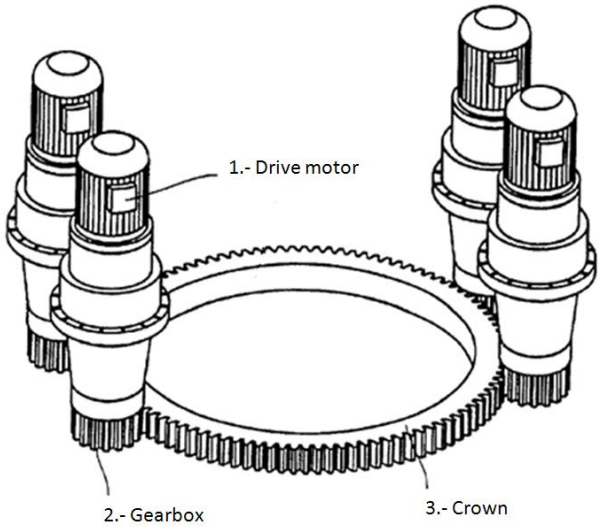

Figure 2.5: Schematic representation of a YAW system adapted from Wobben [9]

Figure 2.5 shows the most important parts of the yaw system of a pinion-crown wind turbine:

1.- Drive Motor: transforms the electric power into angular mechanical power.

2.- Gearbox: decreases the revolutions per minute of the motor to move the nacelle (#1 in Figure 2.1) slowly. The outside gear of the gearbox transmits the power between the gearbox and the top of the tower to the crown.

3.- Crown: the part assembled at the top of the tower to rotate the nacelle around its vertical axis.

When the control detects a change in the wind direction, it activates the drive motor (#1 in Figure 2.5) assembled in the nacelle, which transmits the angular velocity to the crown moving the nacelle around its vertical axis.

During the dynamic operation of the wind turbines, the pitch system bearing repeatedly suffers from sequential traction and consequently compression stresses. According to the blade coordinate system [11], the trailing edge of blade 1 is working under compression stress as shown in Figure 2.6 while traction stresses occur at the blade leading edge (Figure 2.2). Figure 2.6 shows blade 2 in the opposite situation as the blade has initiated the descent: the stress direction affecting each edge of the blade has been interchanged. This cycle is repeated with every revolution causing millions of micro-movements per cycle. Similarly, the yaw system is affected by the same stress cycle but in this case, caused by the different wind thrusts and slight changes in wind direction. Furthermore, the pitch system changes the blade's

aerodynamic characteristics through the pitch angle to adapt the instantaneous wind speed to the power that can be generated. The power generation at low wind speeds is between 60% and 70% of the operating time, which implies that for long periods of time the pitch system remains operating at the same position as shown in Figure 2.7, the position known as the 0 degree position.

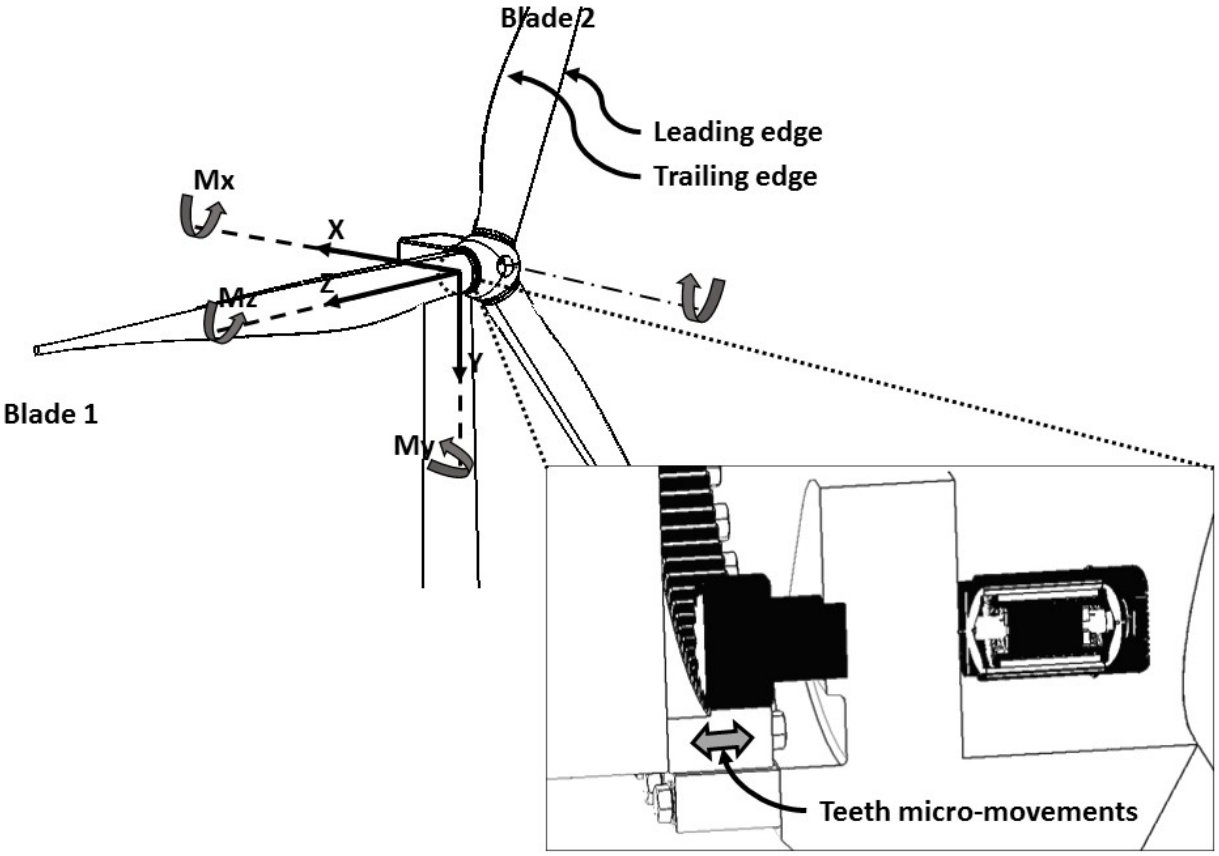

Figure 2.6: Wind Turbine with blade coordinate system. From Germanischer Lloyd Industrial Services GmbH [11]

The traction-compression stresses produce micro-movements due to the gearbox backlash and the elastic deformations that eject the grease layer until the metal between the working teeth starts to come into contact. This phenomenon together with long periods operating the pitch in the same position produces friction between the teeth at the 0º position due to the absence of the grease layer. Wear appears as a change in the tooth's surface involving the removal or displacement of material as defined in ANSI/AGMA 1010-E95 [12]. Wear can be categorized as mild, view Figure 2.8A, moderate, view Figure 2.8B, or severe. Mild wear is considered normal in many applications and moderate may be acceptable in some applications.

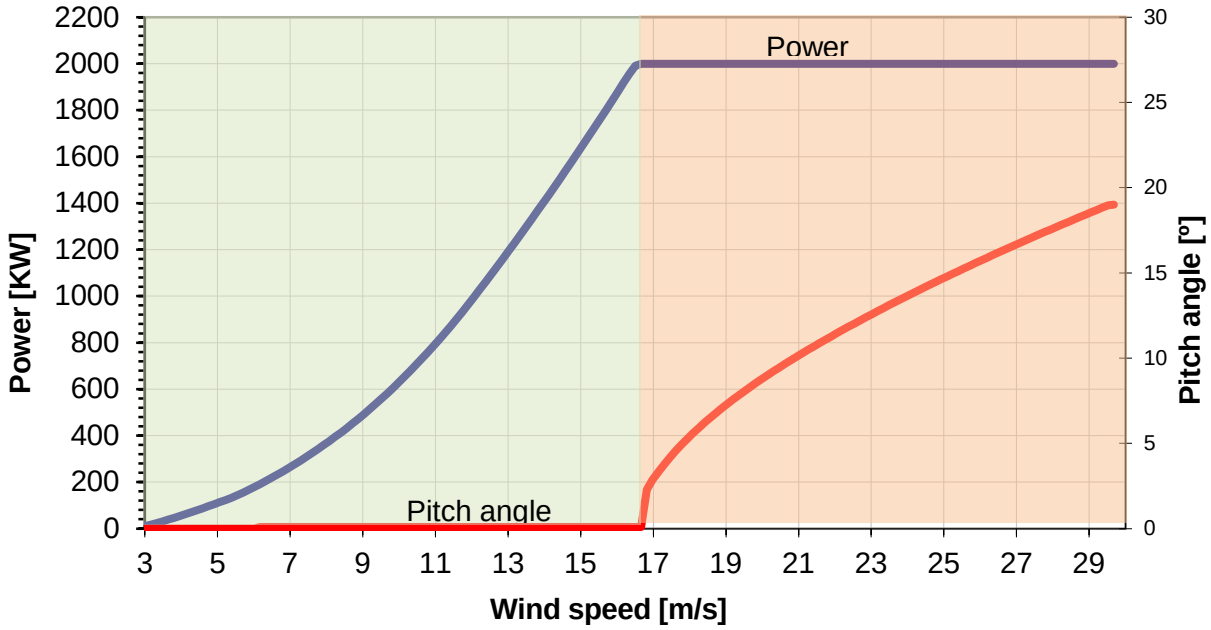

Figure 2.7: Example graph for a 2 MW wind turbine

According to ANSI/AGMA 1010-E95 [12], the wear is acceptable in recently produced gears which may show slight surface imperfections which are eliminated through wear when working in the optimum position. Mild wear is beneficial because it increases the contact region and makes the pressure on the surface of the gear uniform. Moderate wear, as defined in the standard ANSI/AGMA 1010-E95 [12] Figure 2.8B, is also acceptable, since it could allow the machine to achieve its expected life of 20 years. However, if we observe a real picture of a high-power wind turbine gear, the phenomenon of excessive wear can be seen clearly, as shown in Figure 2.9, which would make it impossible to complete the expected life cycle. Furthermore, the tooth wear produces micro-iron particles that contaminate the lubricant and speed up the wear process and the oxidation of the surfaces. These micro-iron particles are retained in the contact region and their abrasive action adds to the rate of surface deterioration as shown in Figure 2.9. This type of corrosion is called fritting corrosion as ISO 10825 [13] reports.

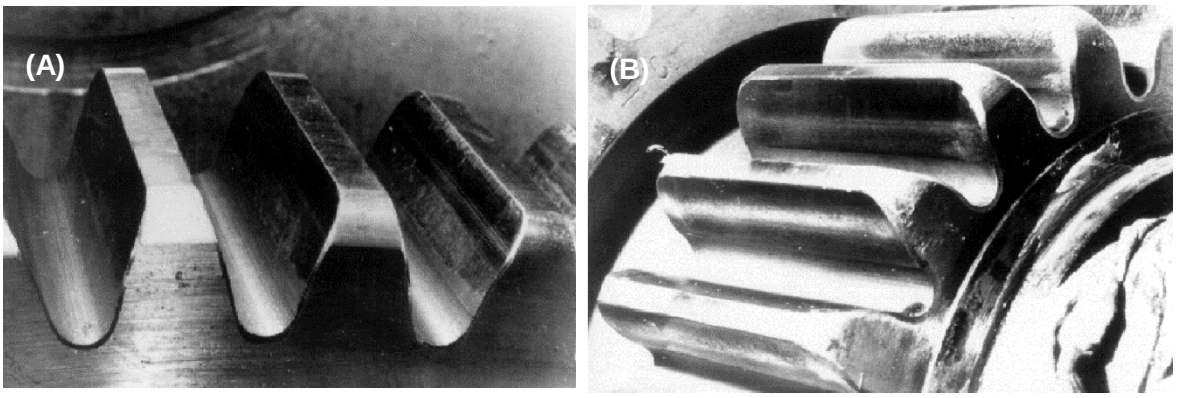

Figure 2.8: (A) Mild Wear and (B) Moderate Wear from ANSI/AGMA 1010-E95 [12]

The state of the art remarks that the problem of excessive wear is still not taken into account because the phenomenon only started to emerge in high-power wind turbines and with long operation times. Nevertheless, it is an issue that is expected to grow in coming years, when the reliability of the systems will predictably decrease.

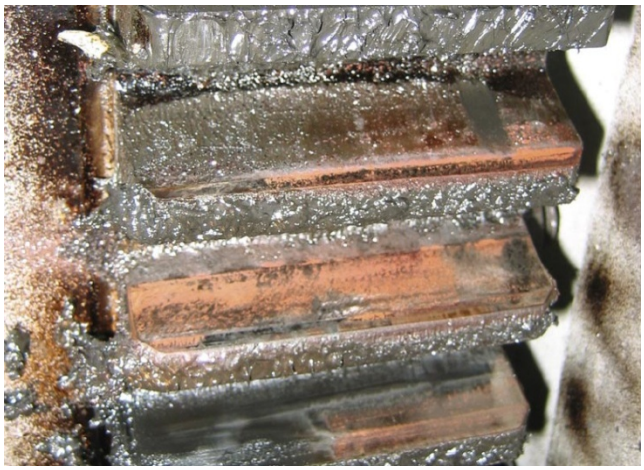

Figure 2.9: Excessive wear in the tooth by Andreas [9]

According to Takadoum [14], eliminating wear is not likely to be achieved, even though the author mentions some parameters that are important to minimize wear:

- Surface state: property related to the material's composition and surface, hardness, residual stress and surface energy.
- Stress in the system: property inherent in the power of the transmission that will condition the expected life.
- Mechanical contact: property related to the geometry and the contact area. Study of the pressure distribution on and below the surface.
- Tribology of the system: property related to the lubricant's characteristics, implementation, periodicity and distribution.

Much effort has been made within the research community to improve all these parameters to minimize the effect of gear wear, except for the stress since it is inherent in the system design.

2.1. Approaches to overcome excessive wear

The excessive wear of the yaw and pitch gears is a central issue in the field. Some of the reported attempts to tackle the problem are set out and discussed below. Therefore, major wind turbine manufacturers have already patented solutions and strategies to monitor, minimize and control the effect of gear wear although the solutions patented are not particularly effective and the main solutions led to energy generation losses.

The proposed solutions essentially tune and modify the system parameters that Takadoum [14] defined as critical to minimize the effects of wear. Mashue [15] proposed changing the **surface state**, see 2.1.1, by setting new on-duty conditions never used before: decreasing the hardness of the pinion compared to that of the crown. Klaus [16] suggested changing the **tribology,** see 2.1.5, of the system by adding special holes to the pinion and the crown through which fresh lubrication could be injected directly to the gear contact surface. Nielsen [17] modified the **mechanical contact,** see 2.1.2, by assembling two pinions to transmit the same torque in order to decrease the pressure at the contact surface.

On other hand, other studies have implemented solutions to repair and control the affected tooth in situ. For instance, Dimascio et al. [18] patented a solution to replace the damaged region of the gears in situ with a new bolt-assembled tooth, see 2.1.1. Mashue et al. [19] patented a method to measure the excessive tooth wear to predict when the failure will occur, see 2.1.3, and Gamesa Innovation [4], see 2.1.4, redesigned a new electric pitch system.

2.1.1. Modification of the surface state conditions

The design concept of the pitch and yaw system is similar to the rack wheel. In the rack wheel, the hardness of the pinion is higher than the hardness of the rack, because the pinion has less teeth and the working time per tooth is higher than that of the wheel. In the design of the ring gear of the pinion in wind turbines, the ring gear is not as hard as the pinion, like the concept of the rack wheel, because the work per tooth in the pinion is higher than in the wheel.

Mashue et al. [15] changed the hardness of both parts, inducing wear in the pinion, and therefore introducing the need to replace the pinion when the wear was excessive. The advantage of this change is that it is the pinion that suffers the excessive wear, which is easier than the bearing to change. Even so, replacing the pinion during maintenance is an expensive and difficult operation. To facilitate maintenance operations Dimascio et al. [18] designed an interchangeable part for the teeth in the bearing, see Figure 2.10. The flank of the tooth is fixed to the bearing with special bolts. This system makes it possible to replace the portion of the ring gear with excessive wear.

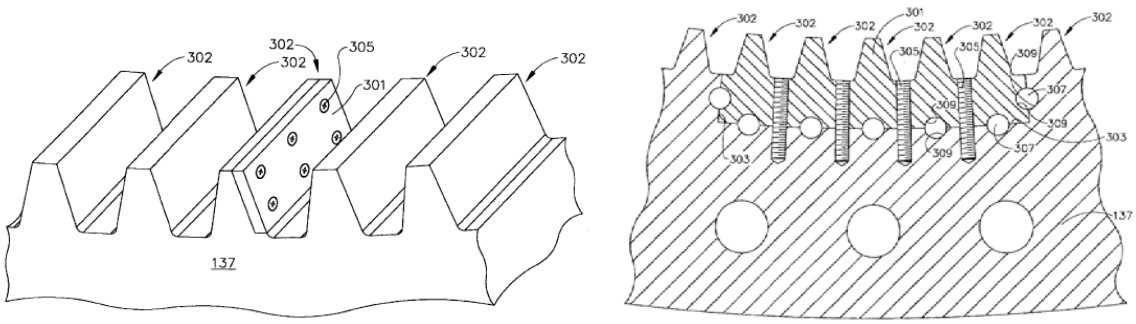

Figure 2.10: Schematics of a reinforcement of the tooth in the bearing gear from Dimascio et al. [18]

2.1.2. Modification of the mechanical contact conditions

Another important factor is the number of teeth in contact at the same time, which increases the surface in contact, and therefore decreases the surface pressure per tooth. Nielsen [17], assembled three gears, one to transmit the power (#4 in Figure 2.11), and the other two (#5 in Figure 2.11) to be in contact with the bearings decreasing the stress per tooth.

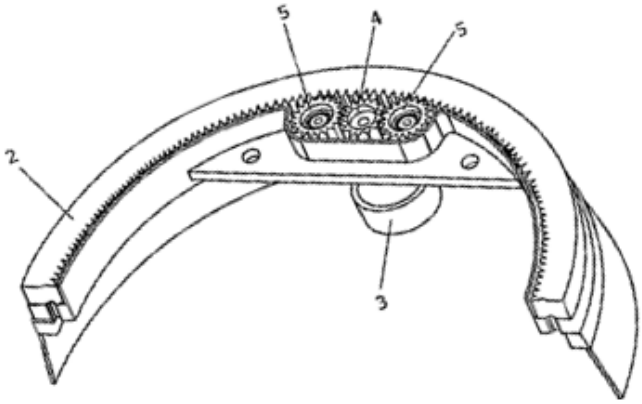

Figure 2.11: Mechanism to decrease the stress on the tooth by Nielsen [17]

2.1.3. Mechanisms to monitor the wear

The previous systems changed some design characteristic mentioned by Takadoum [14]. Another approach is to develop a system to evaluate excessive wear and set-up an accurate maintenance plan. This approach has been used by several research groups or companies such as Mashue et al. [19], who implemented a system to mark the surface of the tooth. These marks can be easily checked and make it possible to determine when to repair the gear system, as seen in Figure 2.12.

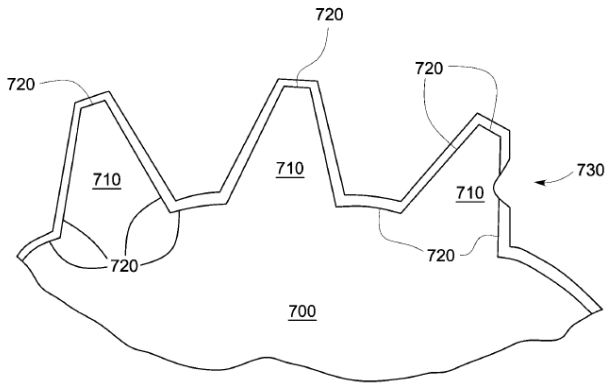

Figure 2.12: Surface marks, at right the wear lead the limit from Mashue et al.[19]

On the other hand, Nordex Energy [20] designed a tool to measure the excessive wear in the tooth. Figure 2.13 shows the system and the system placed along the tooth. Using this tool it

is possible to determine the affectation of the problem, and therefore, to measure the wear at the tooth and predict the time to repair the gear system.

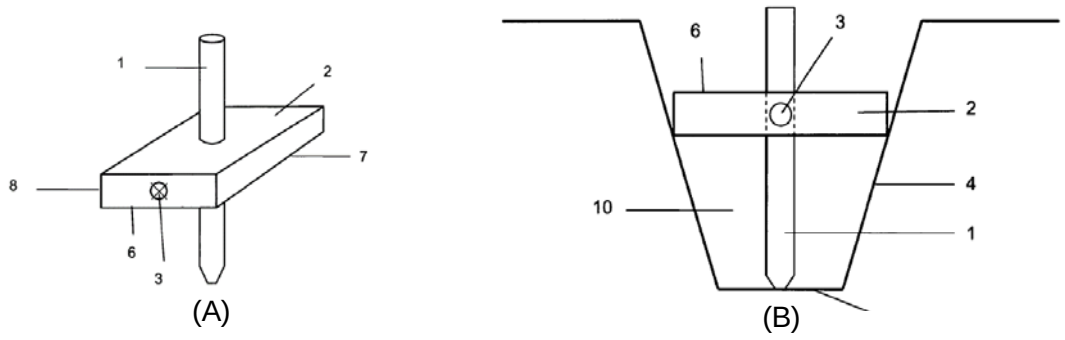

Figure 2.13: (A) Tool to measure excessive wear, (B) Detail of the tool when measuring from Nordex Energy [20]

2.1.4. Changing the pitch system

Gamesa Innovation [4] defined three different pitch systems installed: pinion-crown (the system to improve the lubrication), the hydraulic system [21] shown Figure 2.14 and the cogged belt (similar to the pinion-crown). Gamesa Innovation [4] makes a combination of these three systems and has installed a new electric design, as shown in Figure 2.15. Table 2.1 compares the pinion-crown system with the hydraulic system, the most commonly used technologies. General Electric [5] and Alstom [6] are two companies that are still using electric pitch while Gamesa [3] and Acciona [7] are examples of companies using a hydraulic system.

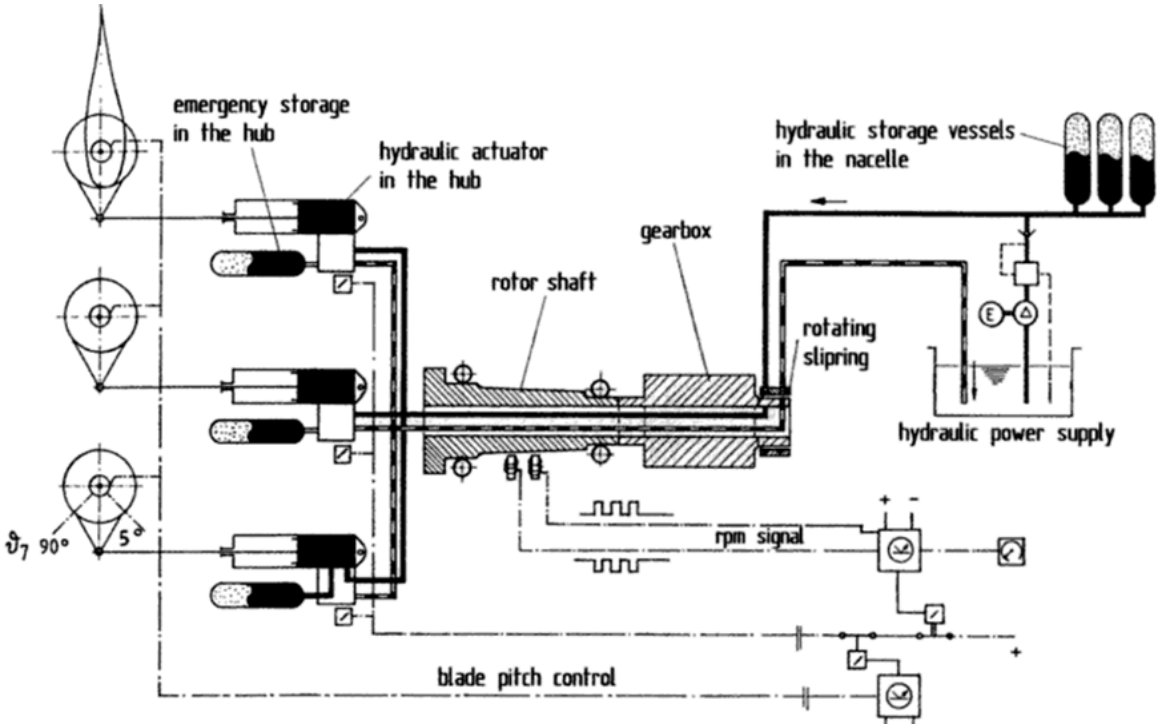

Figure 2.14: Diagram of hydraulic pitch by Hau [21]

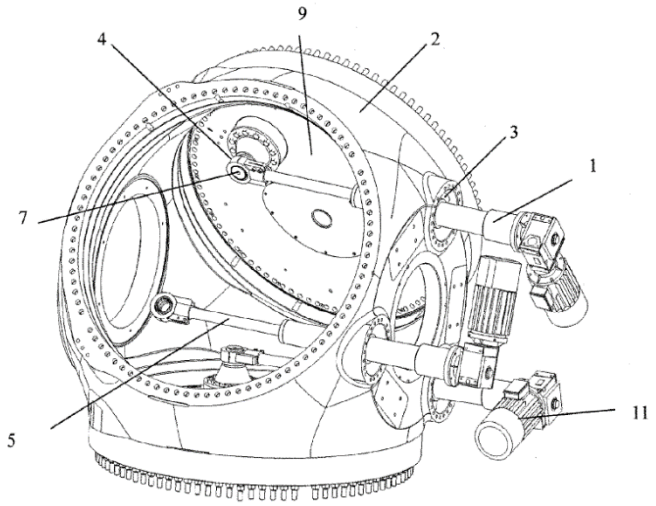

Figure 2.15: New pitch system design from Gamesa Innovation [4]

2.1.5. Modifying the tribology conditions

Some researchers have devoted their efforts to minimizing wear by changing the lubrication system to increase the lubrication layer reduced during the micro-motions. Klaus [16] designed a new shaft of the gear to inject lubricant in the center of the tooth. Figure 2.16A shows a detailed drawing were the pipe (mark #7) injects the lubricant through the hole positioned at the root of the tooth.

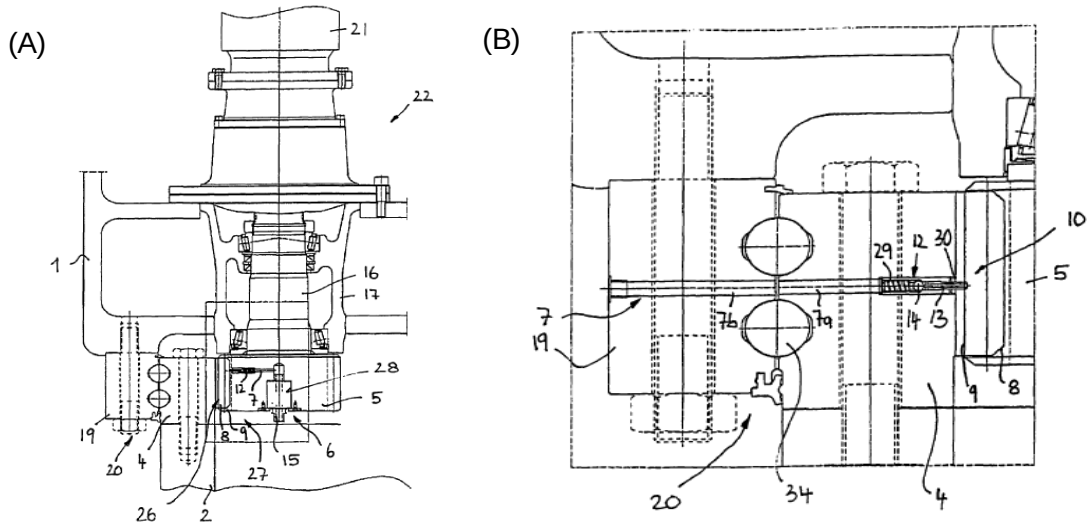

Figure 2.16: Lubricator injector. (A) Injection in the gear. (B) Injector in the bearing by Klaus [16]

Along the same lines, Kürzdörfer [22] designed a special injector that sprays one side of the tooth to lubricate the joint directly, see Figure 2.17.

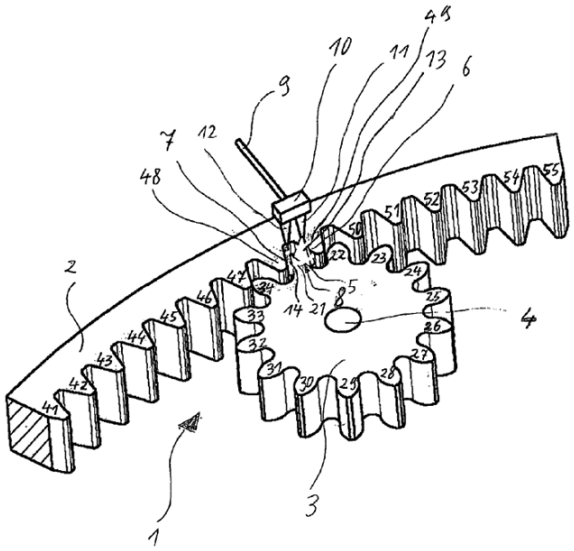

Figure 2.17: Special lubricant injector from Kürzdörfer [22] to spray one side of the tooth directly with lubricant

Another solution to prevent damage to the roller of the pitch and yaw bearings was proposed by Harris [23] and consists of rotating the bearing to move the rollers and refresh the lubrication with this movement. Valero [24] proposed reducing the micro-motions in order to maintain the lubrication layer. To this end, the authors designed a mechanical brake of the pitch gearbox as shown in Figure 2.18 with a pin (reference #300) that mechanically blocks the movement. Stromag [25] installed an electric brake between the drive motor and the gear, see Figure 2.19. The brake disk joined to the bearing (reference #14) is locked by the caliper (reference #15) fixed to the nacelle. Both systems increase the retention power of the pitch bearing and try to minimize its micro-movements.

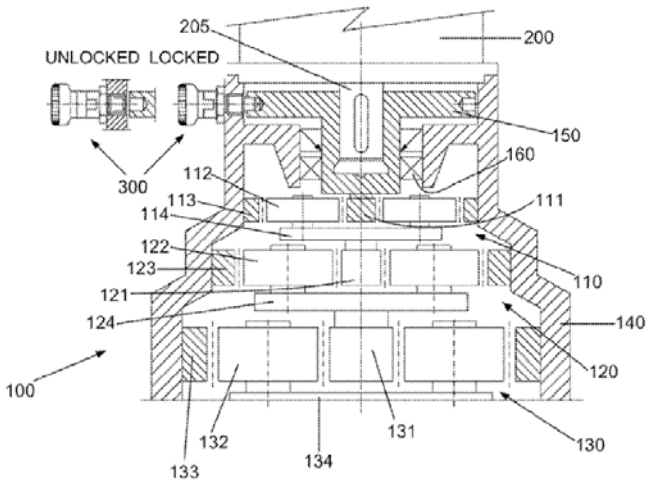

Figure 2.18: Mechanical brake by Valero [24]

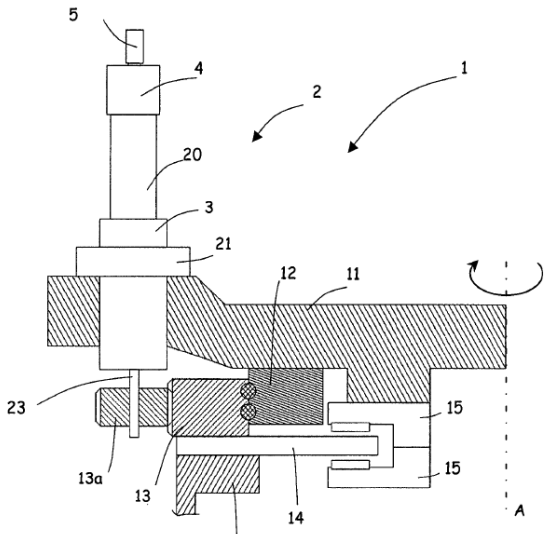

Figure 2.19: Electrical brake by Stromag [25]

This PhD research proposes a decrease in the wear of the teeth by increasing the lubrication layer at the contact tooth flank with a novel lubrication system that injects fresh lubricant directly to the contact tooth flank as presented in the appended PUBLICATION A. Figure 2.20A shows a cross section of a tooth that has a novel injector installed to inject fresh grease directly to the contact tooth flank. Figure 2.20B is a 3D view with the gear transparent to show the concept of the proposed grease injection. In order to develop this new concept of injector, micro-fluidics technology and the micro-manufacturing technology are used. Chapter 3 introduces a novel methodology developed to manufacture micro-channels to test the grease fluency under micron range. Chapter 4 validates the grease fluency performance under the micro-channels manufactured in the previous chapter using micro Particle Image Velocimetry (µPIV) technology.

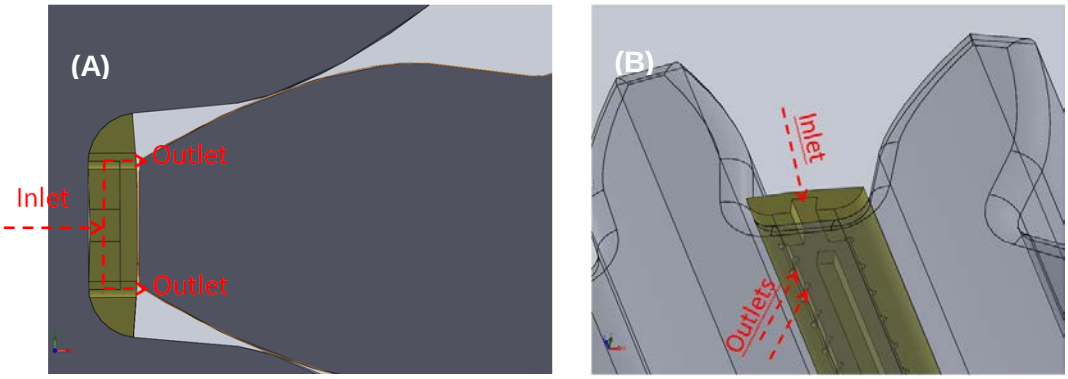

Figure 2.20: MiCRoLuBGeaR concept to integrate in the gear dedendum position. (A) cross section at the injection point and (B) 3D animation view with the gear transparent

3. Manufacturing method for micro-channels

The tendency of the new technologies to make structures smaller led researchers to develop new technologies such as Rebeca et al. [26] and Brittain et al. [27] who report that micro-technology is a new science to make smaller functional machines. The goal of this PhD thesis is to take advantage of the possibilities that micro-fabrication offers to integrate a novel distributed lubrication system into the yaw and pitch gears. There are few publications where micro-manufacturing technology has been applied in the field of tribology. Srinidhi [28] used them to detect and count metal wear particles in lubrication oil while Du [29] used a similar device with a coil to detect the metal wear particles, see Figure 3.1.

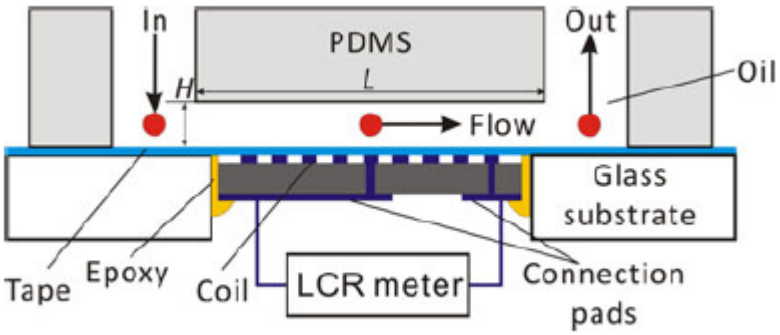

Figure 3.1: Schematic of the microfluidic device for metal particle detection in lubrication oil. Channel dimensions 250 µm(H) x 500 µm(W) x 3500 µm(L) by Du [29]

3.1. Novel micro-fabrication technique to study grease flow using µPIV

Soft lithography is the standard technique used to manufacture micro-channels, mostly in Polydimetyl siloxane (PDMS). It is widely used because micro-channels can be produced quickly and cheaply, although the low hardness of the polymer leads to significant elastic deformations if the channels are working under pressure.

The grease pressure fluency depends on its viscosity – the higher the viscosity, the more the fluency pressure increases. The greases used in open gears, like those present in pitch and yaw gears, have a high viscosity, since this property allows the grease to remain in the position where it is injected, in this case in the tooth flank.

Hence, the grease properties used in pitch and yaw gears cause a significant pressure loss when flowing in micron-sized channels, therefore the use of soft lithography to produce PDMS channels was ruled out. Other methodologies are available to produce micro-channels such as RIE or Electric Discharge Machining (EDM). RIE is normally used for brittle materials (silicon or glass). EDM has been shown to work on channels down to 500 µm [30], but the main problem is the grease leakages through the joint of the plates and the micro-channel size limit. The limitations of the previous technologies in achieving micro-channels that could withstand high pressures motivate the development of a new micro-channel manufacturing method to study the grease flow. The main characteristics of this manufacturing method are to operate under high pressures and to be used in µPIV tests. The proposed manufacturing method uses the 3D printing technology and it can manufacture the micro-channels and the grease connections as one part, preventing leakage. After cleaning the printed part, an ultra violet curing glue is used to assemble a transparent slide on the micro-channel to visualize the flow using µPIV technology. In appended PUBLICATION B this manufacturing method is detailed.

4. Lubrication using micro-channels

In the teeth in contact in a transmission gear two phenomena occur: rolling and slip. The friction between the two surfaces is caused by the slip phenomenon. Figure 4.1 represents the friction force F_R, the pressure of the gear is F_N and F_A indicates the slip direction. The friction coefficient μ is defined as F_R/F_N and prevents movements and generates energy loses.

Lubricant in gear systems produces a layer between both surfaces to prevent the metal-metal contact and to reduce the friction coefficient μ.

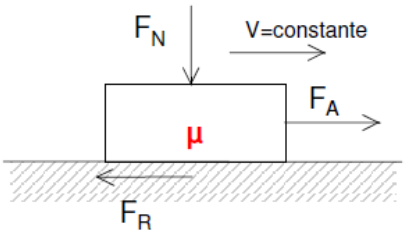

Figure 4.1: Friction forces slip phenomena

Besides the reduction of friction coefficient μ, the lubrication of the gear system:

- Reduces the wear in the systems.
- Reduces friction and increases the efficiency of the system.
- Prevents corrosion in the system.
- Improves the dissipation of the temperature.
- Eliminates the particles.
- Increases the reliability and the life of the systems.

The lubricant to reduce the friction coefficient comprises from refined straight mineral oils to complex blends of fatty oils and synthetic products as ISO 12925 [31] reports. The lubricant viscosity and the special additives vary depending on the type of application as stated in ISO 12925 [31]. The base oil may come from different sources. Table 4.1 shows a comparison of base oils reported by SKF [32]. Another important parameter is the time the oil is expected to maintain its conditions. Figure 4.2 shows the expected time versus the operation temperature for different oils reported by Klüber [33].

Oil property	Mineral	Poli-Alfa-Olefinas (PAO)	Poliglicol
Variation in viscosity versus temperature	8	4	10
Characteristics at low temperature	0	10	4
Wear protection	8	4	10
Friction coefficient	8	4	10
Pitting protection	10	10	10
Neutrality polymer	10	10	0

Table 4.1: Base oil characteristics adapted from SKF [32]. Scale from 0 to 10 where 10 is the best grading

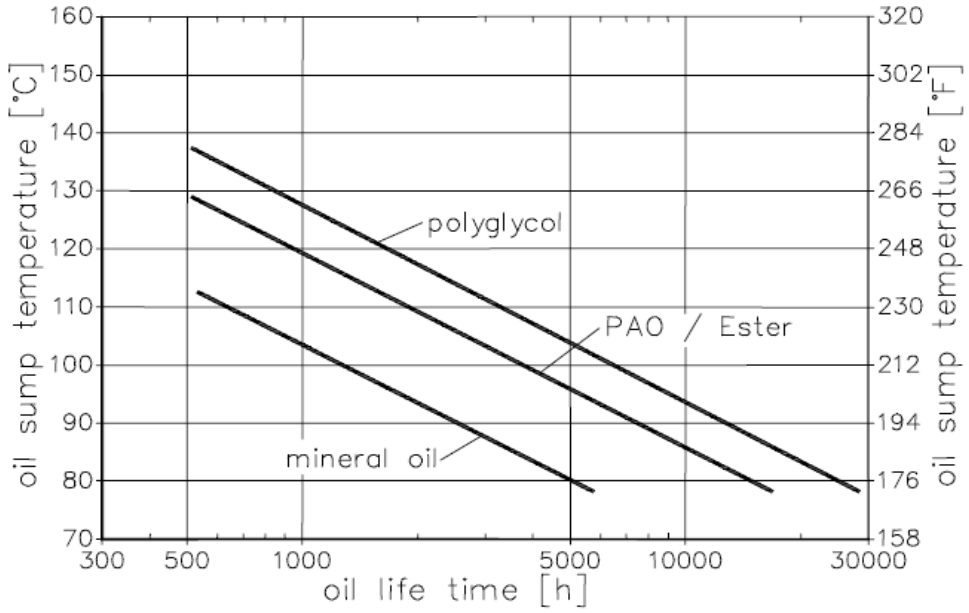

Figure 4.2: Graph of oil life versus operating temperature by Klüber [33]

Another important property that depends on the application is the grease viscosity grades. To obtain grease lubricant with a high viscosity, another component is added to the additives and oil base, a thickening agent, see Table 4.2. This combination of products makes a solid or semifluid texture by the dispersion of a thickening agent in a lubricant liquid as SKF [32] reports.

Thickening agent	Maximum work temperature	Water resistance	Adherence
Calcium	150ºC	Yes	NO
Lithium	150ºC	Yes	Yes
Aluminum	160ºC	No	Yes
Barium	150ºC	Yes	Yes
Sodium	160-180ºC	Less to 90ºC	Yes

Table 4.2: Lubrication thickening agent by Klüber [33]

The thickening agent gives the grease its consistency. Depending on the consistency, the grease is classified using the NLGI grades as Ehrlich [34] reports. NLGI grade 2 is the grease with the highest consistency, and is thus the most non-Newtonian. On the other hand, NLGI grade 00 is the grease with the lowest consistency, thus it is the most Newtonian fluid. The most used greases in the pitch and yaw gears are grade 2 greases or, in extremely cold conditions, NLGI grade 1.

The effects of the grease flow through a micron sized channel had not been reported until now, the closest state of art is the use of micro-technology to manufacture devices to detect and count metal wear particles in lubrication oil by Srinidhi [28] or Du [29]. Therefore, an important milestone in the validation is the high-consistency grease flow through the micro-channels manufactured with the methodology presented in PUBLICATION B, to understand the behavior of the grease, the results of which are presented in PUBLICATION C. The grease fluency is visualized using micro particle image velocimetry (µPIV) technology. The fluency experimental tests show how the channel dimension and the NLGI grease grade affect the slip phenomenon.

5. Results and discussion

When describing the approaches to overcoming excessive wear in the gear tooth, researchers changed the parameters of on-duty conditions following Takadoum's [14] recommendations. This research has focused on the improvement of the lubrication yaw and pitch gears with a novel system to distribute the lubricant along the tooth manufactured taking advantage of micro-fabrication processes as is introduced at point 3. Up to now, no research has applied micro-channel technology to contribute to the improvement of excessive wear in the tooth, as Douglas et al. [35] reports, the new micro-fabrication methods open up new capabilities to research.

5.1. MiCRoLuBGeaR proof of concept

5.1.1. Geometric adaption in the gear dedendum dimensions

Takadoum [14] mentions the tribology of the system as one of the crucial parameters that greatly affects excessive wear. In order to improve the tribology in wind turbine gears, before the verification in Publication C, the assembly of pinion and crown gears with typical dimensions of pitch or yaw gears were carefully analyzed to obtain the volume available to allocate a set of micro-channels that could provide fresh grease directly to the gear tooth flank even when the wind turbine is working. The characteristic parameters of the pinion and the crown are summarized in Table 5.1.

	Module [m]	Number of teeth [z]	Pressure angle [α]	Width of the tooth
Pinion	12	15	20	115 mm
Crown	12	164	20	100 mm

Table 5.1: Pinion and crown gear design parameters

Notice that the Module [m] used in Table 5.1 is similar to the one used in 2MW wind turbines pitch and yaw application systems.

Given the characteristic parameters of Table 5.1 according to Gibert [36] the corresponding gear dimensions are calculated and summarized in Table 5.2. To draw the gear, an involute has been used in Eq. 1 and Eq. 2.

	Ø outside [de]	Ø pitch [dp]	Ø base [db]	Ø internal [di]	Arc pitch [p]
Pinion	204mmm	180mm	169.145mm	150mm	37.699mm
Crown	1944 mm	1968mm	1849.315mm	1998 mm	37.699mm

Table 5.2: Gear dimensions

$$x(t) = \frac{db}{2} \cdot [\cos(\pi \cdot t) + \pi \cdot t \cdot \sin(\pi \cdot t)] \quad (1)$$

$$y(t) = \frac{db}{2} \cdot [\sin(\pi \cdot t) - \pi \cdot t \cdot \cos(\pi \cdot t)], \quad (2)$$

where $0 \leq t \leq 1$ and *db* is the base diameter.

The pinion and crown are modeled with Solid Works 2012 with the parameters obtained in Table 5.2. Figure 5.1 shows the assembly of the pinion on the crown ready to transmit power.

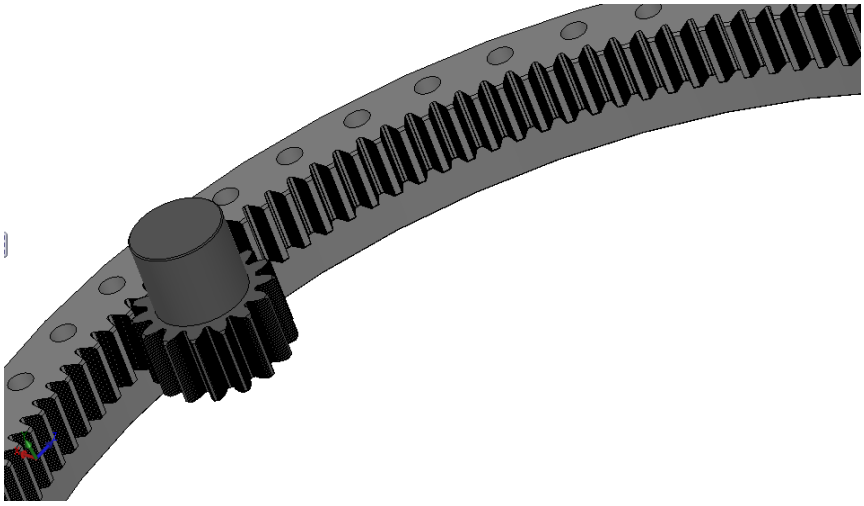

Figure 5.1: Pinion and crown 3D model

According to Gibert [36] and Carreras [37] and also appreciable in Figure 5.1, a gap is formed at the root of the tooth. The minimum value of this gap is in function of the module of the tooth, and DIN 867 [38] defines it as 0.3 times the module [m]. In our model, the value of the gap at the root of the tooth is 3.6 mm in height, see dimension B in Figure 5.2. According to Carreras

[37] at this point the tensions decrease because of the corner cut, eliminating in this way the impact noise against the tooth and absorbing the elastic deformation. Yaw and pitch systems work at a low angular velocity and therefore the impact noise is not relevant. However, the elastic deformation caused by the high loads greatly affects the system.

The goal of this research is to take advantage of the gap volume, see Figure 5.2, to allocate a set of micro-channels (MiCRoLuBGeaR) to supply fresh grease to the tooth root. They will be fabricated and validated using the technology described in PUBLICATION B. In Figure 5.2 the proposed part called MiCRoLuBGeaR with the distributed lubrication system is shown positioned at the root of the tooth in a volume that for the dimensions of Table 5.2 are A=13.4 mm and B=3.6 mm, see Figure 5.2.

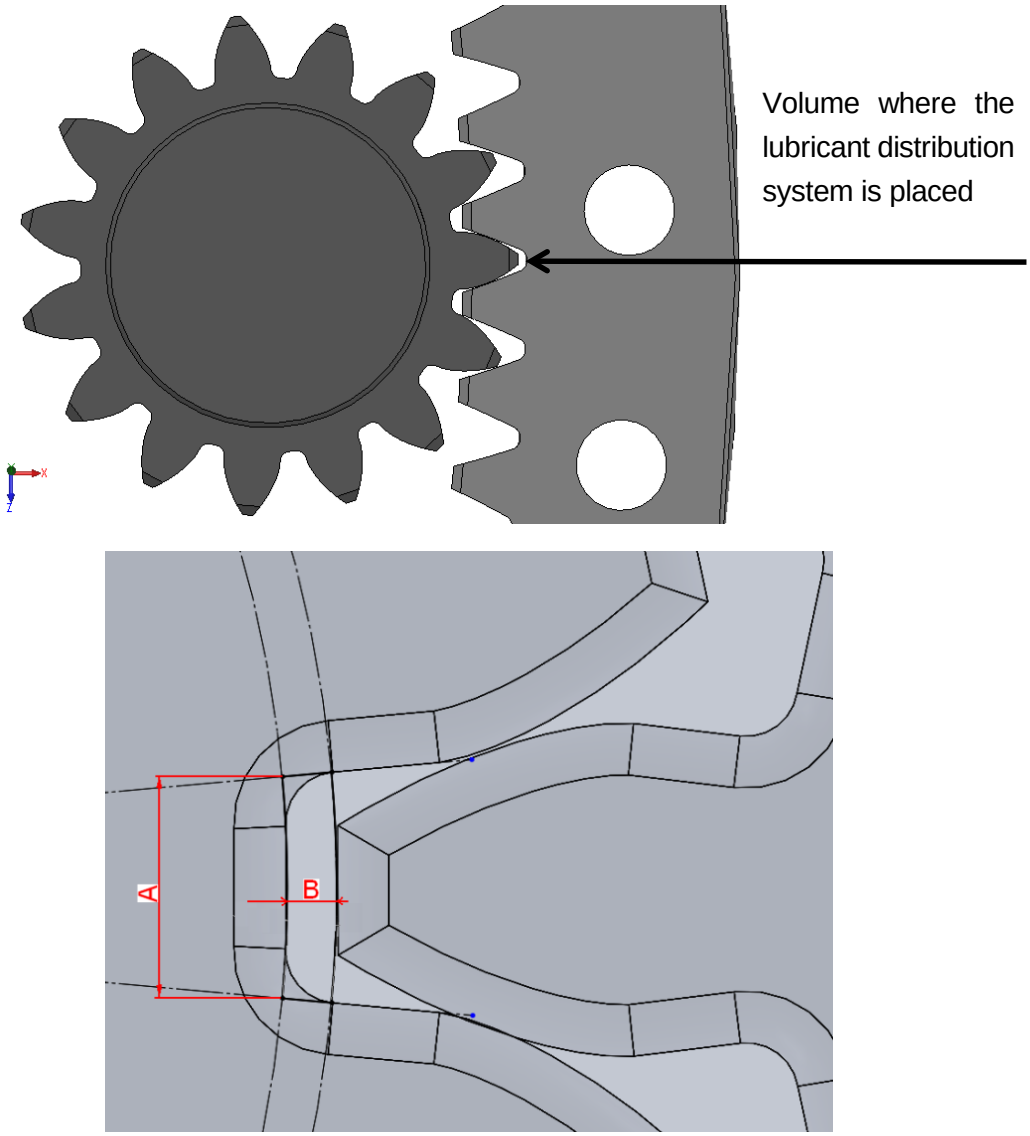

Figure 5.2: View of the available tooth root volume (AxB), where the MiCRoLuBGeaR is positioned

5.1.2. Lubrication flow test

Control the friction and reduce the wear and increase the lifetime and the reliability of the mechanical systems is the aim of the tribology as Takadoum [14] reports. The selection of the correct lubricant depends on different parameters such as the gear type, loads, speed, operating temperatures, input power and reduction ratio. The common feature of the greases used in the pitch and yaw gears is its high consistency, whereas depending on the operation temperature, NLGI grade 1 is used for cold climate conditions while NLGI grade 2 is used for warmer conditions.

The grease flow through micron-sized channels has not been reported until now, so the physical and chemical conditions of the grease after flowing in this kind of channels have been verified. For instance, the grease was checked to see if there were any physical changes such as the separation of the base oil and the thickening agent or chemical changes, such as losing the design properties, additives and components after flowing through a micron-sized channel as DIN 51817 [42] reports. To verify that the grease flows and maintains its physical and chemical characteristics when flowing along a micron-sized channel, a straight pipe from Idex [43], model 1502 with a diameter of 0.03 inches, see Figure 5.3, was chosen and a pump model “Graseby 3200 syringe Pump” was used to induce the flow.

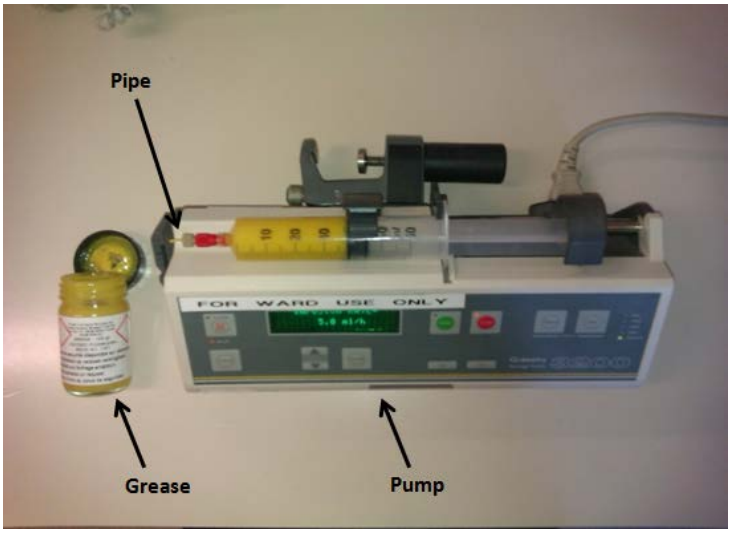

Figure 5.3: Experimental set-up to verify the grease flow in a 20 mm length pipe with a diameter of 0.03 inches

First, NLGI grade 1 greases such as Klüberplex BEM 41-141 were tested due to their lower residence to flow. The grease was forced to flow through the channel and was then analyzed using an infrared spectrum analysis and a consistency analysis to verify that the grease had not suffered any degradation. The infrared spectrum can determine all compounds in the

mixture to be analyzed recording the absorption curve for each hydrocarbon, superimposed on the radiant energy background as Heigl et al. [44] reports. The infrared spectrum results showed a full coincidence of the peaks, therefore from the analysis of the samples, we assumed that there were no chemical changes and that there were no traces of component losses or degradation.

The consistency analysis was used to verify the fact that the grease sample had not suffered the separation of the base oil and the thickening agent. This test was done using the cone penetration test under the ASTM D1403-02 [45]. The test standard defines two procedures for measuring the consistency of small samples of lubricating greases by penetration with a ¼ scale cone or a ½ scale cone. Using ¼ scale cone and cycling machine at "60 full double strokes of the plunger, completed in 1 min ± 5 s" as defined in ASTM D1403-02 [45] the penetration of the samples was quantified as $\mu = 83.05$ mm with and standard deviation of $\sigma = 0.339$. To compare these measurements with the design parameters of Klüberplex BEM 41-141 by Klüber [33], which have a penetration range of 310-340 mm in full-scale penetration, it is necessary convert the results to full-scale penetration using Eq. 3 from ASTM D1403-02 [45].

$$P = 3.75p + 24, \tag{3}$$

where

P is the cone penetration by Test Methods D217
p is the cone penetration by ¼ scale equipment

The average cone penetration measurements in full-scale penetration was $\mu = 335.87$mm and $\sigma = 0.12$, values within the design parameters of Klüberplex BEM 41-141.The standard deviation of the results is small, therefore the test is repetitive and it confirms that the grease does not suffer any physical changes, or the separation of the base oil and the thickening agent, the milled condition of the base oil compared to the thickening agent are in the original concentration and consequently the dynamic viscosity is maintained.

The analysis of the results from both tests, the infrared spectrum and the cone penetration, conclude that the grease Klüberplex BEM 41-141 does not suffer any changes in its chemical or physical structure when flowing through micro-channels. Therefore a preliminary design of a 3D model of the proposed micro-manufactured part to flow grease at the root of the tooth flank was developed and it is presented in Figure 5.4.

PUBLICATION C extends the flow grease study through micro-channels with different NLGI grease grades using micro particle image velocimetry (µPIV) technology.

5.2. 3D modeling and integration

A system was designed to inject fresh lubricant at the tooth flank with the dimensions shown in Figure 5.2 to be assembled in the crown shown in Figure 5.1. The dimensions of the gear were defined in point 5.1 and the pipe dimensions in point 5.1.2.

Figure 5.6 shows a preliminarily design of the MiCRoLuBGeaR that can be assembled in the gear root and allows the tooth flank to be lubricated directly.

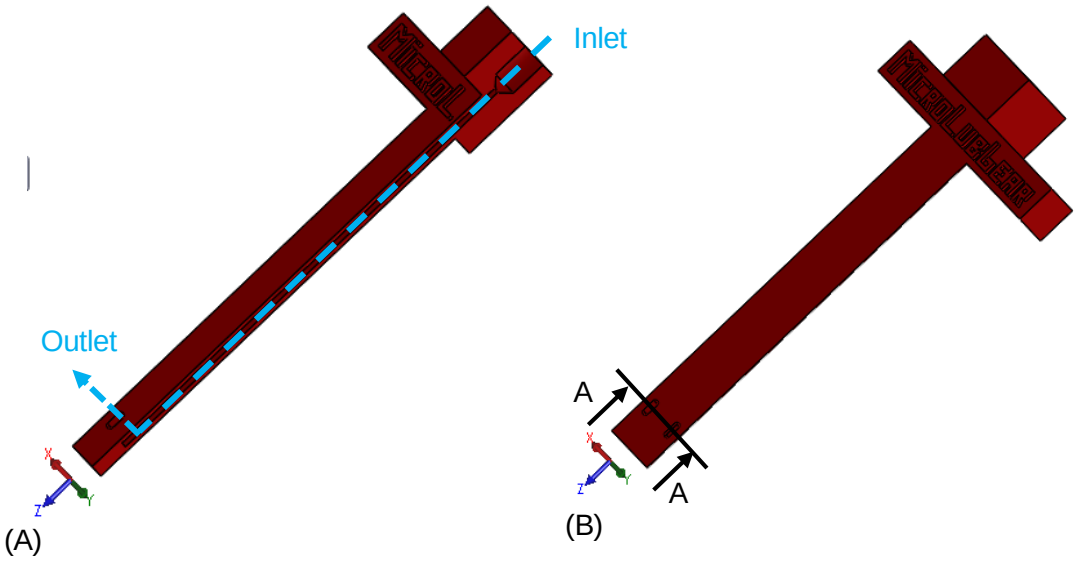

Figure 5.4: (A) MiCRoLuBGeaR symmetrically cross section through the lubrication channel. (B) Isometrical view of MiCRoLuBGeaR

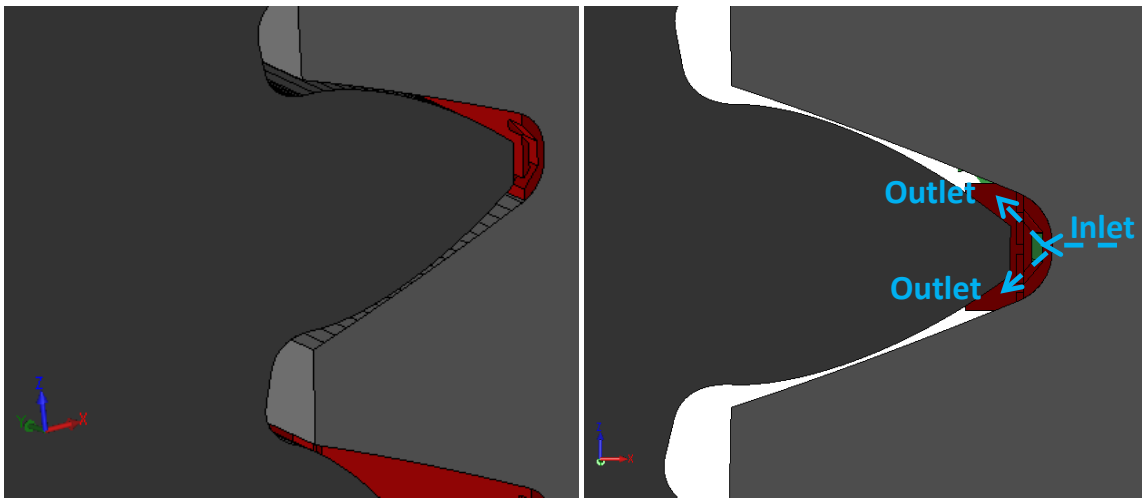

Figure 5.5: MiCRoLuBGeaR assembled in the pitch system. Cross section at position A-A from Figure 5.4B

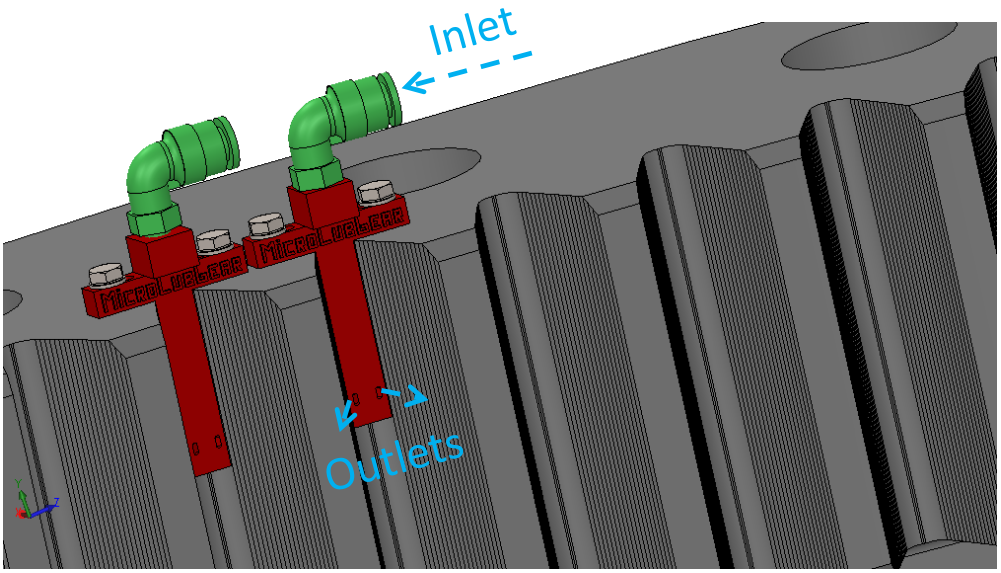

Figure 5.6: MiCRoLuBGeaR assembled in the crown

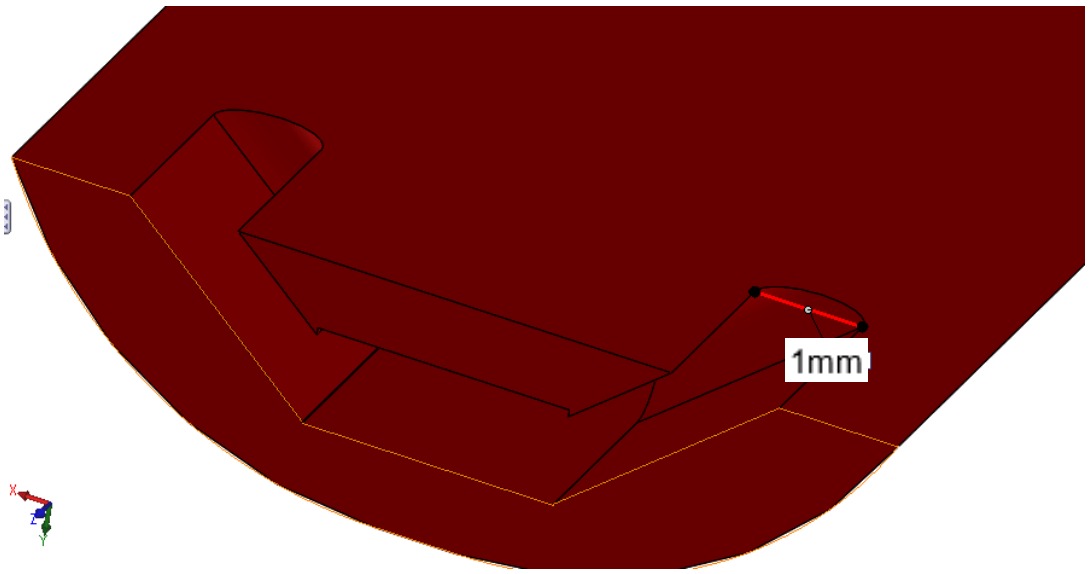

Figure 5.7: Detailed dimensions of the lubrication channel

Figure 5.7 shows a MiCRoLuBGeaR cross-section with a detail of the minimum micro-channel width through which grease flows to the tooth flank. Figure 5.5 is a general view that shows the possibility of lubricating both flanks of the gear tooth with two MiCRoLuBGeaR outlets. The schematic of the MiCRoLuBGeaR part integrated in the wind turbine is shown in Figure 5.8. The motor transmits the power to the gearbox that, through the pinion, moves the gear bearing

assembled, in case of the pitch, at the blade. The wind turbine control activates the system through the electric control. The grease pump is connected by the pressure line to the grease distributor to send the grease to: the bearing lubrication, the gear lubrication and the MiCRoLuBGeaR system, governed by valve 9 to inject fresh grease at the gear only when the gear is at the excessive wear point. The pitch or yaw control can govern valve 9, or it can be governed by a mechanical actuation at the point.

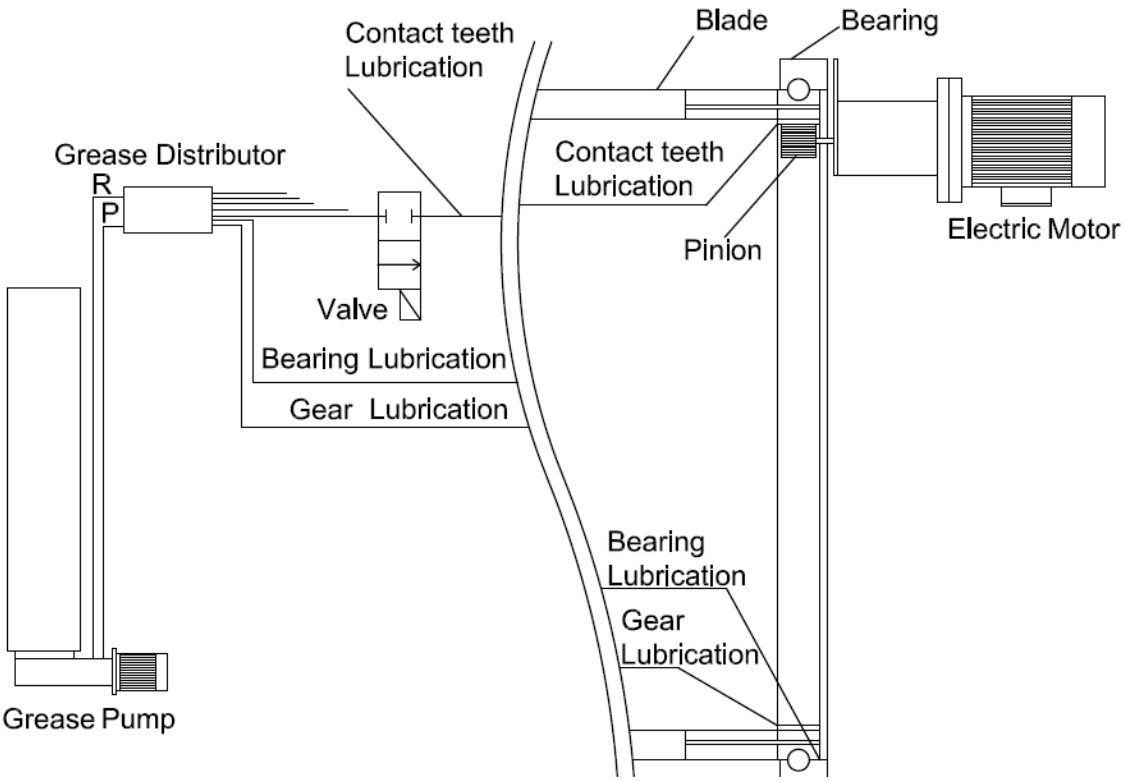

Figure 5.8: Integration of the MiCRoLuBGeaR in an automatic lubrication system

5.3. Grease flow validation using Ansys Fluent

In order to dimension the pump required in the automatic lubrication system, the total pressure loss through the whole set of micro-channels is required. Therefore, ANSYS Fluent is used to model the set of channels through which the grease flows in the MiCRoLuBGeaR. Figure 5.9 shows the mesh used to model the inlet, the micro-channel and the outlets. To solve the finite element model the continuity and momentum equations with a “Pressure-based” solver with coupled algorithm was selected. The inlet was set as a pressure inlet. For calculating cell-face pressures in order to compute pressure gradient using Gauss method, the “PRESTO!” Interpolation Method was selected [46].

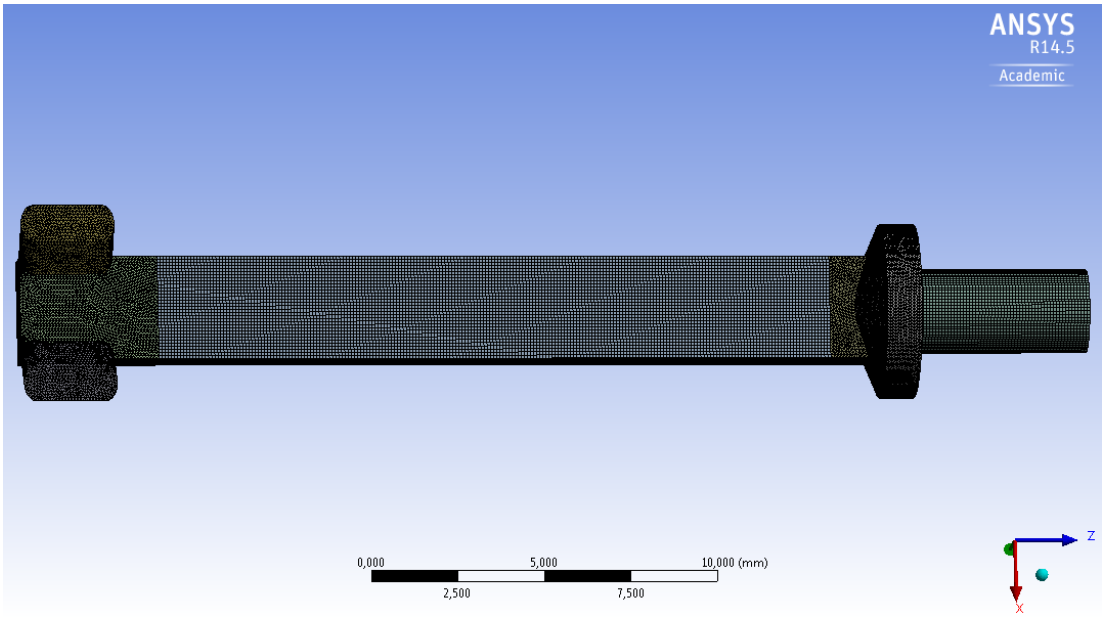

Figure 5.9: Different meshing zones all over the body [46]

After convergence, the velocity contours showed that the grease outlets directed the grease to the tooth flank, as shown in Figure 5.10. Figure 5.11 corroborates the fact that the velocity of the outlets is greater close to the inner faces rather than at the center. This is related to the fact that the outlets are not very long and inclined, so the distance from the main channel to the outlet is longer on the outside flank, increasing the resistance flow.

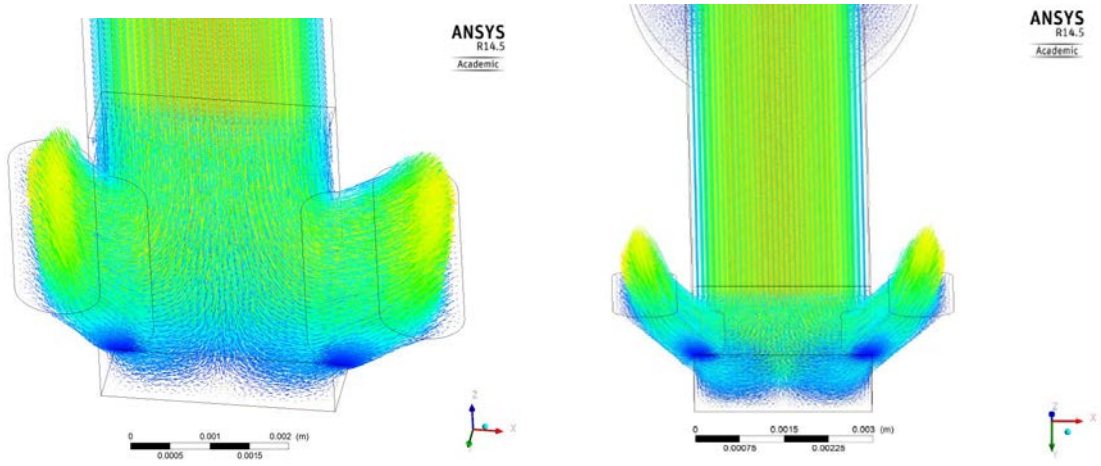

Figure 5.10: Grease flow at the outlets [46]

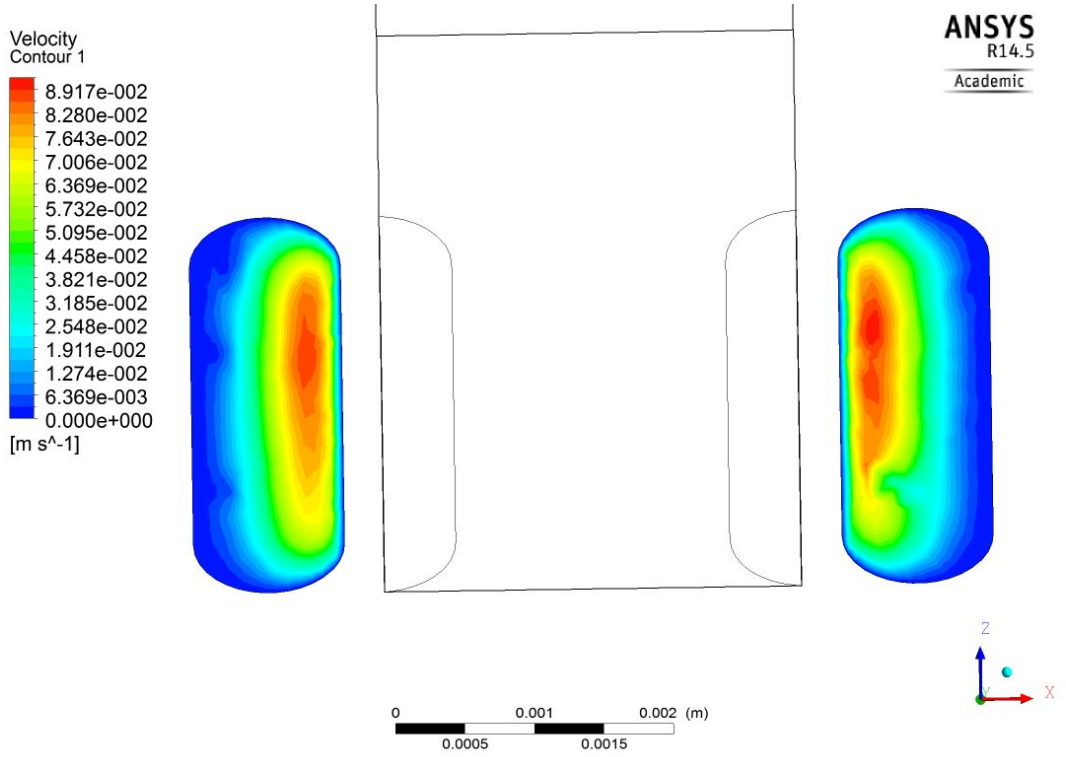

Figure 5.11: Contours of velocity at the outlets [46]

5.4. MiCRoLuBGeaR test bench validation

PUBLICATION D is the MiCRoLuBGeaR test bench validation under real operation conditions. The main factors needed to reproduce the excessive wear at the 0º position due to wind turbine dynamic operation in the test bench are:

- The blade micro-movements caused by the gearbox backlash (at the 0º position the gearbox is braked) due to Mz (as Figure 2.6 shows, aerodynamic forces acting on the blade. $M_{torsion}$ according to Holierhoek's definition [47]).
- The load cycle traction-compression on the blade (Mx and My in Figure 2.6 or M_{edge} and M_{flap} according to Holierhoek's definition [47]) when pitch works at the 0º position (in the example in Figure 2.7 with wind speeds 3 to 17 m/s).

The validation under the previous conditions shows that the optimum MiCRoLuBGeaR length to achieve the most uniform grease distribution is when the injection point is at the center of the gear tooth. Under these conditions the wear evolution between no lubrication and

lubrication with the MiCRoLuBGeaR device was compared. The results showed that without lubrication the wear in the tooth flank appears at $2x10^4$ cycles. Using the MiCRoLuBGeaR, at the same number of cycles, the wear is barely perceptible. Furthermore, the test bench operation showed that there was no interference between the MiCRoLuBGeaR device and the teeth, even with the loads applied.

5.5. Increased grease fluency due to hub rotation

The MiCRoLuBGeaR device is assembled in a position in the hub that is directly influenced by the centripetal acceleration due to the turning of the hub. Figure 5.12A and Figure 5.13A shows the rotor rotation direction (red arrow) and the grease flow direction (yellow arrow) inside the MiCRoLuBGeaR in Figure 5.12A. The MiCRoLuBGeaR cross-section is plotted in Figure 5.13B showing the angle between the rotation axis and the grease flow direction, which is approximately 30º.

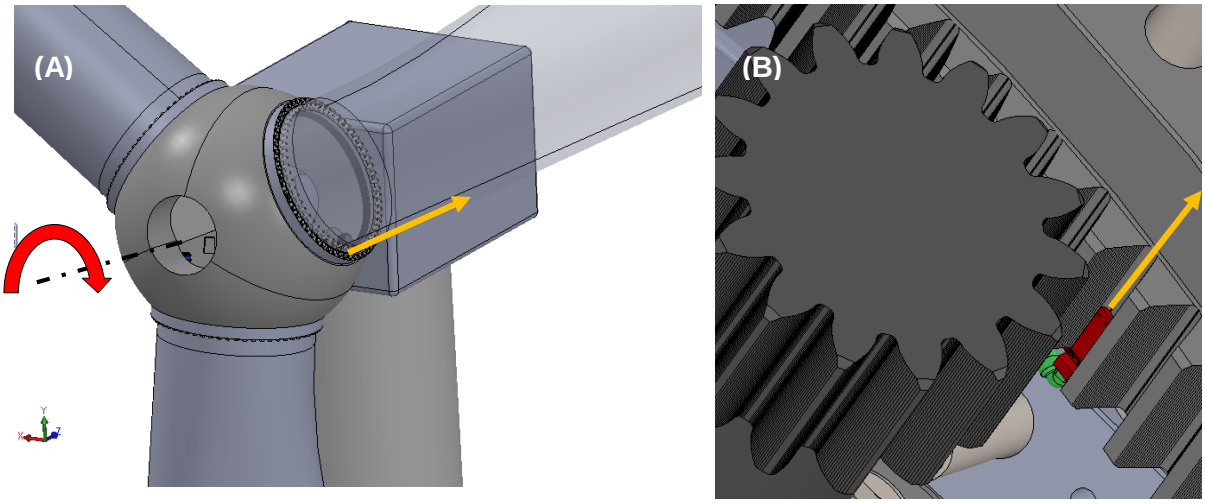

Figure 5.12: (A) Isometric view, the red arrow showing the rotor rotation direction and the yellow arrow showing the grease flow direction inside the MiCRoLuBGeaR. (B) Detailed views of the MiCRoLuBGeaR assembly

The absolute centripetal acceleration is:

$$\left|\vec{a}_{centripetal}\right| = \omega^2 \cdot r \qquad (4)$$

where:

$\vec{a}_{centripetal}$ is the centripetal acceleration
ω is the angular velocity
r is the rotation radius

The absolute Coriolis acceleration is:

$$|\vec{a}_{coriolis}| = 2|\vec{\omega} \times \vec{v}| \quad (5)$$

where:

$\vec{a}_{coriolis}$ is the Coriolis acceleration
ω is the angular velocity
v is the grease velocity into the micro-channel

Assuming values similar to the wind turbine model Alstom ECO100 [6] r = 2 m, w = 18 rpm=1.88 rad/s and the grease velocity thought the micro-channel is a range of 0.01 m/s < v < 0.1 m/s, the Coriolis acceleration according to Eq. 5 is in the range of 0.4 m/s^2 and the centripetal acceleration according to Eq. 4 is 7.1 m/s^2, less than 1 G, insignificant values to affect the simulations but this could help to prevent micro-channel clogging.

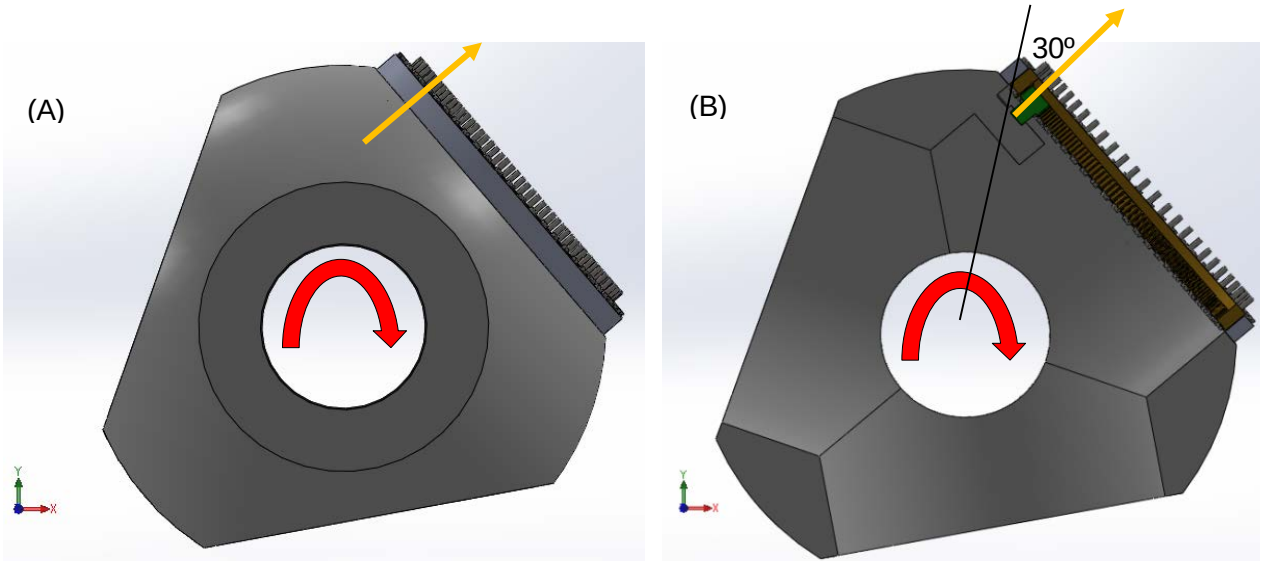

Figure 5.13: (A) Section in the rotation plane (B) Cross section in the plane of rotation. The red arrow shows the rotor rotation direction and the yellow arrow shows the grease flow direction inside the MiCRoLuBGeaR

6. Conclusions and future work

This research has focused on the feasibility of using micro-sized channels to distribute grease directly to the root of the tooth with a view to improve the lubrication on the pitch and yaw gears to avoid excessive wear. It can be considered that the following objectives have already been achieved to a large extent:

The ISA-International Searching Authority of Spain published the ISR-International Search Report PCT/ES2013/070494 of the PUBLICATION A which concluded that the novelty and inventive step of the invention are fulfilled. Furthermore, the report concluded that “the invention differs mainly from the documents of the state of the art in that none of them shows the solution of incorporating micro-fabrication strips whose dimensions are consistent with the geometry of the gear design, which fit into the dedendum space. Each strip has multiple perforations which are micro-channels for distributing the lubrication”.

The new technology should be validated to guarantee its operation with greases, this requirement gives rise to the challenge of manufacturing micro-channels to withstand high pressures. PUBLICATION B presents a novel micro-manufacturing technique that takes advantage of RPT printing and UV curable glue to make it possible to obtain micron-sized channels that can withstand pressures higher than 5 MPa. This manufacturing technique is much faster than previous micro-manufacturing techniques where different steps were needed to obtain the micro-machined parts. However, due to current 3D printer resolutions (around 50 µm) and according to the experimental results, channels smaller than 250 µm x 250 µm in cross-section should not be used to characterize fluid flow behavior using micro Particle Image Velocimetry, since inaccuracies in the channel boundaries can deeply affect the fluid flow behavior which is accentuated in curved sections.

This new micro-manufacturing technique opens the door to the possibility of analyzing the behavior of the grease flow in an elbow channel with a rectangular cross section of 250x1000 µm. PUBLICATION C is the study that comprises a dual experimental/analytical approach where the method of micro Particle Image Velocimetry (µPIV) is used to measure and visualize the flow in the channel. The analytical model is built from the fluid equation of motion considering the Herschel-Bulkley rheology model. Three Lithium-based greases with NLGI grade 00, 1 and 2 respectively have been used and the flow has been analyzed for flow rates in the range 0.002 ml/min to 0.5 ml/min. It is shown that there is a good match between the analytical model of the flow in the elbow and the velocity profiles measured. The analytical solution for the velocity across the elbow section is shown to be sensitive to the pressure in the angular direction (ϕ, considering cylindrical coordinates). As the pressure increases the velocity profile gradually approaches a reversal indicating that flow separation occurs in the

elbow connected to the solid boundaries. This result has a direct application in lubrication systems where an effective feed of grease from the reservoir to the component to be lubricated is highly important. With separation present in the flow, it is no longer possible effectively pump the grease through the pipe system. Another finding with direct relevance to lubrication systems is that for low flow rates the grease experiences large velocity fluctuations in the channel, i.e. a stick-slip type of motion. This effect disappears for high flow rates, concluding that in order to achieve an even flow rate through (for instance) a lubrication system the applied flow rate itself cannot be too low. Flow visualizations show that wall slip is present and it is found to be reduced in the elbow compared to the in- and outlet sections of the channel. The conclusion is that this effect – which is mainly observed for low flow rates and for the thinnest grease with NLGI grade 00, is caused by the higher shear magnitude in the elbow flow caused by the curvature. For high flow rates the slip effect decreases and the overall flow is unaffected by the elbow. Shear banding due to a non-uniform distribution of the shear rate in the channel is also observed.

Once the possibility of manufacturing micro-channels and the grease injection through them has been validated, a test bench analysis under real wind turbine loads was performed. PUBLICATION D shows the test in a pitch gear test bench of a 2 MW wind turbine using conventional wind turbine greases under real loads. The nozzles that injected the grease to the position in the middle of the teeth showed a more uniform grease distribution and, compared with the current lubrication systems, extend the service life of the teeth by more than double and reduce the appearance of wear to $2x10^4$ cycles. Another benefit of the MiCRoLuBGeaR system is that it allows the wind turbine to lubricate and generate at the same time, this being the key difference compared to previous technologies, and consequently increases the wind turbine electricity generation. In addition, the method presented in PUBLICATION D is universally applicable to any pitch gear modules, regardless of the shape, size and the lubrication system available. The wind sector tendency towards an offshore market leads to the use of autonomous systems to reduce preventive and corrective maintenance such as the device presented.

The use of micro-lubrication is a new field of study that provides the possibility of using the advantages of miniaturization in many industrial applications. But there are still some questions to be answered, such as i) the effect of constrictions and/or bifurcation on the grease flow behavior, ii) whether the gears can be made “smart” by integrating sensors in the channels to evaluate the grease or oil quality or other parameters that may be of interest, iii) whether the greases can be flexible, offering channels that can refine their working conditions (for example for high temperatures).

7. DIVISION OF WORK

PUBLICATION A: Jasmina Casals Terré, Josep Farré Lladós. *"Procedimiento y dispositivo para prevenir el desgaste excesivo en engranajes"* Patent WO 2014009588 A1.

The main invention and design setup was developed by all authors. The 3D model and the wind turbine implementation were completed mainly by Farré, in collaboration with Casals. The paper was written by all authors.

PUBLICATION B: J Farré-Lladós, J Casals-Terré, J Voltas and L.G Westerberg *"The use of Rapid Prototyping techniques (RPT) to manufacture Micro channels suitable for high operation pressures and µPIV".* Rapid Prototyping Journal. Volume 22, Issue: 1, in press.

The main design setup was developed by Casals and Farré and the 3D parts were manufactured by Voltas. The micro-channel assembly and the micro-channel measurements were mainly conducted by Farré, in collaboration with Casals. The µPIV experiments with the different depths and post-processing were mainly conducted by Farré, in collaboration with Westerberg. The paper was written by all authors.

PUBLICATION C: Lars G. Westerberg, Josep Farré-Lladós, Jinxia Li, Erik Höglund, Jasmina Casals-Terré. *"Grease flow in an elbow channel".* Tribology Letters (2015) Volume 57, Issue 3, DOI 10.1007/s11249-015-0469-6.

The µPIV experiments with the different depths and post-processing were mainly conducted by Farré in collaboration with Westerberg and Li. The analytical model was developed by Westerberg. The paper was written by all authors.

PUBLICATION D: Josep Farré-Lladós, Lars G. Westerberg and Jasmina Casals-Terré. *"Embedded Micro-nozzles in Pitch Gear Dededum to minimize wear at zero degree position"*. Tribology Transactions, *submitted*.

The 3D model and the test bench implementation were mainly completed by Farré in collaboration with Casals. The µPIV experiments with the different depths and post-processing were mainly conducted by Farré in collaboration with Westerberg, and the test bench validation was mainly conducted by Farré in collaboration with Casals and Westerberg. The paper was written by all authors.

8. REFERENCES

[1] Eduardo Vicente – Lincoln Spain. Lubricación en aerogeneradores. Revista Tope nº 148. Pàgina 20-24 July/August 2009.

[2] Jasmina Casals-Terré, Josep Farré-Lladós. Work Package 0 KIK-Innoenergy Project No: 04_2013_IP54_MiCRoLuBGeaR. March 2013.

[3] Product specification and information concerning Gamesa G90, Available from: www.gamesacorp.com, 2012-04-02.

[4] Gamesa Innovation, patent assignee; 2008 Dec. 01. Sistema de cambio de paso variable accionado eléctricamente. Español Patent ES 2308911-A1.

[5] Product specification and information concerning General Electric GE's 1.6 - 100, Available from: www.ge.com, 2012-04-02.

[6] Product specification and information concerning Alstom ECO100, Available from: www.alstom.com, 2012-04-02.

[7] Product specification and information concerning Acciona AW3000, Available from: www.acciona-energia.com, 2012-04-02.

[8] Product specification and information concerning MOOG, Available from: www.moog.com, 2012-03-28.

[9] Andreas Manjock. Close to the wind: Pitch Systems. Beaufort 6; Edition June 2007. Vol.2 p.1-3.

[10] Wobben, Aloys inventor; 2005 Sep. 20. Azimuthal driving system for wind turbines. United States Patent US 6945752.

[11] Germanischer Lloyd Industrial Services GmbH; 2010 July 1. Guideline for the Certification of Wind Turbines. Hamburg: Germanischer Lloyd.

[12] ANSI/AGMA 1010-E95. Revision of AGMA 110.04; 1995. Appearance of Gear Teeth – Terminology of Wear and Failure. United States of America: ANSI/AGMA.

[13] ISO 10825. First edition; 1995. Gears – Wear and damage to gear teeth – Terminology. Switzerland: ISO.

[14] Takadoum, Jamal; 2008. Materials and Surface Engineering in Tribology. ISBN 978-1-84821-067-7. London: Wiley.

[15] Mashue A, Moorer B.G, Goodwin K, inventors; 2011 Jun. 16. Gear set for pitching blade of rotor of wind turbine utilized for providing electricity to utility grid, has pinion/drive gear comprising set of teeth whose hardness is less than harness of teeth of ring gear. United States patent US 2011142617-A1.

[16] Klaus P, inventor; 2010 Apr 20. Actuator for adjusting a rotor blade pitch angle. United States patent US 7699584-B2.

[17] Nielsen T, inventor; 2008 Jun. 26. A gear system for yaw drive or a pitch drive for a wind turbine. World Intellectual Property Organization WO 2008/074320-A1.

[18] Dimascio P, Close R, Auer G, Grimley R, Hamel A, inventors; 2009 Aug. 29. Hub pitch gear repair method. Canada patent CA 2655691-A1.

[19] Mashue A, Pemrick J, inventors; 2011 Jun. 16. Wind turbine with gear indicating wear. United States patent US 2011138951-A1.

[20] Nordex Energy, patent assignee; 2010 Apr. 08. Device for estimating wear condition of gear teeth of pitch rotary joint of wind turbine, has quadrangular part movably and lockably arranged on pin, where two transverse sides of part are shorter than two longitudinal sides of part. Germany patent DE 202009015263-U1.

[21] Hau Erich; 2006. Wind turbines. Fundamentals, technologies, application, economics. ISBN 978-3-642-27151-9. Germany: Springer.

[22] Kürzdörfer, M inventor; 2007 Mar. 21. Anstellwinkeleinstellvorrichtung für eine Windkraftanlage. European Patent EP 1764544-A2.

[23] Harris T, Rumbarger J.H, Butterfield C.P; 2009 December. Wind Turbine Design Guideline DG03: Yaw and Pitch Rolling Bearing Life. Colorado: National Renewable Energy Laboratory.

[24] Valero S, inventor; 2011 Jan 10. Locking device of a wind turbine auxiliary drive. World Intellectual Property Organization. WO 2011/083155-A1.

[25] Stromag Ag, patent assignee; 2008 Dec 04. Wind turbine adjustment mechanism, for azimuth and/or pitch, has an induction brake between the dive motor and the gearing. Germany patent DE 202008010748-U1.

[26] Rebecca J and George M. Whitesides. Electrochemistry and soft lithography. A route to 3D microstructures. Chemtech: Cambridge, May 1999; Volume 29, Number 5, Pages 18-30.

[27] Scott Brittain, Kateri Paul, Xiao-Mei Zhao and George Whitesides. Soft lithography and microfabrication. Physics World, May 1998; Pages 31-36.

[28] Srinidhi Veeravalli Murali; 2008 December. A microfluidic coulter counting device for metal detection in lubrication oil. Master thesis. Ohio. The Graduate of the University of Akron.

[29] Li Du, Jiang Zhe, Joan Carletta, Robert Veillette. Real-time monitoring of wear debris in lubrication oil using a microfluidic inductive Coulter counting device. Microfluid Nanofluid, 2010 May. Pages 1241-1245. DOI 10.1007/s10404-010-0627-y

[30] Sultan M A, Fonte C P, Dias M, Lopes J C B and Santos J R. Experimental study of flow regime and mixing in T-jets mixers. 2012 Chem. Eng. Sci. 73 388-399. DOI:10.1016/j.ces.2012.02.010

[31] ISO 12925. First edition, 1996. Lubricants, industrial oils and related products (class L) – Family C (Gears). Switzerland: ISO.

[32] Product specification and information concerning SKF Reliability systems. Available from: www.skf.com, 2012-05-08.

[33] Product specification and information concerning Klüber. Available from: www.klueber.com, 2012-02-02.

[34] Ehrlich, M. (ed.): Lubricating Grease Guide, second edition. NLGI, Kansas City, USA (1987).

[35] Douglas B Weibel, Willow R. DiLuzio and George m. Whitesides. Microfabrication meets microbiology. Nature, March 2007; Volume 5 Pages 209-218. DOI:10.1038/nrmicro1616

[36] Gibert Pedrosa, Jaume; 2005. Ingeniería de los engranajes. Barcelona. ISBN: 8460954552

[37] Carreras Soto T; 1970. Engranajes. Trazados teórico y práctico. Sevilla.

[38] DIN 867; February 1986. Basic rack tooth profiles for involute teeth of cylindrical gears for general engineering and heavy engineering. Germany: DIN-Normen.

[39] Product specification and information concerning Mobil. Available from: www.mobilindustrial.com, 2012-02-02.

[40] Product specification and information concerning Castrol. Available from: www.castrol.com, 2012-02-02.

[41] Product specification and information concerning Shell. Available from: www.shell.es, 2012-02-02.

[42] DIN 51817; April 1998. Determination of oil separation from lubricant grease under static conditions. Germany: DIN-Normen.

[43] Product specification and information concerning IDEX, Available from: www.idex-hs.com, 2012-05-07.

[44] J. J. Heigl, M. F. Bell and J.U. White. Application of Infrared Spectroscopy to the Analysis of liquid Hydrocarbons. Analytical Chemistry, May 1947; Volume 19 num 5. DOI: 10.1021/ac60005a003

[45] ASTM D1403-02; Reapproved 2007. Standard Test Methods for Cone Penetration of Lubricant Using One Quarte and One Half Scale Cone Equipment. United States: ASTM.

[46] Ernest Guirao Palacios. Design and characterization of a microlubrication system for minimizing the preventive maintenance of wind turbines. 6 June 2014

[47] J.G. Holierhoek, H. Korterink, R.P. van de Pieterman, H. Braam, L.W.M.M. Rademakers, D.J. Lekou, T. Hecquet, H. Söker. Recommended Practices for Measuring in Situ the 'Loads' on Drive Train, Pitch System and Yaw System. September 2010. Protest ECN-E--10-083.

PART II: Papers

PUBLICATION A

METHOD AND DEVICE FOR PREVENTING EXCESSIVE WEAR IN GEARS

OBJECT OF THE INVENTION

As stated in the title of the present specification, the invention relates to a method and a device to prevent excessive wear in gears.

More particularly, the object of the invention is a method and a device for its implementation, which aims to improve gear performance and prevent excessive wear present in machinery gears working under heavy loads, particularly intended to be applied in wind turbines gears, where the method is based on the application of micro-fluidic technology comprising the development of a grease distribution system through parts of soft material (for example polymers) which are arranged in the contact point between the teeth and the notches of the gear.

FIELD OF THE INVENTION

The application field of the present invention falls within the field of industry devoted to the manufacture of wind turbines, focusing on the field of systems intended to improve gears wear.

BACKGROUND OF THE INVENTION

To design more efficient wind turbines, the current trend of manufacturers is to increase the rotor diameter so that it can capture more wind kinetic energy and thus increase power and generate more energy. Thereby profits are achieved faster. The load

increases in components and connections due to the increase in the size of the entire rotor, and consequently there is also an increase of the deformations present in all the materials forming the parts of the wind turbine. The present static loads increase significantly bringing back a problem that was not evident in previous models of wind turbines with smaller power.

Most systems that make up the wind turbine are assembled in a static manner, not the powertrain system that transmits torque to the yaw and the variable change of pitch systems.

During dynamic operation of wind turbines, the bearings of the variable change of pitch system are subjected to alternating traction and compression stress.

Similarly, the yaw system is affected by the same stress cycle, but in this case due to the different wind speed and the small wind direction changes.

In each of these cycles a gear micro-movement is produced that removes the lubricant and initiates a friction between the two surfaces in contact of the teeth that are working. Contact between the metal produced by the absence of lubricant leads to excessive wear on the gear.

Reliability studies such as those by Ribrant in 2005 [10] show that the ratio of failure of wind turbines is due in a 13.4% to the pitch system and in a 6.7% to the yaw system. So, we could say that about 20% of failures in wind turbines could be related to that

excessive wear and that this failure rate may be increasing, if the same lubrication system and power transmission is maintained, and the wind turbines power is increased.

20% of failure ratio is significant enough to motivate most wind turbine manufacturers to have begun to study the excessive wear of the teeth set having a higher working load caused in the friction region, both in the yaw system and in the variable change of pitch system, and its possible solution.

Kürzdörfer M; 2007 [8] from Baier & Koppel company was the first to patent a system to reduce tooth wear. On their website [11] the different systems developed for this purpose can be seen. The first patented invention was based on a lubrication system that point injects lubricant through the upper part of the tooth in the position of wear.

Following examples can be found in patents such as Dimascio, P et al; 2009 [4] that proposes to replace the damaged region of the bearing crown with a removable part attached by bolts.

Mashue, A; 2011 [2] proposes a marks system to measure the excessive tooth wear and thus predict the repair before failure occurs.

Takadoum J; 2008 [5] published the parameters of the operating conditions to optimize to minimize wear in gears: working surface, loads acting, mechanical contact and tribology of the system.

Mashue, A; 2011 [1] patented new conditions not used until then consisting to increase the hardness

of the bearing crown to become higher than the hardness of the pinion (design concept inherited from the worm pinion gears design) thus causing the wear in the pinion that due to its size it is easier to replace.

Klaus P; 2010 [3] proposed a change in the tribology of the system, as it added to the crown of the bearing or of the pinion holes that inject fresh lubricant at the contact point of the teeth.

Nielsen, T; 2008 [6] proposed a change that involves joining two pinions to transmit the same torque and thus reduce the pressure suffered by each of the pinions at the contact surface.

In general all of the aforementioned patents are aimed to improve the excessive wear modifying those parameters described by Takadoum J; 2008 [5]. Klaus P; 2010 [3] modifies the lubrication system involving complex machining, Nielsen, T; 2008 [6] modifies the mechanical contact by adding new parts, Mashue, A; 2011 [1] modifies the conditions of the working surface having to replace parts for wear. Thus production is complicated obtaining expensive applications which are difficult to implement in wind turbines in operation.

[1] Mashue A, Moorer B.G, Goodwin K, inventors; 2011 Jun. 16. Gear set for pitching blade of rotor of wind turbine utilized for providing electricity to utility grid, has pinion/drive gear comprising set of teeth whose hardness is less than harness of teeth of ring gear. US 2011142617-A1

[2] Mashue A, Pemrick J, inventors; 2011 Jun. 16. Wind turbine with gear indicating wear. US 2011138951-A1

[3] Klaus P, inventor; 2010 Apr 20. Actuator for adjusting a rotor blade pitch angle. United States patent US 7699584-B2.

[4] Dimascio P, Close R, Auer G, Grimley R, Hamel A, inventors; 2009 Aug. 29. Hub pitch gear repair method. CA 2655691-A1.

[5] Takadoum, Jamal; 2008. Materials and Surface Engineering in Tribology. London: Wiley.

[6] Nielsen T, inventor; 2008 Jun. 26. A gear system for yaw drive or a pitch drive for a wind turbine. WO 2008/074320-A1.

[8] Kürzdörfer, M inventor; 2007 Mar. 21. Anstellwinkeleinstellvorrichtung für eine Windkraftanlage. EP 1764544-A2.

[10]Ribrant, Johan; 2005-2006. Reliability performance and maintenance - A survey of failures in wind power systems. Master thesis. Sweden. KTH School of Electrical Engineering.

[11]Baier & köppel Product Specifications, Available at: www.beka-lube.de, 2012-05-07.

SUMMARY OF THE INVENTION

In the present invention a new lubrication system for lubricating the contact point between the two gears that provides the possibility to exactly lubricate the contact area with a control of the amount of grease required, which, moreover, is compatible with both the new wind turbine models and also the currently ongoing wind turbine models in which it allows

lubrication of the contact tooth (5) simultaneously with the generation of electricity, thus avoiding generation losses.

Particularly, the method proposed by the present invention is based on the application of the micro-fluidic technology and thus the micro manufacturing of a grease distribution system that can be adapted to the dedendum of the gear to be lubricated.

For this end it is incorporated a micro-manufactured part with dimensions in accordance to the design geometry of the gear, so in each case the part will be designed to be adapted to the assembly.

In any case, said part consists of a strip adapted to fit to the gap of the dedendum or tooth root, considering, of course, the incorporation of one of these parts in each of the dedendum determining two ridges or teeth in, at least, those teeth that suffer excessive wear.

The lubricant distribution strips are preferably made of soft materials (such as polymer) to avoid damage to the gear in case of accidental contact.

These strips also are provided, each with a plurality of perforations which are lubricant distribution micro-fluidic channels.

If we use design values of module 12 and 15 pinion teeth, similar to those used in Pitch and Yaw gears in wind turbines, we obtain values of width and thickness for the part of 13.4mm and 3mm respectively, values easy to manufacture using micro-technology.

Once the strips in a gear, the lubricant injection through the same will be carried out by integrating them to the own automatic lubrication system usually available in the gears, especially in those of the type to which the invention is primarily intended, that those of wind turbines.

An example of that integration to said lubrication system consists in connecting the grease pump to a distributor with the corresponding return piping to supply the bearing rolling elements, the toothed crown and to supply the strip for lubrication the wear point. To control the action of lubrication in that point, a control valve is provided that can be driven mechanically by the engine itself or by the control of the wind turbine when the latter is located in the working position.

Having regard to the above, it is stated that the here described method and device to prevent excessive wear on gears is an innovation of features previously unknown for this purpose, reasons which together to its practical usefulness, provide a sufficient basis for obtaining the requested exclusivity privilege.

DRAWINGS DESCRIPTION

To complement the description that is being made of the invention, and to assist a better understanding of the distinguishing features, to the present specification, as an integral part thereof, a set of drawings are attached, which, in an illustrative an non limiting manner, represent the following:

Figure number 1.- Shows a perspective view of two meshed gear wheels, to which is incorporated the device according to the invention.

Figure number 2.- Shows a sectional view and in detail of the engagement between the tooth of a wheel with the notch of the other, showing the configuration and arrangement of the strip which forms the device of the invention housed in the dedendum of said notch.

Figures numbers 3, 4 and 5.- Show two views of an embodiment of the strip comprised by the device of the invention, shown, respectively, by means of a top plan view, a bottom plan view and a side elevation view.

Figure number 6.- Shows a diagram of the circuit for lubricating a gear to which the device of the invention has been incorporated.

PREFERRED EMBODIMENT OF THE INVENTION

In view of the mentioned figures, and according to the adopted numbering, a preferred embodiment of the invention is shown, which comprises the parts and elements that are described in detail below.

Thus, the method of the invention comprises the lubrication of the contact point between the two wheels (1) of a gear (2) by microfluidics technique, to which end, as seen in Figure 1, in at least one of said two wheels (1) is provided the incorporation of a microfabrication part (3) housed in each of the notches (4) determining the spaces between the teeth (5) of

said wheel (1), where said part (3) is a part having a planar and approximately rectangular configuration and which fits snugly to the dedendum (6) of each of said notches (4).

Is important to point that the adjustment of each of the parts (3) on the dedendum space (6) of each notch (4) is achieved in each case by dimensioning the part so that the width (a) of the same matches the width of the dedendum (6) in which is housed, and so that the thickness (b) thereof be less or equal than the space between the surface of the crest (7) of the tooth (5) of the engaging wheel and the surface of the dedendum (6) into which the part (3) is housed.

Each of said parts (3) is also provided with means for channeling lubricant in the area in which they are incorporated, preferably but not limited to, using the own lubrication system of the gear assembly (2).

To this end, each of said parts (3), as shown in Figures 3 to 5, has a plurality of through holes (8) passing through the part from its top surface (3a) to its bottom surface (3b), being, at said bottom surface, connected with longitudinal grooves (9) that in one end of the part (3) converge into a notch (10) open laterally, so that, together, constitute a system of distribution channels for the lubricant, where the latter will be injected into the longitudinal grooves (9) through said lateral opening forming said notch (10).

Thus, since the dimensions of the notches of the space of the dedendum (6) are variable depending on the module of the gear and on the gear geometry, in

each case the design of the strip is adapted both in dimensions, width (a) and thickness (b), as in the lubricant distribution system.

Turning to Figure 6, it shows the scheme of operation of the device that, once the parts (3) are assembled, uses for its lubrication the same lubrication system that lubricates the rest of the gear, where the grease pump (11) is shown connected to a distributor (12) with the corresponding return pipe (13), existing a first feed tube (14) supplying grease to the rolling elements of the bearing of the gear (2), a second feed tube (15) grease feeding one of the wheels (1), specifically the toothed crown, and a third feed tube (16) which feeds via the side notches (10) the parts (3) of the device lubricating exactly the wear point. Furthermore, to control the action of the lubrication of said point, in said third feed tube (16) a control valve (17) is arranged which can be mechanically driven by the engine (18) itself or by the control of the wind turbine when located at the working position.

Thus, the device described can be applied to any type of machine, but advantageously, in wind turbines in the change of pitch gear and in the yaw gear.

The device allows an independent supply of lubricant to each gear of the system, enabling lubricate the tooth (5) in contact while supporting loads.

The width (a) and thickness (b) of the strips can be adapted to the geometric characteristics of any gear to allow its mounting thereon, and also the

geometry and positions of the holes that constitute the lubricant distribution channels system of the strips are also variable.

Sufficiently described the nature of the present invention, as well as how to put it in practice, it is not considered necessary to further explain the invention to allow any person skilled in the art understand its scope and the advantages derived therefrom, stating that, in its essence, the invention can be put in practice in other embodiments that differ in detail from that indicated by way of example, and which are also covered by the protection claimed provided they do not alter, change or modify its fundamental principle.

CLAIMS

1.- METHOD TO PREVENT EXCESSIVE WEAR IN GEARS of the type that includes an injection of lubricant to a contact point between two wheels (1) of a gear (2), characterized in that said injection of lubricant to said contact point is performed through parts (3) housed in at least one of the notches (4) determining the spaces between teeth(5) of one of said wheels (1), wherein said lubricant is injected into said parts (3) via a channels system with lateral opening provided in said parts (3) for this purpose.

2.- METHOD TO PREVENT EXCESSIVE WEAR IN GEARS, according to claim 1, characterized in that the injection is performed using the same system that lubricates the rest of the gear, including therein a third feed tube (16) which adds to those already provided normally.

3.- METHOD TO PREVENT EXCESSIVE WEAR GEARS according to claim 2, characterized in that for controlling the action of lubricating of the wheels contact points a control valve (17) is arranged in said third feed tube (16), which can be mechanically driven by an engine (18) or by a wind turbine control.

4.- DEVICE TO PREVENT EXCESSIVE WEAR IN GEARS, according to the method described in any of claims 1-3 characterized in that it comprises parts (3) having a planar and approximately rectangular configuration, which snugly fit the dedendum (6) of each of the notches (4) of the wheel (1) that incorporates them; and in that said parts (3) have a system of distribution channels for lubricant.

5. DEVICE TO PREVENT EXCESSIVE WEAR IN GEARS according to claim 4, characterized in that the width (a) and thickness (b) of the parts (3) is variable and adapts in each case, respectively, to the width of the dedendum (6) in which is housed and to the space between the surface of the crest (7) of the tooth (5) of the engaging wheel and the surface of the dedendum (6) in which the part (3) is housed.

6.- DEVICE TO PREVENT EXCESSIVE WEAR IN GEARS, according to claim 4 or 5, characterized in that the lubricant distribution channels system is variable in number according to the geometry of the gear adapted to the position of the dedendum of the gear tooth.

7.- DEVICE TO PREVENT EXCESSIVE WEAR IN GEARS, according to claim 6, characterized in that the lubricant distribution channels system comprises a plurality of through holes (8) connected, at the lower surface of the part, with longitudinal grooves (9) that in one of the ends of the part (3) converge into a notch (10) open laterally.

8.- DEVICE TO PREVENT EXCESSIVE WEAR IN GEARS, according to any of claims 4-7, characterized in that the parts (3) are of soft material, preferably polymer.

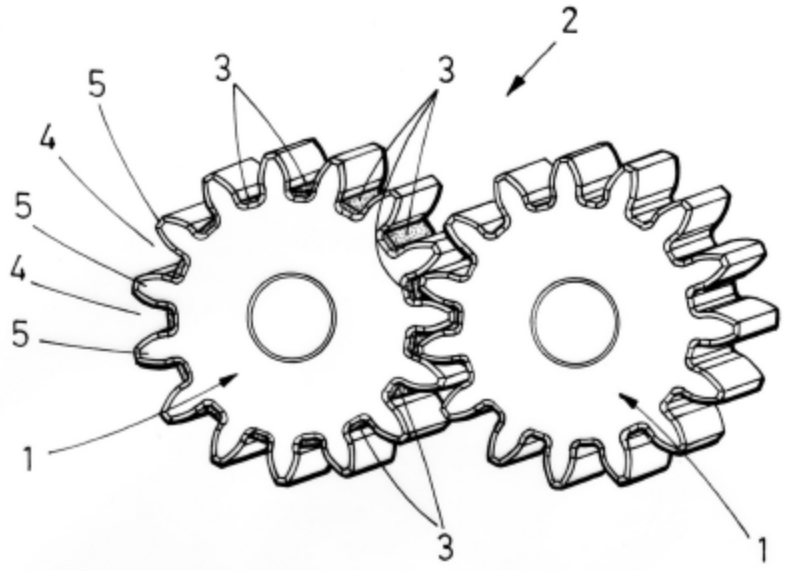

FIG.1

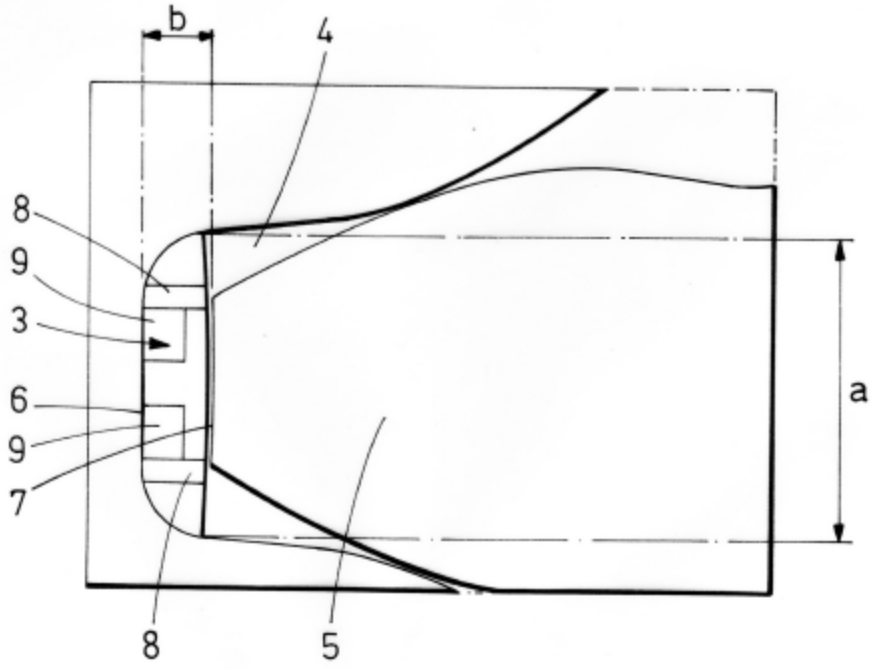

FIG.2

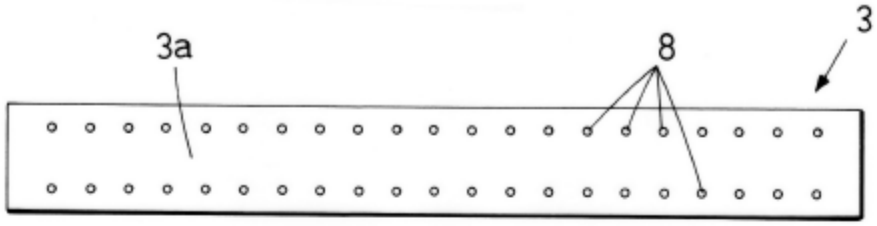

FIG.3

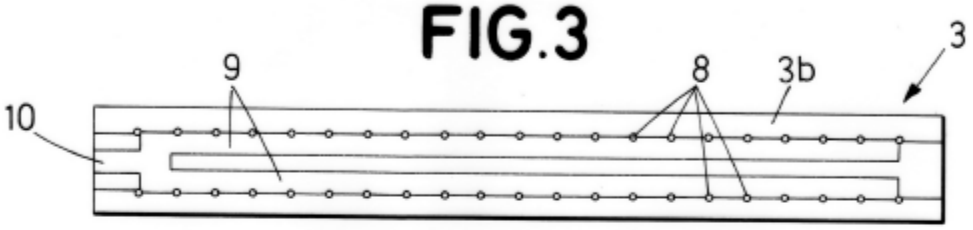

FIG.4

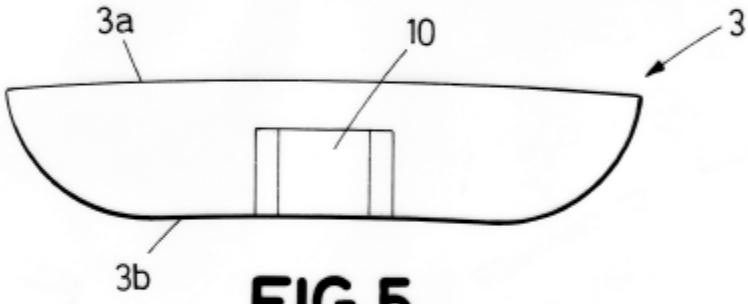

FIG.5

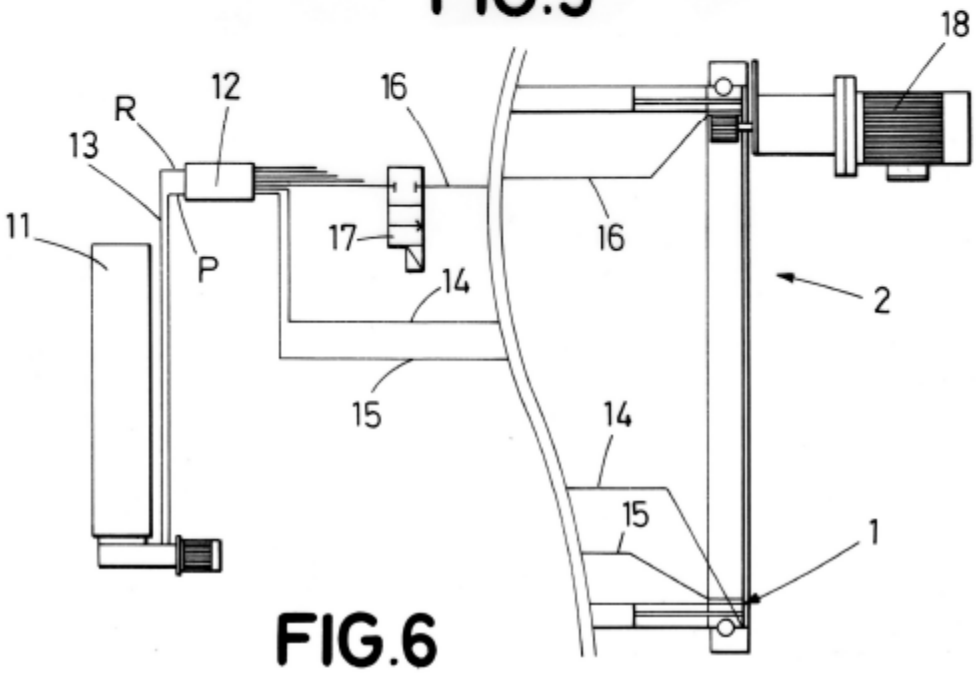

FIG.6

ABSTRACT

METHOD AND DEVICE FOR PREVENTING EXCESSIVE WEAR IN GEARS, involving lubricating the contact point between the wheels (1) of a gear (2), injecting lubricant into said point via parts (3) housed in the notches (4) that determine the spaces between teeth (5), via a system of channels with a lateral opening provided in said parts (3). The width (a) and thickness (b) of the parts (3) coincide respectively with the width of the bottom of the valley of the notch (4) and with the space between the surface of the crest (7) of the engaging tooth (5) and that of the valley of the notch(4)which houses it. The parts (3) have through-holes (8) connected to longitudinal channels (9) that, at one of the ends thereof, meet in a laterally open notch (10). The same system that lubricates the rest of the gear assembly is used to inject the lubricant.

PUBLICATION B

The use of Rapid Prototyping techniques (RPT) to manufacture Micro channels suitable for high operation pressures and µPIV

1. Abstract

The use of microfluidics is extensively related to bioapplications where the devices normally actuate at atmospheric pressures. The advantages of miniaturization are also valuable in many industrial applications, but building microfluidic circuits that withstand high pressures is still a challenge. This paper presents a new methodology to manufacture micro-channels suitable for high operating pressures and micro Particle Image Velocimetry measurements using a rapid-prototyping high-resolution 3D printer. This methodology can fabricate channels down to 250 µm and withstand pressures of up to 5 ± 0.2 MPa. The manufacturing times are much shorter than in soft lithography processes since there is no need to create a mold and the material can be chosen from a range of different UV curable resins that present a Young Modulus ranging from 2000 to 3000 MPa.

2. Introduction

Current research in the field of microfluidics using micro Particle Image Velocimetry (µPIV) covers investigations of the fundamental flow properties of e.g. complex fluids like grease (Green et al., 2011; Li et al., 2013; Li et al., 2012; Baart et al., 2011; Westerberg et al., 2010) or flow in medical devices (Madadi et al., 2013; Lewpiriyawong et al., 2008). The method used to manufacture the channels depends on its dimensions where, in the case of devices of the order of 1 mm in size, conventional manufacturing processes such as chip removal or electrical discharge machining are commonly used, while for channels with smaller dimensions, different micro-fabrication techniques have proven more suitable (Brittain et al., 1998, Weibel et al., 2007). Weibel et al., 2007 showed that for the micro-scale channels the typical manufacturing technique is soft lithography (Armani et al., 1999) where the base material is polydimethylsiloxane (PDMS), or some other polymer with similar characteristics. This polymer has a low Young Modulus (360-870 kPa), implying it can be easily deformed and 3D structures are not easily manufactured. There is a clear need of a straight forward manufacturing technique that provides the finished part from the AUTOCAD drawing, for instance Wu et al., 2011 proposed to use a high accuracy positioning table with a novel ink which allowed the direct fabrication of micro-channels.

Many engineering applications operate under elevated pressures as illustrated by Egham, 2006, who used an oleo-hydraulic pump that operated up to about 500 atmospheres, and Sanches et al., 2013 showing oil distributors or new flushing bearings methods operating at up to 60 MPa. In most of these devices there are micro-channels where grease and/or oil flows, and the behavior of the lubrication materials in these channels can modify the expected life of all actual components. It is of great interest and importance to analyze the flow behavior of greases in channels dimensioned in the micron range in order to be able to optimize the lubrication of the actual component. However, conventional micro-manufacturing processes such as soft lithography or Reactive Ion Etching (RIE) on silicon or glass (Ciftlik et al., 2012) have shown different challenges when operating at high pressures. PDMS channels are manufactured using soft lithography, where the pressure influences the channel deformation which in turn leads to experimental results far removed from realistic values (Gervais et al., 2006; Hardy et al., 2009), unless the channels are modified by adding other materials such as glass to make them more rigid (Inglis et al., 2010) or layer of UV-curable thiolene resins (Madadi et al., 2013). This reason has motivated the use of other technologies to manufacture the micro-channels, such as RIE or Electric Discharge Machining (EDM). RIE is normally used for

brittle materials (silicon or glass) which can easily break if they suffer an impact, and EDM has been shown to work on channels down to 500 µm (Sultan et al., 2012), but the main problem was the grease leakages through the joint of the plates and the micro-channel size limit.

Previous micromachining processes such as soft lithography, RIE, and EDM have shown different challenges when operating at high pressures. Either the low Young Modulus of PDMS causes elastic deformation of the channels which in turn affect the agreement between the experimental results and the expected results, or the number of manufacturing steps is increased. Moreover, the interconnections with external pipes and pumps are difficult to integrate in all the aforementioned processes. The novel manufacturing method presented in this paper can thanks to the use of a high resolution 3D printer with a wide material range (Young Modulus from 2000 to 3000 MPa) produce micro-channels that can operate at high pressures and also have integrated hose connections to pipes and pumps. In precise machining technologies such as Electric Discharge Machining (EDM) it is extremely difficult to machine accurately channels smaller than 500 µm. In previous studies (Li et al., 2012; Baart et al., 2011; Westerberg et al., 2010) this methodology was used but the main problem was the grease leakages through the joint of the plates and the micro-channel size limit.

The recent improvement in 3D printer resolution has made 3D printers a viable alternative for machining microfluidic circuits. Here polyjet technology has made it possible to manufacture faster and cheaper than EDM. Bonyar et al., 2010 used this technology to manufacture molds used in soft lithography to build PDMS micro-channels, substituting the lithography step used on another photopolymer called SU8. According to Bonyar et al., 2012, 3D-printed molds could be manufactured much faster than conventional ones. However, focusing on the accuracy of the printed parts it was concluded that the accuracy is higher for the glossy printing mode (resulting in a glossy surface finish) compared to the corresponding matt mode. A disadvantage with the glossy mode however, is an induced channel widening due to the leaning of the photopolymer material after deposition, which limits the achievable channel dimensions (Bonyar et al., 2012).
In their study, Bonyár et al., 2012 always used the 3D printer for mold manufacturing but they never used it for micro-channel manufacturing.

In this paper, we propose a novel manufacturing technique based on building the micro-channels by using a 3D printer directly and then sealing them using glass slides and ultra violet (UV) curable glue. The main advantages of this system are that it is faster than the current technologies and it is more cost-effective. Furthermore, it is possible to build micro-channels that withstand high pressures without the elastic deformations that other common micro-manufacturing materials such as PDMS suffer.

3. Materials and methods

The novel manufacturing method developed takes advantage of the recently improved resolution in 3D printers to manufacture a RPT part that contains the hose connections and a micro-channel useful for microfluidics. In this section a method to assemble one wall of the micro-channel using UV curable glue with a glass slide is presented – an operation required to prepare the channel for µPIV measurements.

3.1 Materials

The materials used to perform the channel construction and flow measurements are listed below.

- Microscope glass slide of dimensions 76 x 26 x 1 mm according to ISO 8037-1:1986.
- Standard hydraulic hose from Lincoln Industrial Corp., model WEDK4-M6x1. 4 mm diameter tube and M6 x 1 metric thread.
- 31G syringe type (0.25 mm diameter needle).
- UV curable glue (Delo-photobond GB368 curing from 320 till 420 nm). The curing time is 15 s at 55 mW/ cm^2.
- 3D Printing Object 30 Printer from Stratasys using VeroWhitePlus RGD835 modelling material and FullCure 705 support material. The resolution of the printer is 600 dpi (42 µm), 600 dpi (42 µm) and 900 dpi (34 µm) in the x, y and z-axis respectively according to its datasheet. All fabricated structures were first cleaned with pressurized water and subsequently submerged in a 4% NaOH solution for 15 minutes. SolidWorks 2012 was used for designing the objects and STL format was used to export the file to the 3D printer.
- Grease pump from Lincoln Industrial Corp. model QLS 401 - 230VAC. The minimum flow rate in a single output is 0.2 cm^3 and the pressure relief valve actuates at 20.5 MPa.
- Ø6 x 1.5 pressure plastic tube 7.5 MPa at 20ºC (with triple safety) from the manufacturer Lincoln Industrial
- 6 ± 0.1 MPa manometer.
- Polytetrafluoroethylene (PTFE) used at the manometer and hydraulic hose threads.
- Syringe pump KDS410 from KD Scientific.
- Laser from Litron Lasers, model LDY301-PIV.
- Microscope from Leica, model 090-135.003 with 20X objective.
- Software DynamicStudio version 3.40.82 from Dantec Dynamics.
- Micro-particles type MF-Rhodamine B particles with a diameter of 3.23 µm ± 0.06 µm.
- Lithium grease, NLGI grade 1.
- 20 ml syringe.
- Sensofar, microscope confocal model PLu neox with 10X objective.
- Software SensoSCAN version 3.3.1 from Sensofar.

3.2 Methods

In the present study a Rapid Prototyping Printer (RPT) from Stratasys, model Object 30, is considered to directly print channels 250 µm wide and 250 µm thick using VeroWhitePlus, which is a rigid thermoplastic of acrylic type, and microscope glass slides to close the channel configuration. The attachment of both parts will be done using UV curable glue.

The use of RPT allows integration of the connection in the same part where the channel is created. Figure 1a shows an example of the RPT part together with the glass-bottomed part (enclosure) to make µPIV measurements possible. The part manufactured by RPT embeds the micro-channels and the standard hydraulic hose to connect the inlet pipe.

A detail of the RPT part directly manufactured by the printer is shown in figure 1b and figure 1c. Here subfigure 1b shows the top view of the part containing the channel inlet and outlet. Figure 1c is the corresponding bottom view of the part, where two details are emphasized: four centering columns that help during the bonding procedure and an embedded seal around the channel to

prevent the channel from clogging when fixing the glass plate using a UV curable adhesive. The four columns and the seal are the same height.

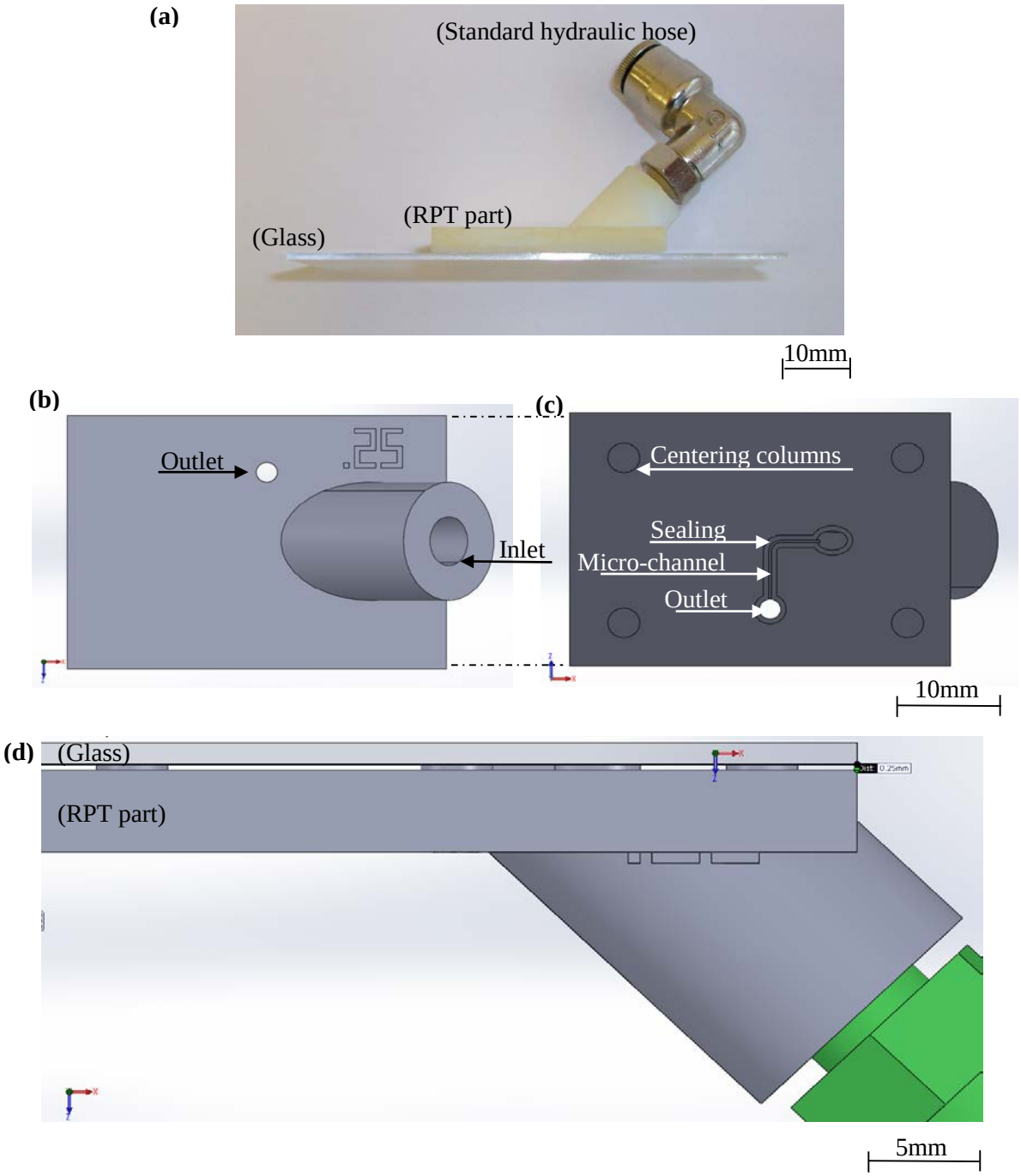

Figure 1. (a) View of the micro-channel assembly. (b) RPT part top view and (c) RPT part bottom view. (d) Assembly detail of the gap between the RPT part and the glass.

The micro-channel and the connection to the hydraulic hose have been manufactured as a single, integrated part using the 3D printer; see figure 1b and figure 1c. The 3D printer has two different surface finishes: firstly a glossy finish having a surface roughness (Ra-value) of the order of 10 nm and secondly a matt finish having a Ra-value of the order of 1.5 µm. According to Bonyár et al., 2012 the glossy surface finish distorts the final dimensions of the channel, which would consequently generate more reflections during µPIV measurements (Stanislas et al., 2003). Therefore a matt surface finish has been considered.

Once the actual part has been printed, the support material is removed using pressurized water and the thread to connect the hydraulic hose is hand-tapped. The RPT part is then first submerged in a 4% NaOH solution for 15 minutes and thereafter in de-ionized water for 15 minutes. To seal the top surface of the micro-channel, standard glass slides with a dimension of 26 mm x 76 mm x 1 mm are used; see figure 2a-b. In order to withstand the high pressure, the glass is bonded to the RPT part using a flexible UV curable adhesive labeled Delo-photobond GB368. Before the bonding procedure all the parts are cleaned and compressed air is used to dry the RPT part. To clean the glass substrate, it is submerged in acetone for 10 min. and methanol for 10 min. respectively. Subsequently, it is boiled in a piranha solution (H_2SO_4:H_2O_2 = 3:1) for 15 min. The slides are then immersed in de-ionized water for 5 min. and dried using nitrogen gas. Finally, the cleaned glass substrates are placed in a conventional oven for 20 min. at 85 ºC and after that dried using compressed air.

To start the bonding procedure two glue drops are placed near the columns in order to hold the glass in place and mechanical pressure is applied to ensure good contact (figure 2a), whereafter a first UV curing is carried out; see figure 2b. Then the gap between the glass and the surface of the RPT part is filled with glue using a syringe of type 31G (needle Ø 0.25 mm); see figure 2c. This step is critical because if the glue arrives at the seal and it is not cured fast enough it can fill the channel due to the generated capillarity forces. Finally the part is placed under the UV exposure lamp just when the glue is near the seal; see figure 2d. After the perimeter of the channel is sealed, the rest of the surface is filled with glue in order to distribute the pressure uniformly during working conditions.

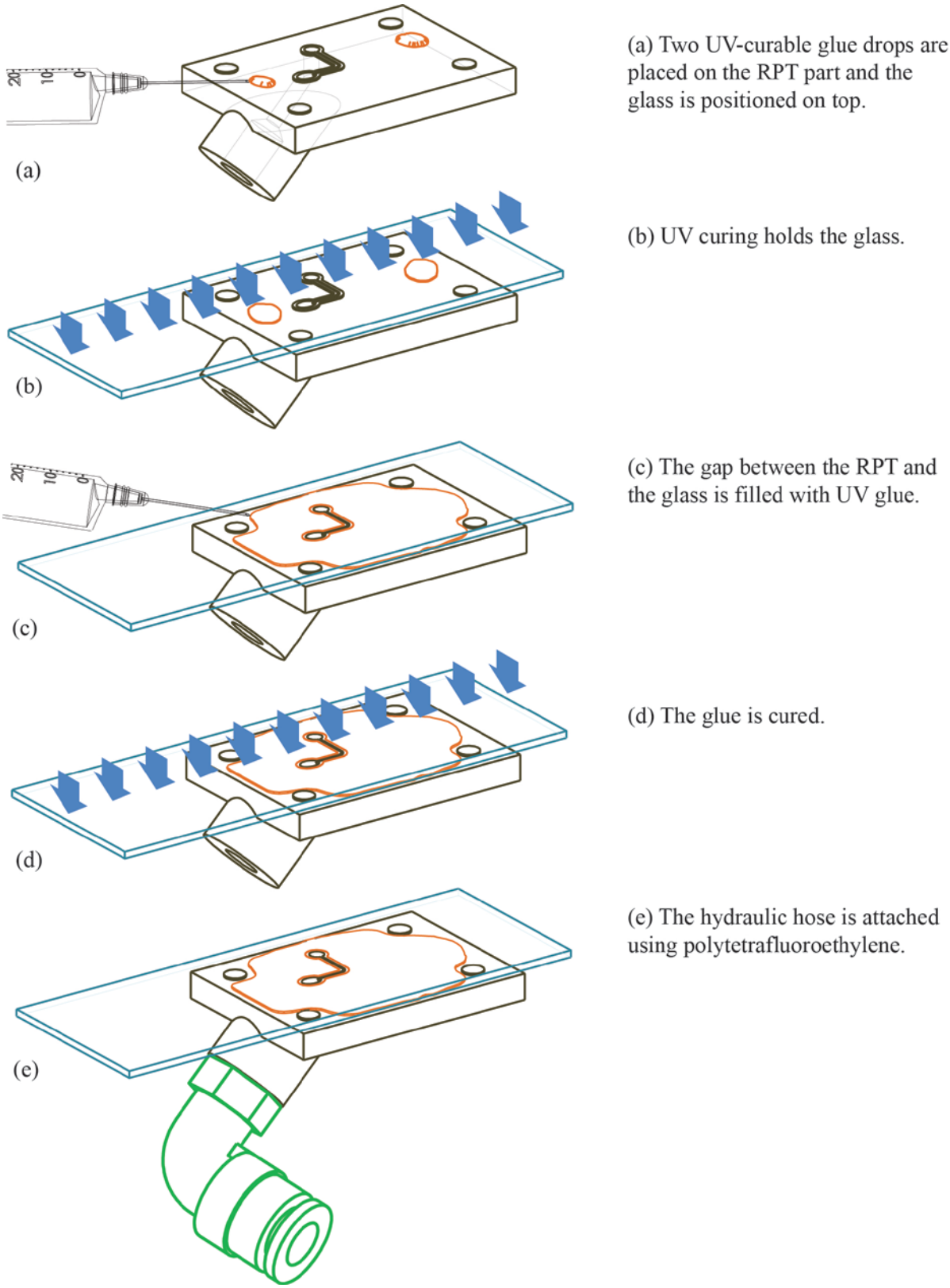

Figure 2. Fabrication steps of micro-channels suitable for high operating pressures and µPIV measurements.

4. Experiments

To verify the quality of the RPT micro-channels and the possibility to use them in high-pressure µPIV measurements, two parameters are evaluated: firstly the maximum pressure without leakages at the channels, and secondly the channel transparency without µPIV reflections. To evaluate these parameters, two experimental setups are prepared. In figure 3 the experimental setup to determine the maximum pressure without leakages at the channels is presented. Here the RPT part was specially designed to connect a manometer at the outlet measuring the pressure at the end of the micro-channel. The obtained value is compared to the pump manometer to verify that the pressure is transmitted along the grease circuit and to measure the pressure losses in the pipe connecting the grease pump outlet with the micro-channel. The pump is set for manual injection of the grease and when the manual injection button is pulsed, the grease pump will inject 0.2 cm^3 of grease in the circuit shown in figure 3. So at the beginning of the experiment, the grease circuit is filled using the manual button without the manometer at the outlet. When there is grease flow at the outlet, the manometer is connected to close the circuit. The pressure difference between the inlet and outlet is 0.2 MPa at 20 ºC.

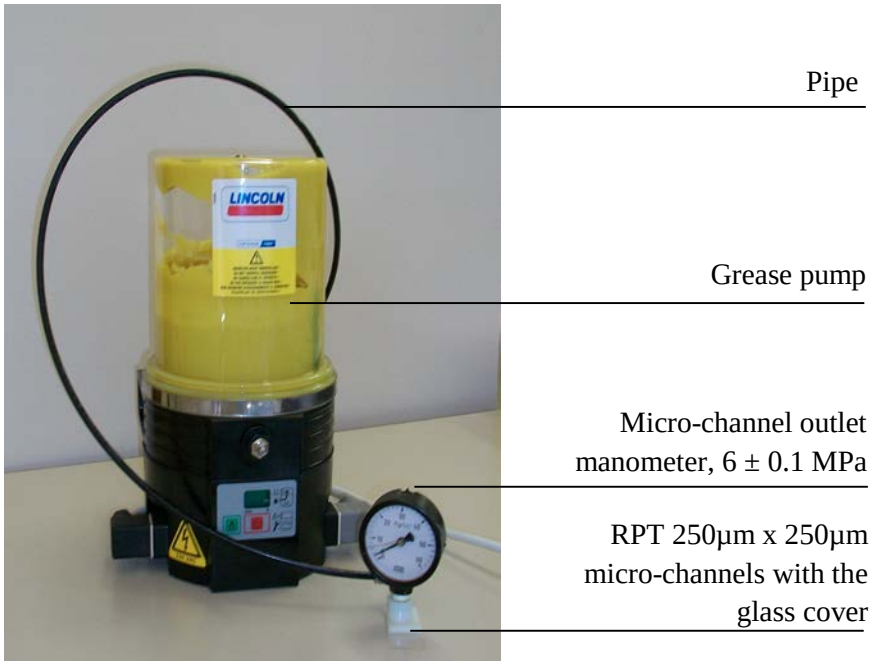

Figure 3: Experimental setup to determine the maximum pressure without leakages and fractures at the channel structure.

In order to reach the maximum pressure, the amount of grease is increased manually using the greasing button on the grease pump. The procedure to obtain the maximum pressure is as follows: inject grease, wait until the pressure difference between the pump manometer and the channel outlet manometer is 0.2 MPa, and when the pressure remains unchanged for 10 minutes proceed to inject grease using the manual greasing button. The detection of leakage is then ocular, done by monitoring the outlet manometer pressure.

Figure 4 shows the experimental setup used to validate the manufacturing technology with respect to µPIV characterization. The main principle behind PIV is to take pictures of a particle-seeded material (fluid); grease in this case. The light source is a doubled-pulsed laser enabling a series of double-framed pictures separated by a given time difference. PIV is non-intrusive meaning no probes have to be inserted into the fluid to perform the measurements – hence avoiding the possible problem of an inserted object perturbing the flow motion. The method is also indirect as the analysis is performed on the motion of the seeded particles – which in turn makes it crucial that the particles follow the flow motion. Suitable particles are chosen with background to the fluid density and the required light signal to be obtained. The motion of the particles is tracked using Fast Fourier Transform (FFT) and a correlation algorithm resulting in data of the fluid velocity in the actual plane of measurement. Compared to PIV in macroscopic geometries where the plane is set by a laser sheet formed by imaging optics, the plane in µPIV applications is set to the focal plane of the microscope objective as the laser light illuminates the whole volume. In the present study the tracer particles used are fluorescent MF-Rhodamine B particles having a diameter of 3.23 µm ± 0.06 µm. As shown in figure 4 the RPT part micro-channel is positioned over an inverted microscope and a high-speed camera is used to take pictures of the particle-doped grease flow.

Also, in terms of details of the micro-channel (material and manufacturing process) - which is the prime objective the present paper - it is of specific importance to have channels which prevent reflections from the laser light as these will impair the quality of the measurements.

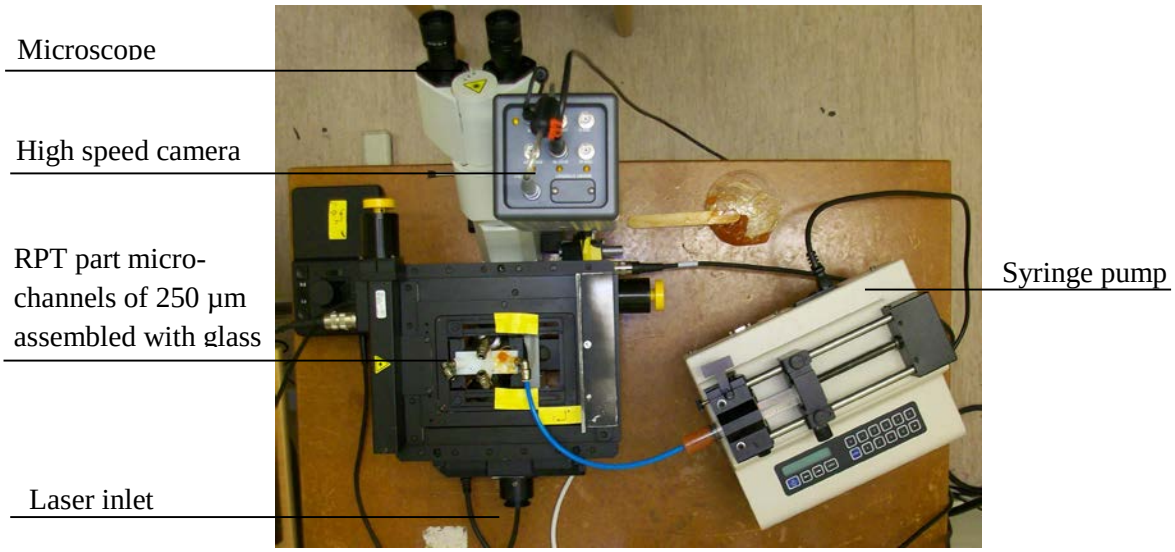

Figure 4. Setup of a µPIV experiment using an RPT part with a 250 µm square micro-channel.

The channel is validated through µPIV measurements, which test whether reflections are present, as well as monitoring the velocity distribution in the channel; see figure 5b for a measured velocity profile in the channel. This novel method investigates the possibility to continue the work in (Green et al., 2011; Li et al., 2013; Li et al., 2012; Baart et al., 2011; Westerberg et al., 2010) to also comprise high pressure flow and flow in a new set of smaller dimensions introducing shear rates being at least of an order of magnitude greater than what has been considered in the studies cited above. Based on these objectives, two flow rates were considered: a very low flow rate of 0.012 ml/

min., corresponding to a maximum velocity of the order of 0.0032 m/ s, and a higher flow rate of 0.125 ml/ min., corresponding to a maximum velocity of the order of 0.03 m/ s.

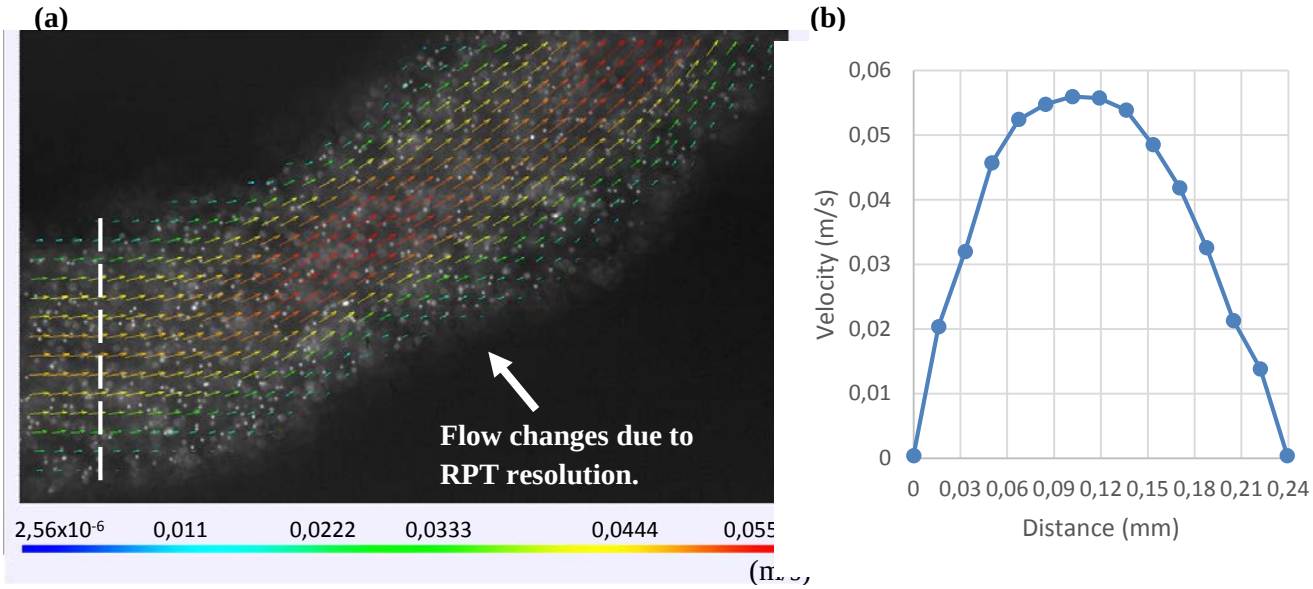

Figure 5. Flow rate of 0,125 ml/min. at straight micro-channel of 250 µm x 250 µm. (a) Microscope picture with an objective of twenty times superposed with the average vectors velocity calculated from the µPIV measurements. (b) Velocity profile at the dotted line of figure (a), the elbow entrance.

5. Results and discussion

The pressure tests were performed three times with different micro channels of 250x250 μm^2 and the results indicate that the micro channel can withstand pressures of up to 5 MPa (μ = 5 MPa, σ = 0.2 MPa) without leakages. Leakage was observed to first appear in the hose connector threads, hence indicating this to be the weakest point of whole setup. The channel material performed properly however and no cracks were observed on it.

Since the tensile strength of the glue is 20 MPa (Delo Technical Information, 2012) and the cross section of the expected channels are in the micron range (i.e. 250x250 µm), the channel- to bonding area ratio is much lower than 1 and the effect of the channel dimensions to the withstand pressure is negligible. If larger channels are required, this ratio could be increased keeping at least the ratio equal to 1.

Figure 5b shows the velocity profile at the middle of the straight inlet section of the channel (cf. Figure 1c) and figure 5a presents the velocity vector field at the elbow. The visible dots are the tracer particles in the grease. The µPIV measurements performed show that is possible to obtain high quality velocity measurements in the channel. However, some perturbations in the flow were detected close to the elbow boundaries of the channel; see figure 5a. These perturbations are caused by dimensional changes in the channel due to the printer resolution (accuracy) in the x, y, and z directions: 42 µm in x and y direction and 34 µm in the z direction respectively. In Figure 5a a

bump is visible at the lower boundary at the beginning of the elbow which causes a locally distorted flow around this region. Therefore, it is important to analyze the accuracy of the printer when manufacturing micron-sized-channels, to evaluate the limits of this novel fabrication technique.
The part shown in figure 6 has been printed to evaluate the quality of the micro channels containing elbows and/or curves, either aligned with the printer axis (bottom of the printer part) or at 45º angle (top of the printed part). Printing these geometries requires synchronization between the x- and y-axis of the printer, and always in the curved section and in the 45º channels.

The six manufactured micro channels have a square cross section with a side length ranging from 150 µm to 650 µm, with 100 µm increments. In each channel 5 different cross sections (see figure 6) were measured using confocal microscopy and since the part are thought to study tribology applications the grease intake has also been analyzed. The parts were completely submerged in grease during 7 days (168h) at 40ºC. The part weight was measured before the test and after. The weight change is summarized in Table 1. After the test, pressure was applied to the channels to verify that the glue withstanded the same pressure. According to the results, the parts absorbed less than 1% in weight and suffered a little change in colour.

Conditions	Not submerged, only 168h at 40ºC	Submerged with grease type NLGI-2 during 168h at 40ºC	Submerged with grease type NLGI-1 during 168h at 40ºC
Weight change	-0,11%	0,07%	0,21%

Table 1: Grease intake of VeroWhite material

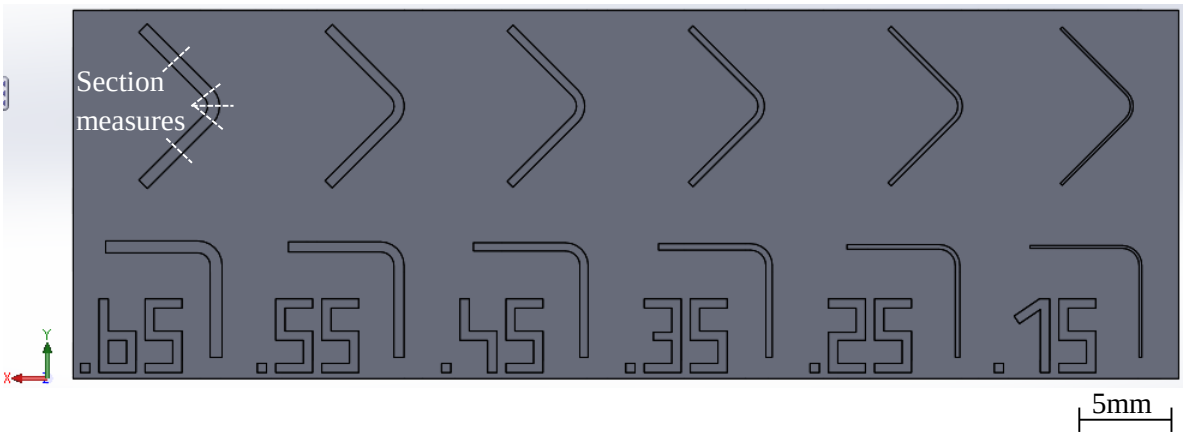

Figure 6: RPT part to evaluate the printing quality between micro channels oriented 45º to the x axis of the 3D printer and micro channels oriented in the same direction as the x-axis of the 3D printer.

Confocal microscopy provides the whole topography of the channel, see figure 7a and the topography can be analyzed at each cross-section, see figure 8. Figure 8a clearly illustrates the building process layer by layer, where we notice minimum layer thickness of resolution in z (Δz). Figure 7b plots the histogram of the different heights presents in the confocal image and we can see the two side bands around the expected height showing the effect of the resolution of the printer in some cross-sections. But the effects of the printer resolution in x and y-axis are shown in figure 7a where we can appreciate the waviness of the wall, due to the positioning precision of the laser head. As illustrated in figure 7a due to x/y resolution, the width is not constant all along the channel, causing constriction points in the x and y direction, which as a consequence narrows the channel at some locations down to 210 µm and hence affects the channel flow at the boundaries. These two effects have been analyzed the six mentioned samples and the results are summarized in figure 9 and figure 10, where the average value of channel-depth and channel-width is plotted for both cases when the printer axis are aligned with the manufactured channel and when they are tilted 45º.

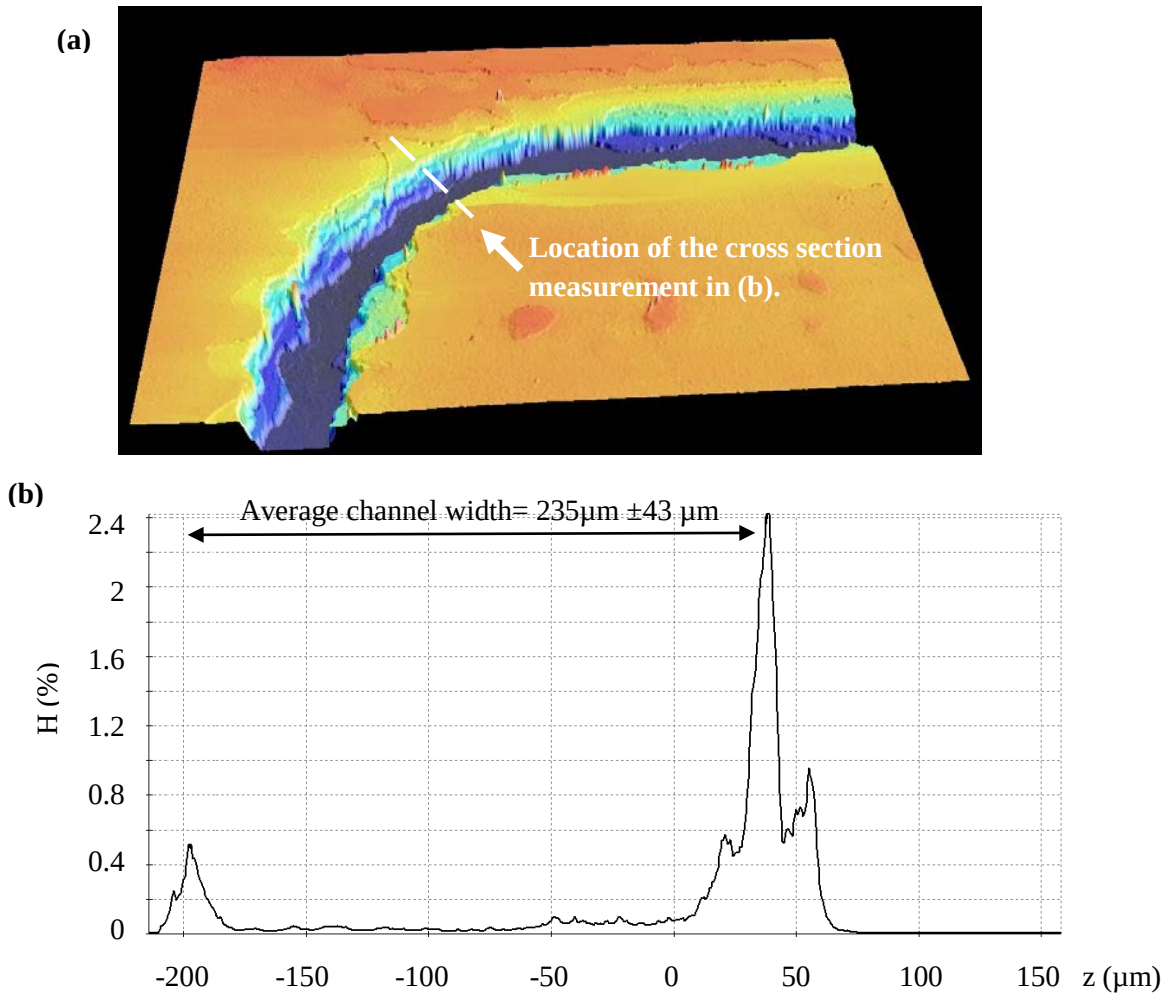

Figure 7: Microscope confocal topology analysis. (a) 3D view of the micro-channel. Figure 10 shows the cross section at the elbow. (b) Histogram of the micro-channel.

According to the results shown in Figure 9, the manufacturing depth is reliable and does not depend on the micro-channel orientation with respect to the axis of the 3D printer. In terms of the channel width accuracy/reliability, the channels tilted 45º with respect to the manufacturing axis tend to be up to 25 µm wider than the micro channels manufactured with the same x/y-axis direction. Concerning the repeatability of the channel width for the manufacturing process, it is shown that micro channels manufactured at an angle of 45º to the axis of the 3D printer have two times higher standard deviation at lower dimensions (250 µm) compared to the 650 µm width case. In terms of curvatures, even though the printer can print acute angles (< 45º), sealing this type of channels is challenging since the strong capillary flow generated in the acute angle area that can drive the glue inside the channel is clogging it. Furthermore, the current printer accuracy (42 µm in the x- and y direction and 34 µm in the z direction respectively) makes this process not feasible to manufacture channels smaller than 250 µm since the measured topography of the channels with a width of 150 µm shows that the desired width is impossible to obtain. In order to manufacture a channel using the 3D Printing Object 30, the ratio between the channel dimension and the manufacturing axis accuracy should not be less than 4.7. The required distance between channels should be in the same range (at least 200 µm) not only to ensure the channel definition but also to fill the cavities between them accurately with the UV glue and therefore provide good sealing.
This condition is illustrated when the orientation of the micro channel coincides with the x- and y-axis of the 3D printer. For this case it is shown that a micro channel up to 150 µm can be manufactured; however, the length scale of the deviation from an ideally flat wall due to the printer accuracy is of the same order of magnitude as the width of the channel, meaning the flow may be restricted at some locations in the channel. But for the case of a channel with 45° orientation, a width of 150 µm is impossible to obtain, meaning the minimum width should be 250 µm. Caution should though be considered before bonding as the channel surface at the elbow may have irregularities perturbing the flow.

Figure 8 shows two channels with a width of 250 µm. In figure 8a the channel is oriented along the manufacturing axis while in figure 8b it is tilted 45º. It is clear that the worst case in terms of the waviness of the channel wall is for the channel oriented 45° to the axis of the 3D printer. But as the dimensions are increased up to 350 µm the relative waviness improves and consequently the positive effect from tilting the channel with respect to the manufacturing axis is reduced; see figure 12 which corresponds to the 350 µm wide channel oriented 45º to the x-axis of the 3D printer.

The surface roughness measured at the bottom of the micro-channel shows that for channel sizes smaller than 250x250 µm its standard deviation increases as the micro-channel size decreases. Moreover, in micro-channels bigger than 250x250 µm the roughness is shown to not depend on the micro-channel dimension; the average Ra value is 1.87 µm and the standard deviation is 0.78 µm. Figure 11 shows the results for the Ra measurements for each micro-channel cross section.

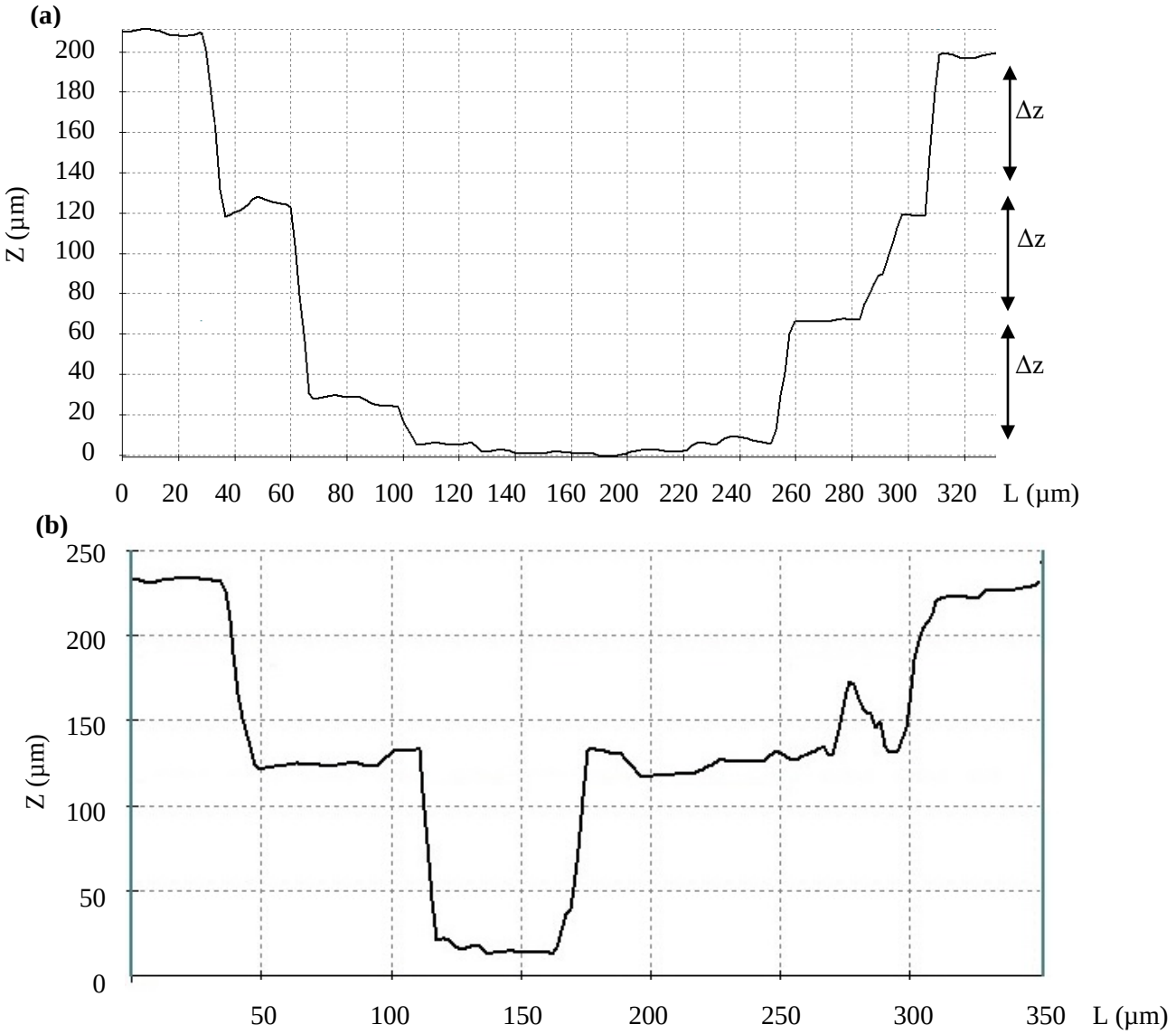

Figure 8: Cross section of the 250 µm micro channel figure 7a). (a) Printed oriented along the 3D printer manufacturing axis (b) Printed 45º to the x-axis of the 3D printer.

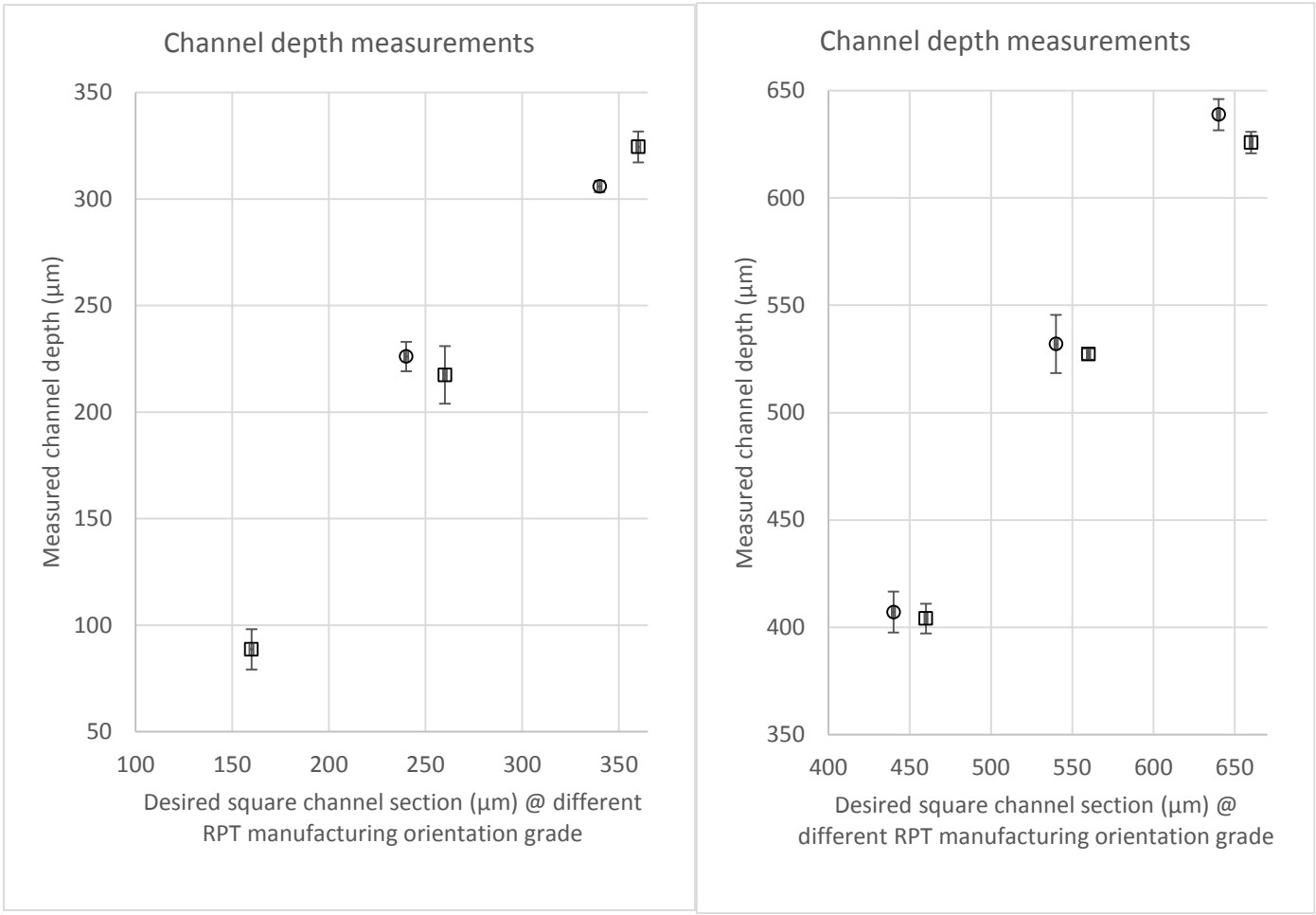

Figure 9: Channel depth measurements. The squares represent channels manufactured where the x- and y-axis coincide with the axes of the 3D printer. The circles represent the corresponding case where the channel is oriented 45º to the x-axis of the 3D printer.

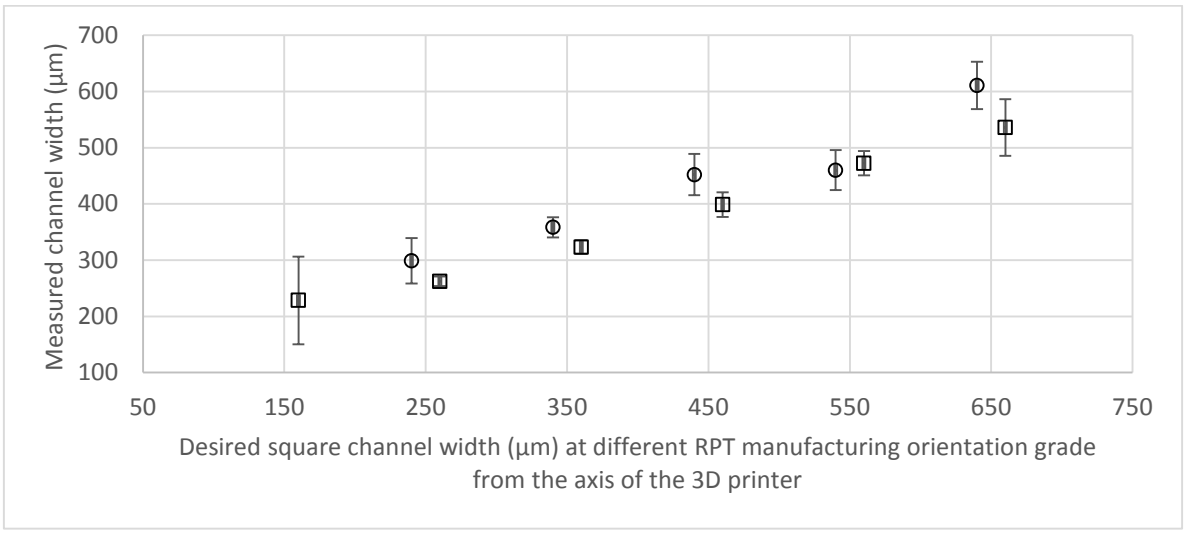

Figure 10: Channel width measurements. The squares represent channels manufactured where the x- and y-axis coincide with the axes of the 3D printer. The circles represent the corresponding case where the channel is oriented 45º to the x-axis of the 3D printer.

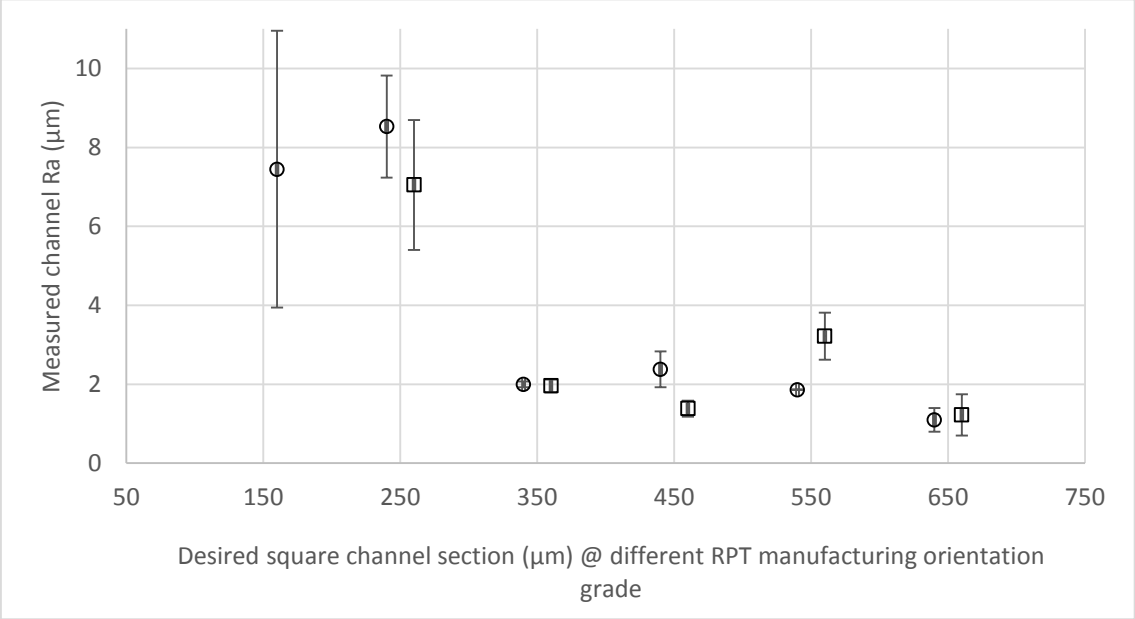

Figure 11: Channel roughness measurements. The squares represent channels manufactured where the x- and y-axis coincide with the axes of the 3D printer. The circles represent the corresponding case where the channel is oriented 45º to the x-axis of the 3D printer.

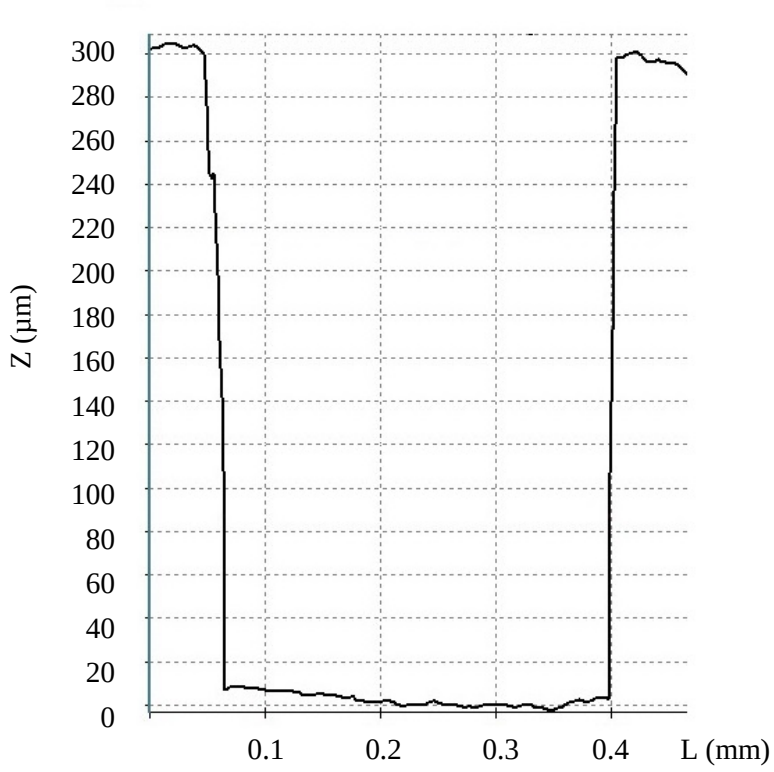

Figure 12: Cross-section of the 350 µm micro channel printed 45º to the x-axis of the 3D printer

The printer time of the RPT part used in Figure 1 is 102 minutes. This time could be minimized integrating more micro-channels in the same RPT or printing more than one RPT at the same time. The assembly time depends on the skill of the technician; for the proposed part the average time is 15 minutes. The material consumption to print the RPT parts is presented in Table 2. Therefore, the average manufacturing time and material consumption makes this process very competitive compared to previous methods using micro-fabrication technologies such as soft lithography or micro-machining.

VeroWhitePlus RGD835 consumed (1€/gr)	FullCure 705 Consumed support material. (1€/gr)	Microscope glass slides cost	UV glue cost (2€/ml)	Total cost
9gr (9€)	6gr (6€)	0.1€	0.2ml (0.4€)	15.5€

Table 2: RPT material consumption by the RPT part of Figure 1.

6. Summary and conclusions

The presented novel micro-manufacturing technique that takes advantage of RPT printing and UV curable glue opens the possibility to obtain micron-sized channels that can withstand pressures higher than 5 MPa. This manufacturing technique is much faster than previous micro-manufacturing techniques where different steps were needed to obtain the micro-machined parts. However, due to current 3D printers resolutions (around 50 µm) and according to the experimental results, channels smaller than 250 µm x 250 µm in cross-section should not be used to characterize fluid flow behaviors using micro Particle Image Velocimetry, since inaccuracies in the channel boundaries can deeply affect the fluid flow behavior which is accentuated in curved sections.

7. References

Armani D, Liu C and Aluru N (1999), "*Re-configurable Fluid Circuits by PDMS Elastomer Micromachining*" Proc. Annual International Workshop on Micro Electro Mechanical Systems, Orlando, Florida 17-21 January 222-227.

Baart P, Green T, Li J, Lundström T S, Westerberg L G, Höglund E and Lugt P (2011), "*The influence of speed, grease type, and temperature on radial contaminant particle migration in a double restriction seal*" Trib. Trans. 54 867-877.

Bonyar A, Santha H, Ring B, Varga M, Kovacs J G and Harsanyi G (2010), "*3D Rapid Prototyping Technology (RPT) as a powerful tool in microfluidic development*" Proc. Eng. 5 291–294

Bonyár A, Sántha H, Varga M, Ring B, Vitéz A and Harsányi G (2012), "*Characterization of rapid PDMS casting technique utilizing molding forms fabricated by 3D rapid prototyping*" Int. J. Mater. Form. doi: 10.1007/s12289-012-1119-2

Brittain S, Paul K, Zhao X M and Whitesides G. M (1998), "*Soft lithography and microfabrication*" Physics World May 13 1998 31-36.

Ciftlik A T and Gijs M A M (2012), "*Parylene to silicon nitride bonding for post-integration of high pressure microfluidics to CMOS devices*" Lab Chip 12 396-400.

Egham W EP (2006), "*High pressure lubricant pump for steelworks*". European Patent EP1914425B1.

Green T, Baart P, Westerberg L G, Lundström T S, Höglund E, Lugt P and Li J (2011), "*A new method to visualize grease flow in a double restriction seal using microparticle image velocimetry*" Trib. Trans. 54 784-792.

Hardy B S, Uechi K, Zhen J and Kavehpour H P (2009), "*The deformation of flexible PDMS microchannels under a pressure driven flow*" Lab Chip 9 935-938.

Inglis D W (2010), "*A method for reducing pressure-induced deformation in silicone microfluidics*" Biomicrofluidics 4 026504 doi: 10.1063/1.3431715.

Lewpiriyawong N and Yang C (2008), "*Dielectrophoretic manipulation of particles in a modified microfluidic H filter with multi-insulating blocks*" Biomicrofluidics 2 034105.

Li J, Höglund E, Westerberg L G, Green T, Lundström T S, Lugt P M and Baart P (2012), "*μPIV measurement of grease velocity profiles in channels with two different types of flow restrictions*" Trib. Int. 54 94–99.

Li J, Westerberg L G, Höglund E, Lundström T S, Baart P, Lugt P (2013), "*Lubricating grease shear flow and boundary layers in a concentric cylinder configuration*" Proc. 3rd International Tribology Symposium of IFoMM (International Federation for the Promotion of Mechanism and Machine Science), Luleå, 19-21March 2013.

Madadi H, Mohammadi M, Casals Terré J and Castilla López R (2013), "*A novel fabrication technique to minimize PDMS-microchannels deformation under high-pressure operation*" Electrophoresis 4(22-23), 3126–3132 doi: 10.1002/elps.201300340.

Sanchez J, Rudyk S and Spirov P (2013), "*Removal of Grease from Wind Turbine Bearings by Supercritical Carbon Dioxide*" Chem. Eng. Trans. 32 1909-1914.

Stanislas M, Okamoto K and Kähler C (2003) "*Main results of the First International PIV Challenge*" Measure. Sci. Tech. 14 R63–R89.

Sultan M A, Fonte C P, Dias M, Lopes J C B and Santos J R (2012), "*Experimental study of flow regime and mixing in T-jets mixers*" Chem. Eng. Sci. 73 388-399.

Gervais Thomas, El-Ali Jamil, Günther Axel and Jensen Klavs F. (2006). "*Flow-induced of shallow microfluidic channels"* Lab Chip 6(4), 500-507, doi: 10.1039/b513524a.

Weibel D B, DiLuzio W R and Whitesides G. M (2007), "Microfabrication meets microbiology" Nature 5 209-218.

Westerberg L G, Lundström T S, Höglund E and Lugt P (2010), "*Investigation of grease flow in a rectangular channel including wall slip effects using micro particle image velocimetry"* Trib. Trans. 53 600-609.

Wu Willie, DeConinck Adam, and Lewis Jennifer A. (2011), "*Omnidirectional Printing of 3D Microvascular Networks*" Advanced healthcare materials 23 178-183.

Delo Technical Information. (2012). "*Delo-photobond GB368 Technical Information*", available at http://www.syneo.net/pdf/Colle/PB/colle-acrylate-uv-verre-DELO-PHOTOBOND_GB368_%28TIDB-GB%29.pdf (accessed 15 May 2014).

PUBLICATION C

Grease flow in an elbow channel

Lars G. Westerberg • Josep Farré-Lladós • Jinxia Li • Erik Höglund • Jasmina Casals-Terré

Tribol Lett (2015) 57:30
DOI 10.1007/s11249-015-0469-6

PUBLICATION D

Embedded micro-nozzles in the pitch gear dededum to minimize wear at zero degree position.

Josep Farré-Lladós[1], Lars G. Westerberg[2] and Jasmina Casals-Terré[1]

1. Mechanical Engineering Department, UPC - Technical University of Catalonia, Terrassa, Spain.
2. Division of Fluid and Experimental Mechanics, Luleå University of Technology, Luleå, Sweden.

ABSTRACT

In this paper, we present a novel method for automatically lubricate the pitch gear teeth while they are in contact and the wind turbine is generating. A micro-nozzle to continuously inject fresh grease in between the teeth in contact has been designed, manufactured and installed in a test bench of a 2 MW wind turbine pitch system. The test bench has been used to characterize the fatigue behavior of the gear surface using conventional wind turbine greases under real cyclic loads, showing a delay of $2x10^4$ cycles in the appearance of wear.

KEYWORDS

Power Generation, Gears, MEMS Devices, Open Gears, Grease Application, Greases, Abrasive Wear, Corrosive Wear, Oxidative Wear

1 INTRODUCTION

Renewable energies and more specifically wind power generation have, in recent years, been a sector that has grown in market share with significant energy generation. In the wind sector, this

growth has led to the design and implementation of machines with greater power generation capacities.

In order to design more efficient wind turbines, manufacturers are increasing the rotor diameter to capture more kinetic energy from the wind and increase energy generation; therefore the stresses and deformations are increasing in all parts of the wind turbine, such as the foundations, yaw, nacelle, tower and drive train unions. Most of these unions are static, except for: the drive train that transmits torque, the yaw system that turns the nacelle and the pitch system that turns the blade around its axis as Germanischer Lloyd Industrial Services (1) reports. During dynamic operation of the wind turbine, the yaw and pitch bearings suffer from sequential traction – compression stresses that cause millions of micro-movements per cycle between the gear teeth. Therefore the thickness of the lubricant between the teeth is reduced and direct contact between metal surfaces occurs. The wind turbine manufacturers observed a new phenomenon that appears in high power wind turbines: excessive wear in the tooth located at 0º in the pitch bearing. Currently, to slow this phenomenon the pitch gear lubrication at the zero degree position is carried out during unwind periods or programmed stops. These programmed stops cause important losses in electricity generation.

Figure 1 shows, as an example, the operation graphic (ideal power curve) of a 2MW wind turbine at the different wind speeds. At low winds (in the example in Figure 1 with wind speeds 3 to 17m/s) being this the 0º position. When the wind turbine arrives to its nominal power (high wind speeds) the pitch system starts to actuate resulting in a system stable in oscillation (the pitch is continuously in movement due to the thrust and velocity wind changes). In a wind farm, the wind rose distribution under low winds is the most common situation, more than 60% of the operation time, during this time the wind turbine works at pitch 0º position.

Focusing on the pitch systems, Gamesa Innovation in 2008 (2) described the different types of pitch systems that are currently installed in wind turbines: pinion-corona, hydraulic system and cogged belt. The excessive wear at pitch is only present in pinion-corona systems, and it is currently a major issue as Holierhoek (3) reports. Furthermore the wind turbine manufacturer's tendency is to increase the rotor diameter to capture more wind kinetic energy and increase energy generation; therefore the stresses and deformations are increased in all parts of the wind turbine, even in non-static unions such as: the drive train that transmits torque, the yaw system that turns the nacelle and pitch system that turns the blade around its axis, factor that contribute to accelerate the wear at the gears.

During the dynamic operation of the wind turbines, the pitch bearing system repeatly suffers from sequential traction and consequently compression stresses causing millions of micro-movements per cycle. This phenomenon together with long periods operating the pitch in the same position produces friction between the teeth at the 0º position due to the absence of the grease layer, as mentioned Holierhoek (3) and Andreas (4).

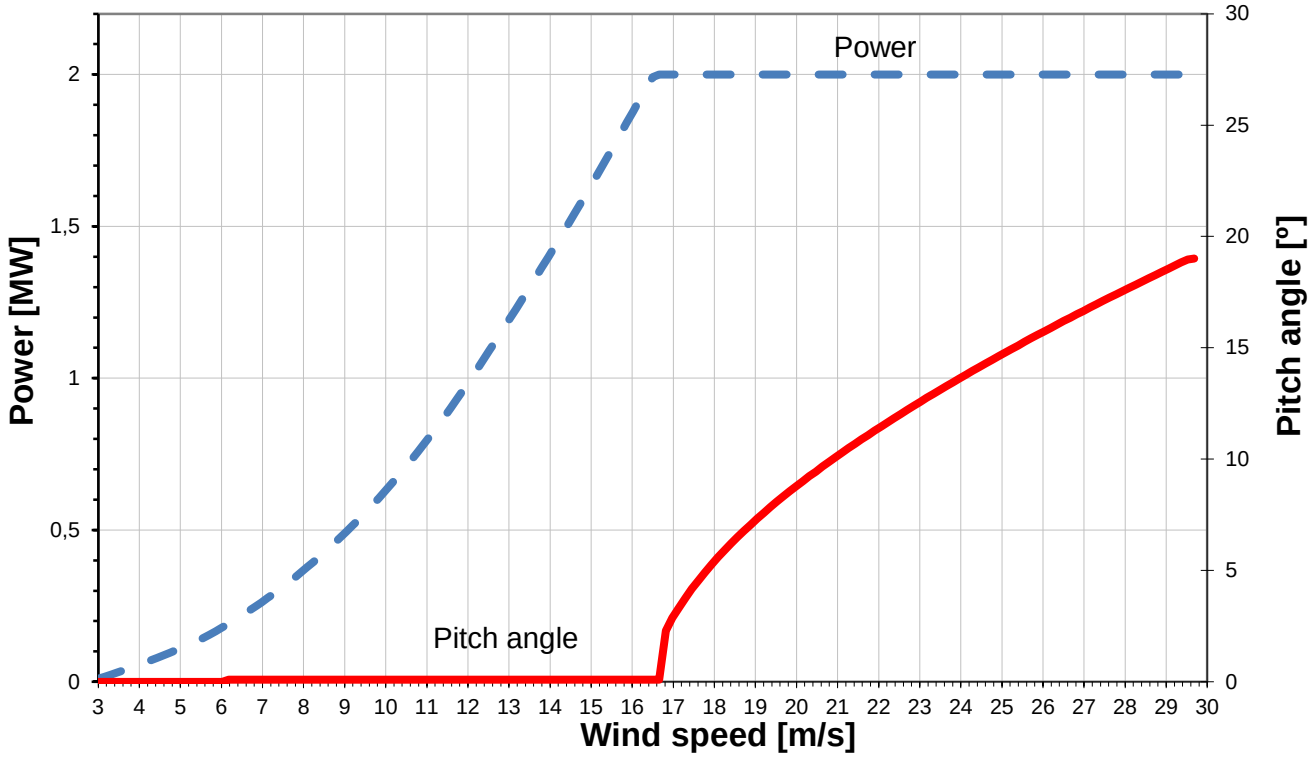

Figure 1: 2MW wind turbine operation graphic. Wind velocity -horizontal axis-. Y-axis: Wind turbine power generated -ideal power plot- and Pitch angle.

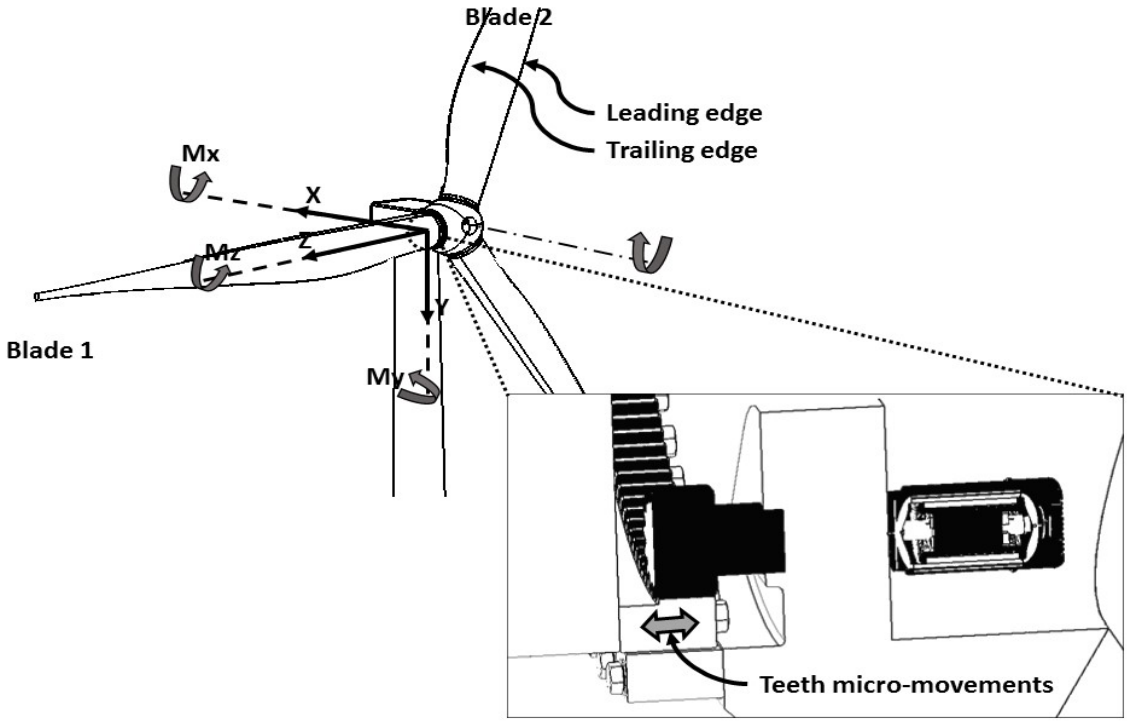

Figure 2: Wind Turbine hub with the blade coordinate system from the Germanischer Lloyd Industrial Services (1). The arrow represents the micro-movements in the pitch teeth system due to the dynamic wind turbine operation. More details of the cross section in Figure 6.

Some researchers have already presented solutions and strategies to minimize the gears wear at specific positions like zero degree position in the pitch system. The proposed solutions essentially tune and modify the system parameters such as surface state (5-6), stress, mechanical contact (7) and tribology (8-10). Parameters that Takadoum in 2008 (11) defined as critical to minimize the effects of wear. The current solutions (5-6) cannot eliminate the preventive maintenance, (7-8) and require expensive parts (another pinion and a compressor respectively). In (9) lubrication is done while the wind turbine operates causing generation loses and (10) is difficult to integrate in ongoing wind turbines due to the necessity of pinion replacement. Methods to measure the excessive tooth wear to predict when the failure will occurs were presented by Mashue et. al. in 2011 (12) or Nordex Energy (13).

This paper research proposes a decrease in the wear of the teeth by increasing the lubrication layer at the contact tooth flank with a novel lubrication system that injects fresh lubricant directly to the contact tooth flank. Figure 3 shows a cross section of a tooth that has a novel injector installed to inject fresh grease directly to the contact tooth flank. In order to develop this new concept of injector, micro-fluidics technology and the micro-manufacturing technology are used. The main advantage of the new system is that extends the tooth lifetime and prevents lubrication stops that consequently increases energy generation per each wind turbine.

The paper is organized as follows: materials and methods introduces the device design principle and its integration in a wind turbine pitch gear. The results and discussion section presents the experimental results of the grease flow test and the test bench validation and points out how this novel method improves the lubrication over current installed solutions and conclusion remarks are presented in the following section.

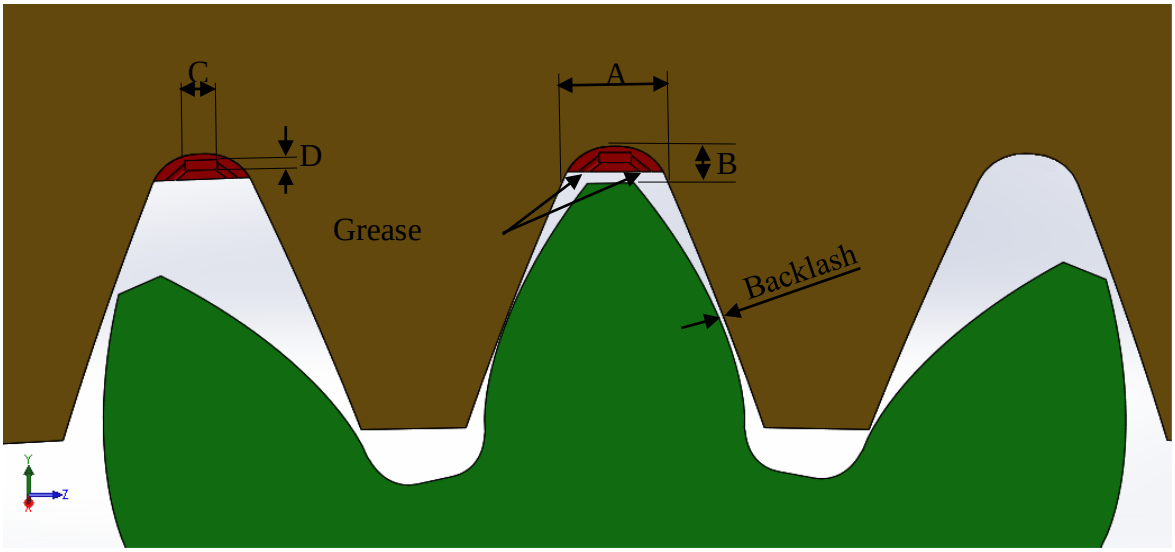

Figure 3: Gear cross-section according to DIN867; 1986 (14). The gear geometry has a dedendum free space (dimensions A per B) where the proposed part is embedded. The dimension B is 0.15 times the dedendum space (50% of the total volume).

2 MATERIALS AND METHODS

2.1 Design Principle

This paper introduces a novel lubrication system that injects fresh grease directly between the contact teeth using a micro-fabricated part embedded in the dedendum position. Figure 3 shows a gear cross-section geometry according to DIN867; 1986 (14), highlighting its maximum dimensions A and B. The standard defines that the dimension B will be between 0.1 and 0.3 times the gear module and in specials cases up to 0.4 times the gear module. Focusing on wind turbine field with pinion-corona pitch systems. If a 2MW wind turbine is used, the module is 12. This module and the common free space (B dimension in Figure 3) is 0.3 times the module, being 3.6 mm for 12-module.

The new micro-nozzle has been designed to fit in only 0.15 times of the module space (50% of the total volume) to prevent the contact between the teeth and the part during elastic

deformations. The final dimensions of the micro-channel are plotted in Figure 3 (D in the range of 500-1000µm and C in the range of 1000-2000µm) and the length of the injector depends on the gear width.

The greases used in open gears, like those present in pitch and yaw gears, have a high viscosity, and its behavior is complex, as Westerberg (15) reports. This property allows the grease to remain in the position where it is injected, in this case the tooth flank but its fluency thought the proposed micro-nozzle should be verified.

2.2 Grease Fluency

Therefore, Micro Particle Image velocimetry (µPIV) technique has been used to analyze the flow behavior of NLGI2 greases in channels that could be integrated in a 12-module gear, see the experimental set up in Figure 4a. The µPIV set up uses a double frame mode, see Figure 4b.

A curved 250x1000 µm2 micro-channel manufactured according to the process presented in Farré-Lladós et. al (16) were used, see Figure 7a. The channels have a minimum width equal to the elbow that the micro-nozzles part has near the outlets Figure 7b. Flow velocity field, see Figure 7c and velocity profile in the cross-section marked Figure 7d could be obtained using this technique. The velocity profile changes along the time and to capture the changes on the time µPIV measurement were done approximately every 5-6 minutes.

The micro-channel was filled using a syringe pump (KD scientific model KDS410) until the grease leaked through the outlet and the pressure was stable to **static pressure point** (circuit losses). After, the experimental flow rate was set to the pump without removing the circuit pressure, flow grease started at lower velocity than theoretical one during the **transitory flow period** (see Figure 8 and Figure 9 the yellow zone). When the grease reaches the theoretical

velocity the **stationary flow period** started (see Figure 8 and Figure 9 the red zone). Two different flow rates were studied: a high flow rate (0.5ml/min) simulating an injection of grease, when the wind turbine starts to work at zero degree position and a low flow rate (0.002ml/min) to simulate the continuous lubrication mode of the zero degree position (few quantity of grease injected). After that, grease samples was checked to see if there were any physical changes such as the separation of the base oil and the thickening agent or chemical changes, such as losing the design properties, additives and components after flowing through a micron-sized channel as DIN 51817 (17) reports. The grease was analyzed using an infrared spectrum analysis and a consistency analysis under the ASTM D1403-02: 2007 (18) to verify that the grease had not suffered any degradation. The infrared spectrum can determine all compounds in the mixture to be analyzed recording the absorption curve for each hydrocarbon, superimposed on the radiant energy background as Heigl et al. (19) reports.

The amount of grease needed per micro-nozzle –each tooth- was determined. Grease manufacturers recommend in the gear's datasheet, 2kg per year in a 139 teeth crown that only works in a 90º degrees section. Therefore, considering that only 35 teeth works, each tooth consumes 57 gr/year. Using a wind industry common grease pump, model QLS 401 from Lincoln, the minimum grease injection is 0.2 cm^3. If NLGI2 grease is used (density 0.99gr/cm^3) 0.198 gr are provided, therefore fresh lubricant should be injected every 30 hours.

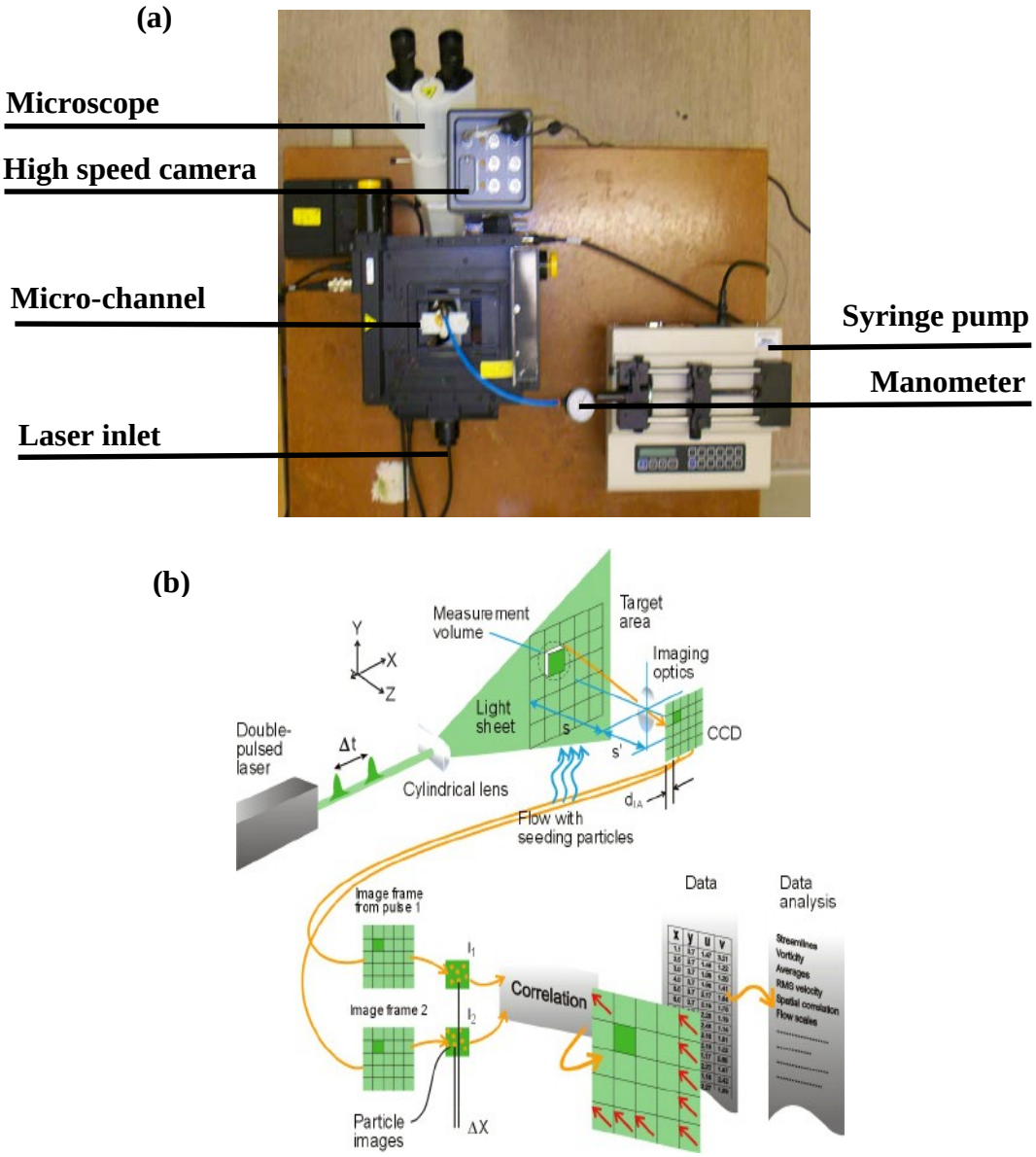

Figure 4: µPIV experimental setup. (a) Top view of the test set up. (b) µPIV

2.3 Micro-nozzle integration in a Wind Turbine Gear Pitch

Later, to analyze the effect of the lubrication through the micro-nozle part on the gear teeth of the pitch system, the part was integrated in a conventional Pitch system with automatic lubrication. Figure 5A shows the schematics of its integration in an ongoing wind turbine lubrication system. The grease pump is connected to an additional selective valve that through an additional grease distributor (teeth) turn aside the grease flow when the wind turbine works at the gear tooth through the proposed micro-nozzle, respecting the original grease schematic system that will

lubricate the rest of the crown through the progressive grease distributor. Figure 5B is a blade detail to show where the grease outlets are connected to each lubrication micro-nozzle (lubrication of the crown and proposed micro-nozzle). The blade is assembled to the pitch bearing and is actuated by the motor through the gearbox. The wind turbine control activates the system through the electric control. Figure 6 shows a 3D view of the integration of the micro-nozzle in a 12-module pitch bearing. This integration can be carried out using a suplementary plate with two thread holes or with two thread holes at the crown to fix the new system.

A

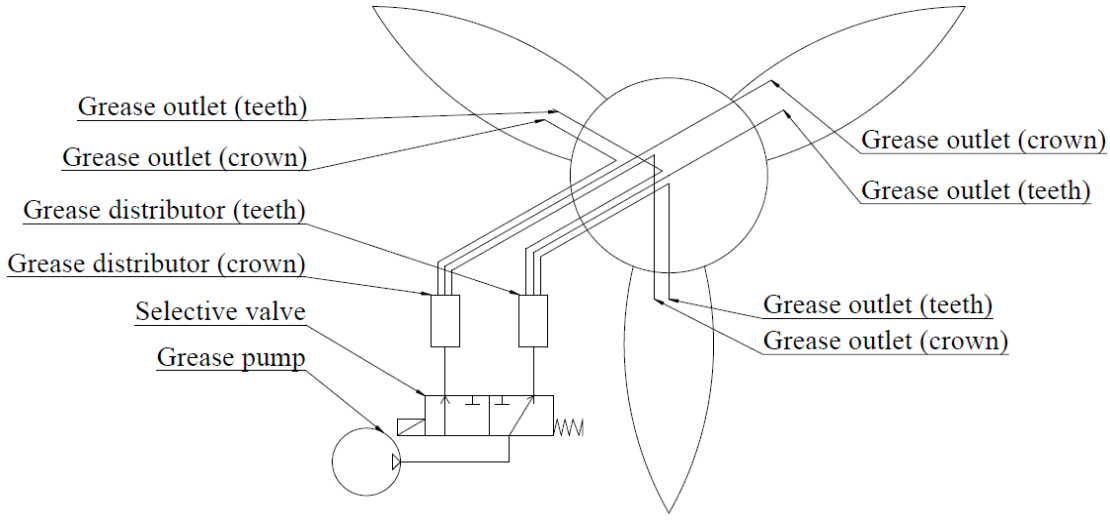

B

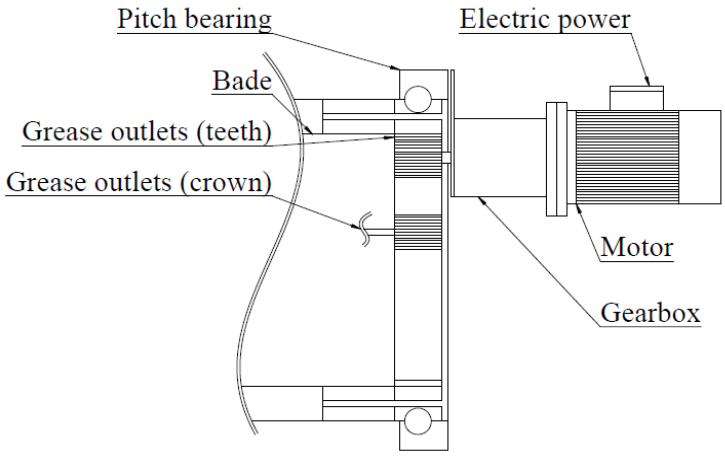

Figure 5: A is the schematic drawing of the micro-nozzles integrated in the wind turbine lubrication system, and B is the integration per each blade.

Finally, the micro-nozzle part is mounted in a test bench, capable to reproduce the phenomena of the excessive wear at 0º position. The test bench simulates operating conditions where the trailing edge of blade 1 (view Figure 2), is values under compression stress while traction stresses occur in the blade leading edge. When the blade is located in the position of the blade 2, the situation is just the opposite as the blade has initiated the descent. The force direction affecting each blade edge has been interchanged, generating a torque Mx. Moreover, an My torque is generated due to the wind turbine regulation with the wind velocity that induces similar traction-compression cycle. Finally each blade suffers an Mz caused by the aerodynamic forces that make it turns around its axis, load that is balanced by the gearbox through the pinion. These main factors needed to reproduce the excessive wear due to wind turbine dynamic operation in the test bench are:

- The blade micro-movements caused by the gearbox backlash (at 0º position the gearbox is braked) due to Mz (as Figure 2 shows, aerodynamic forces acting on the blade. $M_{torsion}$ according to Holierhoek (3) definition).
- The load cycle traction – compression on the blade (Mx and My in Figure 2 or M_{edge} and M_{flap} according to Holierhoek (3) definition) when pitch works at the 0º position (in the example of Figure 1 with wind speeds 3 to 17m/s).

The load operation scenario is summarized in Table 1. The crown hardness is at 58±3 HRC and the pinion hardness is at 24±3 HRC. The lower pinion hardness allows a faster appearance of the wear and in the test bench facilitate the tooth replacement as Mashue (5) reports.

Backlash	Mz/ $M_{torsion}$	Mx/ M_{edge} and My/ M_{flap}
0.5mm at 0.2Hz	Constant ±40KNm	2000 kNm at 0.3Hz

Table 1: Test bench load situation according to Laualgun Bearings Manufacturer.

Using this set up, the grease distribution on the tooth flank was analyzed for different micro-nozzle lengths in a 12-module gear 0.1 m wide. The micro-nozzle cross-section used is represented in Figure 3 (D=250µm and C=1000µm). Table 2 summarizes the different micro-nozzle lengths tested. Each micro-nozzle injected the grease in different position along the gear width; see Figure 10 a Micro-nozzle A, Micro-nozzle B and Micro-nozzle C respectively.

Micro-nozzle (250x 1000µm^2)	Length (m)
A	0.02
B	0.04
C	0.03

Table 2: Micro-nozzle sizes tested.

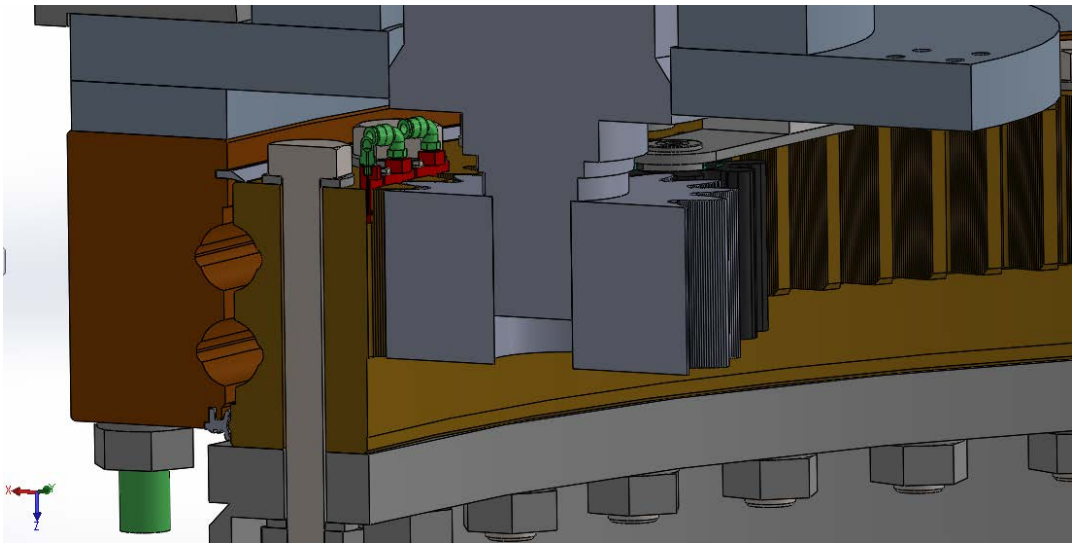

Figure 6: Pitch cross-section at zero degree position

3 RESULTS AND DISCUSSION

3.1 Grease flow test

Figure 8 and Figure 9 show the time evolution of the maximum velocity in the velocity profile and the circuit pressure at 0.002 ml/min and 0.5ml/min respectively. The grease is injected into the circuit and the experiment starts at the static pressure point up to the stationary flow period.

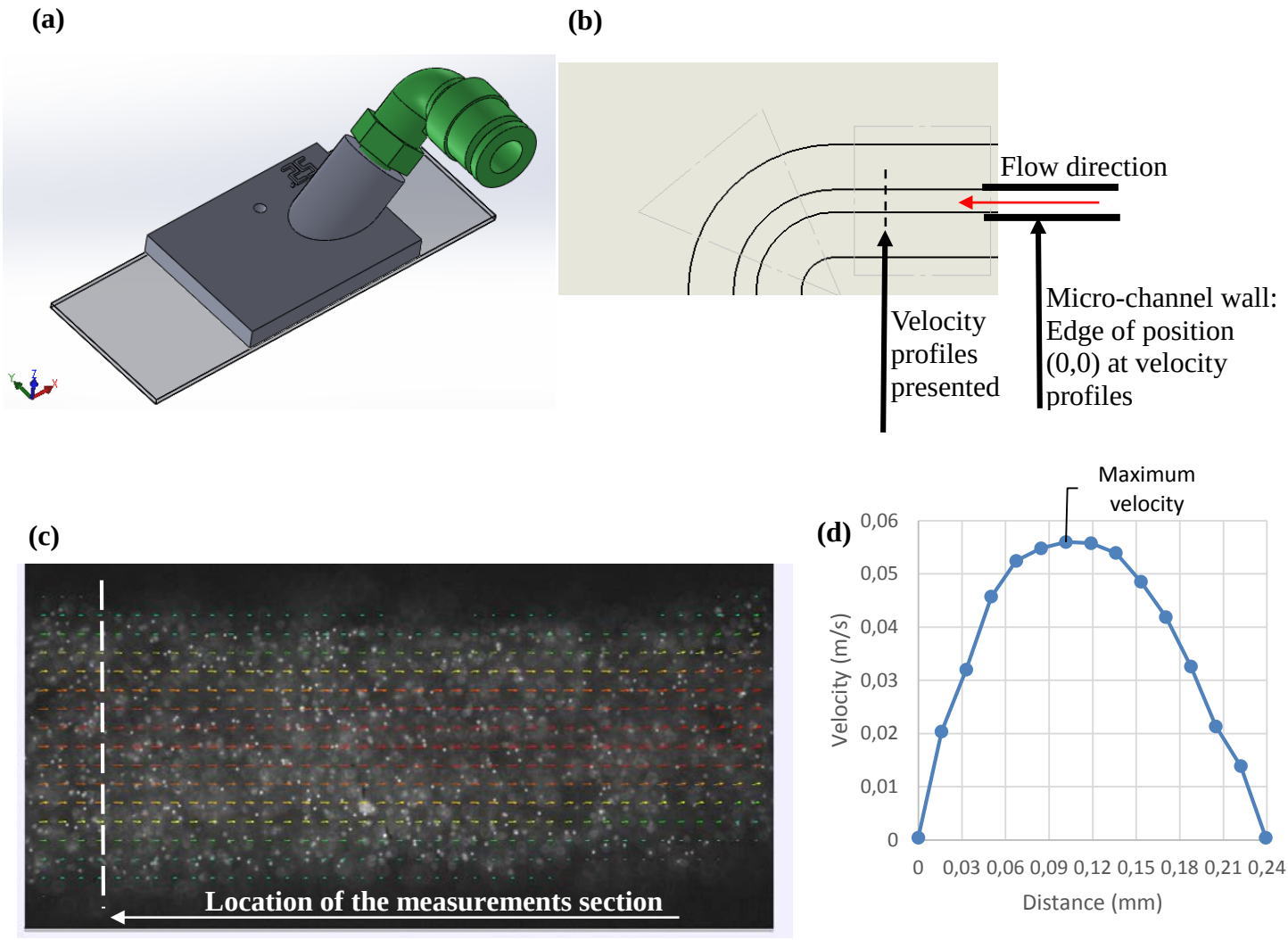

Figure 7: Grease flow at curved micro-channel of 250 µm x 1000 µm. (a) 20X objective microscope picture superposed to the average velocity vectors calculated from the µPIV measurements. (b) Velocity profile at the cross-section marked. (c) Micrsocpe picture with an objective of twenty times superposed with the average vectors velocity calculated from the µPIV measurements. (d) Velocity profile at the dotted line of figure (c), the micro-channel entrance.

µPIV analysis showed that the grease could flow in a 250-µm-width x 1000-µm-height channel. In low flow rates, as Figure 8 shows, the lubrication is more continuous but it is difficult to control the volume of injected grease. On the other hand, using high flow rates, the required volume of grease is injected almost instantaneously. Figure 9 show that in only 6 minutes the grease flows at the theoretical velocity in the outlet.

The infrared spectrum results showed a full coincidence of the peaks, therefore from the analysis of the samples, we assumed that there were no chemical changes and that there were no traces of component losses or degradation. The consistency analysis was used to verify the fact that the grease sample had not suffered the separation of the base oil and the thickening agent. This test was done using the cone penetration test under the ASTM D1403-02 (18).

The average cone penetration measurements in full-scale penetration was $\mu = 335.87$mm and $\sigma = 0.12$, values within the design parameters of NLGI grade 2 grease used. The analysis of the results from both tests, the infrared spectrum and the cone penetration, conclude that the grease does not suffer any changes in its chemical or physical structure when flowing through micro-channels.

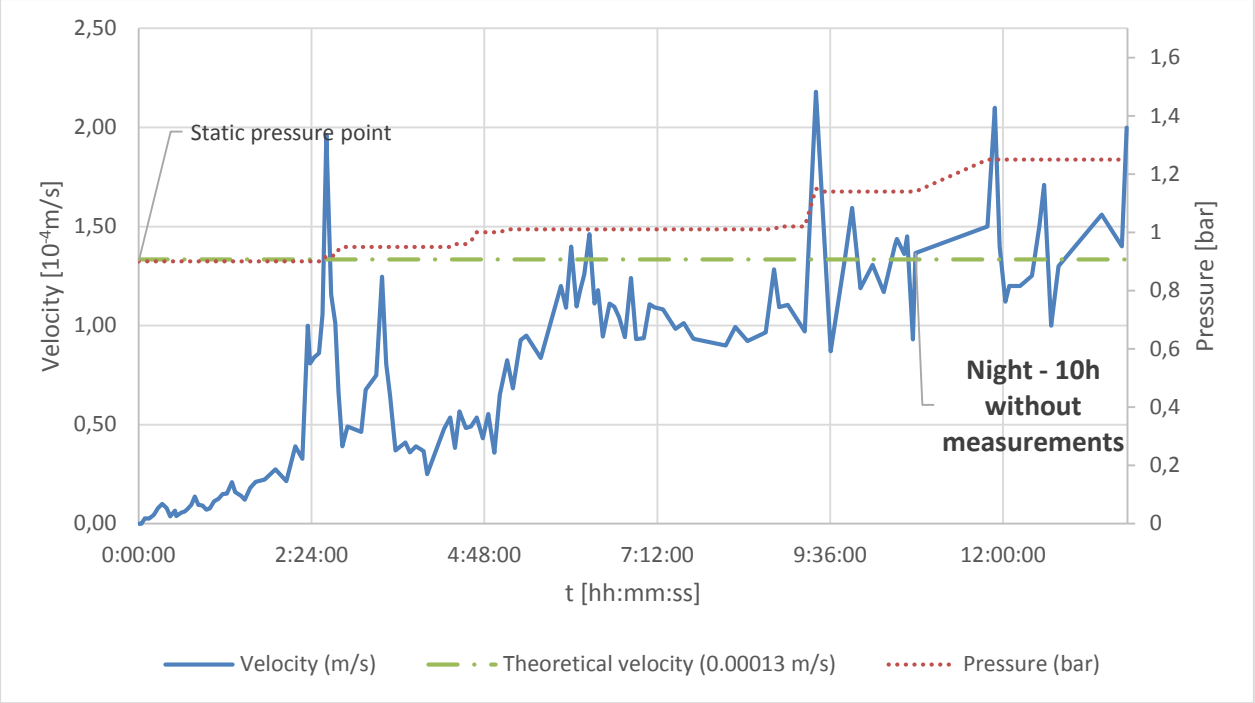

Figure 8: Maximum velocity and the Pressure change versus time of an NLGI2 grease flowing at 0.002ml/min in a 250-µm x 1000-µm micro-channel.

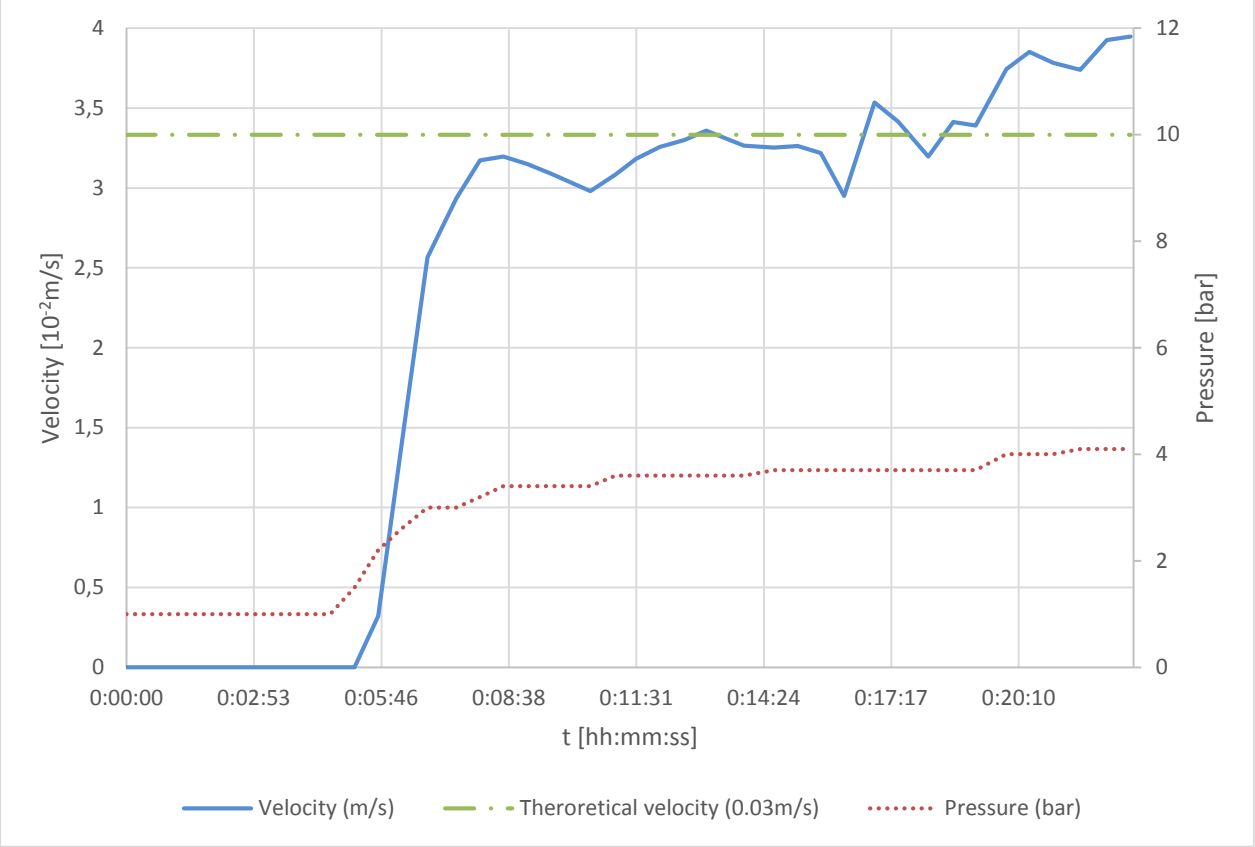

Figure 9: Maximum velocity and the Pressure change versus time of an NLGI2 grease flowing at 0.5 ml/min in a 250-µm x 1000-µm micro-channel.

3.2 Test bench validation

Three different positions of the injection point hs been tested (see Figure 10 a) and when the injection point is at the center of the gear tooth, the grease distribution is more uniform, see Figure 10b.

The test bench was used to determine the Number of fatigue load cycles (Table 1) needed to appreciate wears in the tooth flank without lubrication. At 10^4 cycles the wear appeared as shown Figure 11A. After, lubrication was applied to the tooth through the micro-nozzles and the same number of load cycles was applied, noticing that in this case wear does not appear as shown Figure 11B. The test bench operation showed that there was no interference between the micro-nozzle and the teeth, even with the loads applied.

Continuing the test bench cycling until $2x10^4$ cycles Figure 11D shows the tooth flank with lubrication and the Figure 11C is the tooth flank without the lubrication system. If it is compared both pictures it is possible appreciate that at Figure 11C excessive wear appear against the Figure 11D that starts to appear the mild wear as ANSI/AGMA 1010-E95 (20) defines.

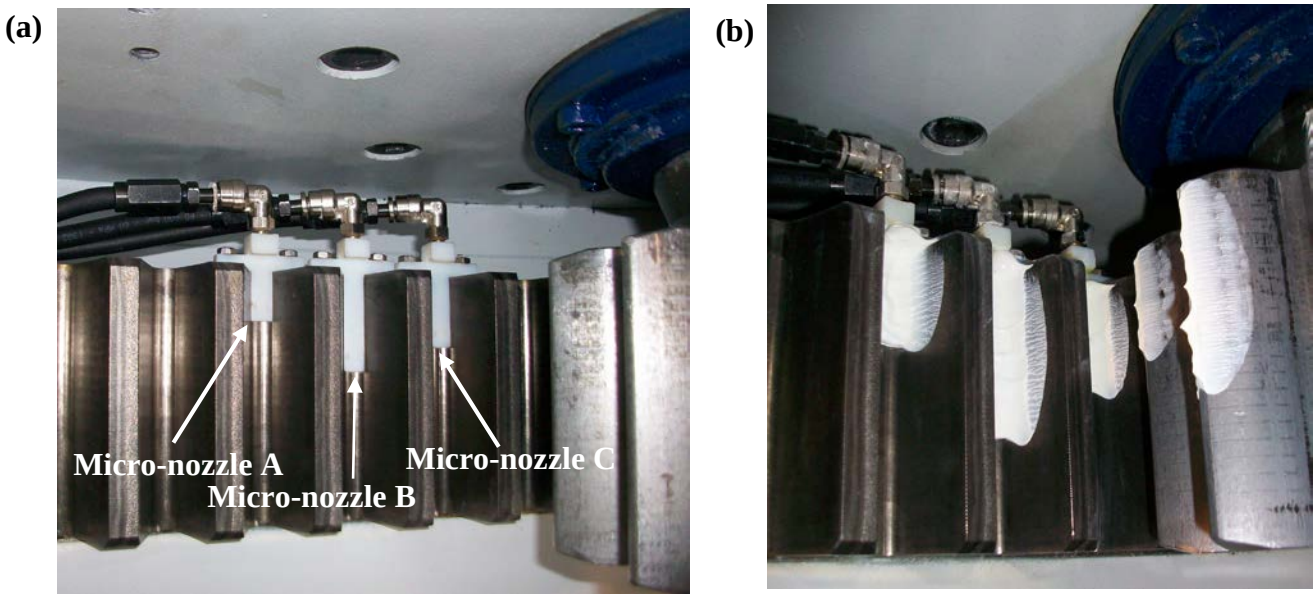

Figure 10: Micro-nozzle integration in a pitch gear. (a) 2-cm, 4-cm and 3-cm length micro-nozzle tested. (b) Grease distribution on the tooth flank for the A, B and C micronozzles.

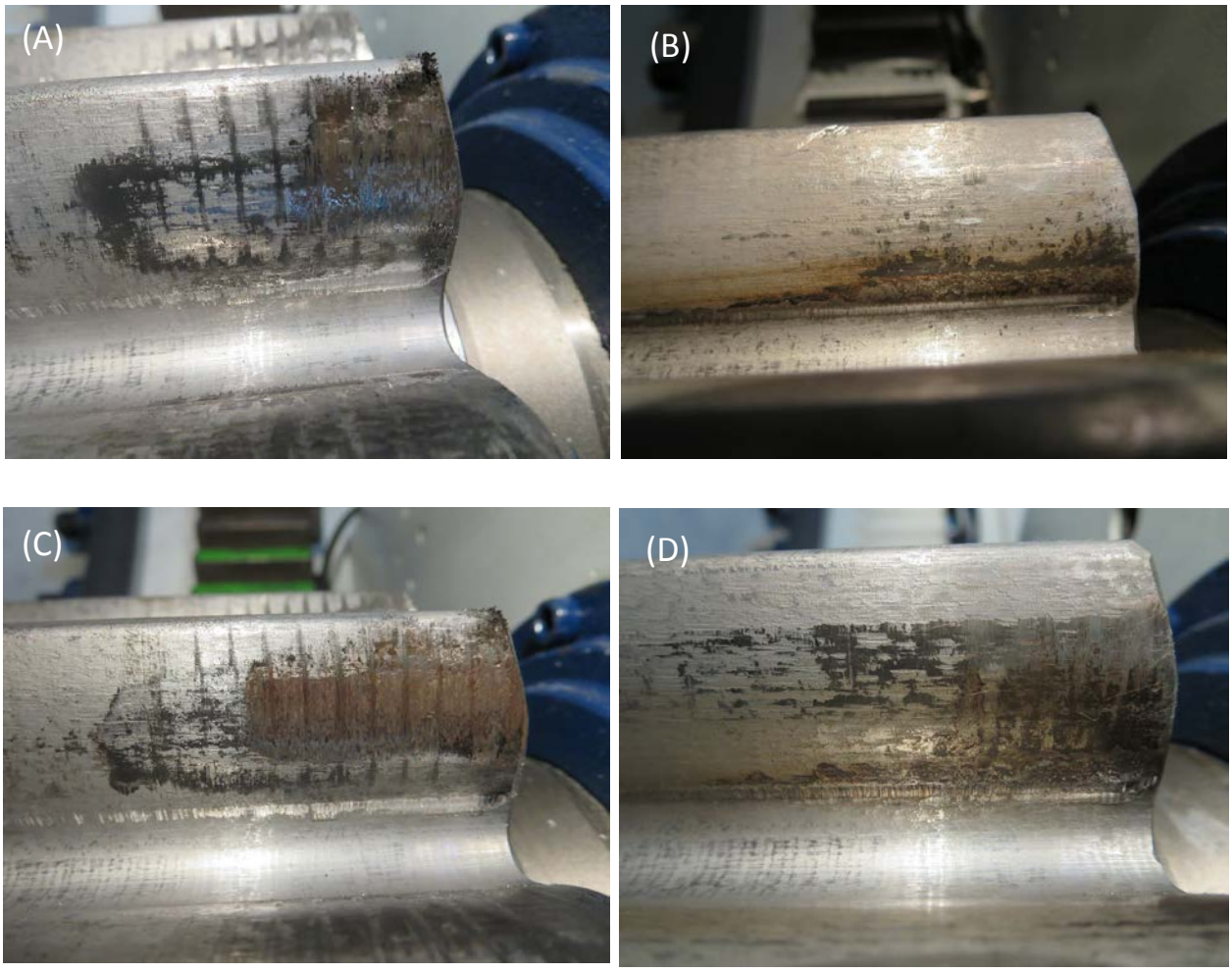

Figure 11: wear evolution at the test bench. (A) Test bench analysis after 10^4 cycles without the lubrication system. (B) Test bench analysis after 10^4 cycles with the lubrication system. (C) Test bench analysis after $2x10^4$ cycles without the lubrication system. (B) Test bench analysis after $2x10^4$ cycles with the lubrication system

4 DISCUSSION

According to the results, grease NLGI grade 2 can flow in a 250-µm-wide and 1000-µm-height channel, useful for wind turbine pitch gears without any degradation. The µPIV tests concluded that at the lower flow rates (0.002ml/min) the grease does not flow through the micro-nozzle at the theoretical velocity till hours later than the pump has been started, that will depend on the pipe length, distributor and valves but mainly to the compression of the grease in the system. On other hand, at higher flow rates (i.e. 0.5ml/min) the transitory period is shorten to a few minutes.

Therefore using low flow rates, results presented on Figure 8, a continuous lubrication can be achieved but it is difficult to warranty the volume of grease injected. On the other hand, using high flow rates, results presented on Figure 9, a less continuous lubrication is achieved but the volume injected is more stable.

According to μPIV, a high flow rate is selected since it guarantees the required amount of grease in minutes and it can avoid the appearance of metal to metal contact. Figure 12 shows the evolution of lubricant for different lubrication strategies compared to the optimum quantity required (square blue line). The proposed micro-nozzle achieves a more accurate strategy to inject the lubricant at zero degree position while the wind turbine can keep producing

The proposed micro-nozzle part to reduce the wear at the gears modifies a parameter that Takadoum in 2008 (11) defined as critical: the tribology. Takadoum (11) defined four parameters that are important to minimize wear: surface state, stress in the system, mechanical contact and tribology of the system. Mashue et. al in 2011 (5) proposed changing the surface state, by decreasing hardness of the pinion compared to that of the crown, which is of difficult implementation in the ongoing wind turbines. In the same direction Dimascio et. al in 2009 (6) presented a solution to replace the damaged region of the gears in situ with a new bolt-assembled tooth. Systems (5-6) change the surface state but do not eliminate the wear, therefore preventive maintenance is required, operation that the technology presented in this paper would minimize. Nielsen in 2008 (7) changed the mechanical contact, since he assembled three gears, one to transmit power and the other two to be in contact with the bearing decreasing the stress per tooth,

but the wear was not eliminated and the preventive maintenance is still required. Kürzdörfer in 2007 (8) designed a special injector that sprays one side of the tooth to lubricate the joint directly;

this cannot be easily implemented since there is no compressed air in the wind turbines and oil is difficult to be kept in the tooth flank. Zdravko in 2007 (9) proposed to inject grease through the lubrication pinion, solution that it is easy to implement in the wind turbines but requires to stop the wind turbine to lubricate the pinion at the 0º position with its associated energy generation losses. Klaus in 2010 (10) presented a solution that used holes in the dedendum to inject fresh grease while the wind turbine operates. Until now this solution is the best but in ongoing wind turbines the gear replacement costs are difficult to justify. The presented technology is easy to integrate in ongoing wind turbines and together with the lubrication pinion presented by Zdravko in 2007 (9) can increase the energy generation since it eliminates the programed wind turbine stops to lubricate.

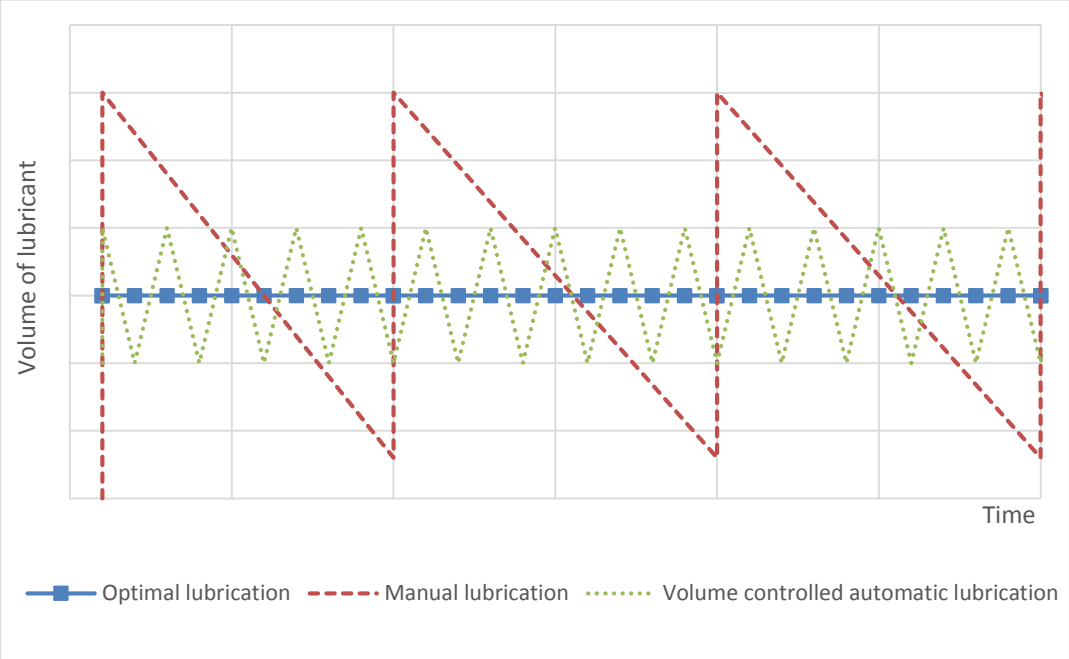

Figure 12: Graphical representation of the different technologies to lubricate. The square line represents the optimum amount of grease needed for that application and the other two lines represents the different methodologies to apply that lubricant.

CONCLUSIONS

A micro-nozzle to provide fresh grease in the Pitch gear teeth in contact has been designed and fabricated. The fabricated parts were tested in a pitch gear test bench of a 2 MW wind turbine using conventional wind turbine greases under real loads. The µPIV analysis shows that a high flow rate is better to warranty the amount of lubrication when is required and the nozzles that injected the grease to the position in the middle teeth showed a more uniform grease distribution and compared to the current lubrication systems, extend the service life of the teeth by more than double and reduce the appearance of wear $2x10^4$ cycles.

Another benefit of this novel lubrication system is that it allows the wind turbine to lubricate and generate at the same time, this being the key difference compared to previous technologies and consequently increases the wind turbine electricity generation. In addition, the method presented in this paper is universally applicable to any pitch gear modules, regardless of shape, size and the lubrication system available.

The wind sector tendency towards an offshore market leads to use of autonomous systems to reduce preventive and corrective maintenance such as the device presented.

5 ACKNOWLEDGMENTS

This project/research has been supported by KIC InnoEnergy. KIC InnoEnergy is a company supported by the European Institute of Innovation and Technology (EIT), and has the mission of delivering commercial products and services, new businesses, innovators and entrepreneurs in the field of sustainable energy through the integration of higher education, research, entrepreneurs and business companies.
The work is also financed by Laulagun Bearings S.A, Klüber lubrication Gmbh and Grupo Tecnico Rivi-Lincoln, companies that have also provided all his technical knowledge on his field.

6 REFERENCES

(1) Germanischer Lloyd Industrial Services GmbH; July 2010. Guideline for the Certification of Wind Turbines. Germanischer Lloyd, Hamburg.

(2) Gamesa Innovation, patent assignee; 2008 Dec. 01. Sistema de cambio de paso variable accionado eléctricamente. Español Patent ES 2308911-A1.

(3) J.G. Holierhoek, H. Korterink, R.P. van de Pieterman, H. Braam, L.W.M.M. Rademakers, D.J. Lekou, T. Hecquet, H. Söker; September 2010. Recommended Practices for Measuring in Situ the 'Loads' on Drive Train, Pitch System and Yaw System. Protest ECN-E--10-083.

(4) Andreas Manjock. Close to the wind: Pitch Systems. Beaufort 6; Edition June 2007. Vol.2 p.1-3.

(5) Mashue A, Moorer B.G, Goodwin K, inventors; 2011 Jun. 16. Gear set for pitching blade of rotor of wind turbine utilized for providing electricity to utility grid, has pinion/drive gear comprising set of teeth whose hardness is less than harness of teeth of ring gear. United States patent US 2011142617-A1.

(6) Dimascio P, Close R, Auer G, Grimley R, Hamel A, inventors; 2009 Aug. 29. Hub pitch gear repair method. Canada patent CA 2655691-A1.

(7) Nielsen T, inventor; 2008 Jun. 26. A gear system for yaw drive or a pitch drive for a wind turbine. World Intellectual Property Organization WO 2008/074320-A1.

(8) Kürzdörfer, M inventor; 2007 Mar. 21. Anstellwinkeleinstellvorrichtung für eine Windkraftanlage. European Patent EP 1764544-A2.

(9) Zdravko Paluncic, Andreas Schöenfeld inventors; April 26 2007. Lubricating device with lubricating pinion. European Patent DE202006011330-U1

(10) Klaus P, inventor; 2010 Apr 20. Actuator for adjusting a rotor blade pitch angle. United States patent US 7699584-B2.

(11) Takadoum, Jamal; 2008. Materials and Surface Engineering in Tribology. London: Wiley.

(12) Mashue A, Pemrick J, inventors; 2011 Jun. 16. Wind turbine with gear indicating wear. United States patent US 2011138951-A1.

(13) Nordex Energy, patent assignee; 2010 Apr. 08. Device for estimating wear condition of gear teeth of pitch rotary joint of wind turbine, has quadrangular part movably and lockably arranged on pin, where two transverse sides of part are shorter than two longitudinal sides of part. Germany patent DE 202009015263-U1.

(14) DIN 867; February 1986. Basic rack tooth profiles for involute teeth of cylindrical gears for general engineering and heavy engineering. DIN.

(15) Westerberg, L., Lundström, T., Höglund, E., Lugt, P.: Investigation of grease flow in a rectangular channel including wall slip effects using micro particle image velocimetry. Trib. Trans. 53, 600–609 (2010). DOI: 10.1080/10402001003605566

(16) Farré-Lladós, J., Casals-Terré, J., Voltas, J., Westerberg, L.G.: The use of rapid prototyping techniques (rpt) to manufacture micro channels suitable for high operation pressures and μpiv. Rapid Prototyping Journal (2014). Accepted.

(17) DIN 51817; April 1998. Determination of oil separation from lubricant grease under static conditions. Germany: DIN-Normen.

(18) ASTM D1403-02; Reapproved 2007. Standard Test Methods for Cone Penetration of Lubricant Using One Quarte and One Half Scale Cone Equipment. United States: ASTM.

(19) J. J. Heigl, M. F. Bell and J.U. White. Application of Infrared Spectroscopy to the Analysis of liquid Hydrocarbons. Analytical Chemistry, May 1947; Volume 19 num 5. DOI: 10.1021/ac60005a003

(20) ANSI/AGMA 1010-E95. Revision of AGMA 110.04; 1995. Appearance of Gear Teeth – Terminology of Wear and Failure. United States of America: ANSI/AGMA.